MONASH University

INVESTIGATING MEK INHIBITION IN THE TREATMENT OF MULTIPLE MYELOMA

Jay Hocking

MBBS, FRACP, FRCPA

A thesis submitted for the degree of Doctor of Philosophy at Monash University

2018

Department of Clinical Haematology
Monash University / Alfred Hospital
Melbourne, Australia

Copyright notice

TABLE OF CONTENTS

ABSTRACT

Multiple myeloma is an incurable haematologic malignancy. Therapeutic advances continue to improve overall survival, but there remains a need for the ongoing development of novel treatment approaches. Activating mutations in the RAS mitogen activated protein kinase pathway (RAS-MAPK) are present in approximately 50% of cases. These mutations function as secondary oncogenic drivers and are thought to play a significant role in disease progression, as these mutations are virtually never seen in the precursor condition monoclonal gammopathy of uncertain significance (MGUS) and have a higher prevalence at relapse. Additionally, the t(4;14) translocation is present in approximately 15% of cases, which signals via inputs into the RAS-MAPK. Together, this provides the rationale for therapeutically targeting the RAS-MAPK. Trametinib is a small molecule inhibitor directed against MEK, a kinase belonging to the RAS-MAPK. Herein we investigate a potential role of MEK inhibition with trametinib in MM.

We show trametinib inhibits proliferation in human myeloma cell lines (HMCLs) that harbour *RAS* mutations (*RAS*^{M}). This effect is mediated by abrogation of signalling through the RAS-MAPK with loss of phosphorylated ERK, cell cycle arrest at $G_{0/1}$ in *p53* wild type cells, and loss of nuclear accumulation of both ERK and cyclin B. Despite the loss of phosphorylated ERK in all HMCLs, virtually no effect is observed in either t(4;14) or WT (neither RAS^{M} or t(4;14)) HMCLs with trametinib monotherapy. In a *RAS*^{M} murine xenograft model, trametinib monotherapy delayed tumour progression, but did not improve survival. Further, treatment with trametinib in combination with dexamethasone results in synergistic cytotoxicity in *RAS*^{M} HMCLs and a single t(4;14) HMCL. As such we find *RAS*^{M} to be a predictive of MEK inhibitor sensitivity and that MM exhibits oncogenic addition *RAS*^{M}.

We interrogated global kinase changes in response to trametinib treatment, identifying both CK2 and BCL-2 activity as causes of early resistance to trametinib. Trametinib treatment in combination with silmitasertib (an inhibitor of CK2) causes synergistic cytotoxicity in *RAS*^{M} HMCLs, and induced a cytostatic response in t(4;14) HMCLs. Trametinib in combination with venetoclax (an

inhibitor of BCL-2) results in synergistic cytotoxicity in *RAS*^{M} and t(4;14) HMCLs that express phosphorylated BCL-2 at baseline, identifying this as a potential biomarker of sensitivity to the combination.

Using RNA-sequencing we recapitulated the findings of MEK-inhibitor sensitivity gene signatures identified in other solid tumours.

Finally, we show that azacitidine pre-treatment of t(4;14) HMCLs resulted in profound sensitisation to subsequent treatment with trametinib. We demonstrate DNMT3b, a known target of azacitidine, is overexpressed in t(4;14) HMCLs and predicts sensitivity the combination. In a t(4;14) murine xenograft model treatment with azacitidine followed by trametinib significantly delayed tumour growth. Despite this, the combination failed to prolong survival compared to azacitidine alone.

Collectively, our results confirm inhibiting the RAS-MAPK with the MEK inhibitor trametinib as a feasible, targeted therapeutic strategy in MM. Combination therapy can optimise the response to MEK inhibition, from cytostatic to cytotoxic. Our findings represent a novel approach in the treatment of MM, and support further clinical evaluation of MEK inhibition in MM.

DECLARATION

This thesis contains no material which has been accepted for the award of any other degree or diploma at any university or equivalent institution and that, to the best of my knowledge and belief, this thesis contains no material previously published or written by another person, except where due reference is made in the text of the thesis.

Signature: ……

Print Name: ……

Date: …….

ACKNOWLEDGEMENTS

I would firstly like to thank my PhD supervisor Professor Andrew Spencer, for his insight in all matters myeloma, his guidance, support and persistence throughout this project. To Dr Tiffany Khong, who has taken a scientific novice and taught him everything needed to become a laboratory researcher, and for being a friend as much as a supervisor. To Dr Sridurga Mithraprabhu for her scientific insight and teaching me scientific rigour.

I would also like to thank Ioanna Savvidou for her support, friendship and philosophy. To both Brianna Xureb and Sophie Whish who have helped with oh so many mice. To all the members of MRG and the ACBD who have helped along the way.

And finally, to Callum, for supporting me and putting up with this for four years.

PUBLICATIONS & CONFERENCE ABSTRACTS DURING CANDIDATURE

- *Demethylation sensitises t(4;14) multiple myeloma to RAS-MAPK pathway inhibition.* Jay Hocking, Sophie Whish, Sridurga Mithraprabhu, Tiffany Khong, Andrew Spencer. European Haematology Association 2018, poster presentation

- *Demethylation sensitises t(4;14) multiple myeloma to RAS-MAPK pathway inhibition.* Jay Hocking, Sridurga Mithraprabhu, Tiffany Khong, Andrew Spencer. Haematology Association of Australia (HAA) 2017, oral presentation

- S Mithraprabhu, T Khong, M Ramachandran, A Chow, D Klarica, L Mai, S Walsh, D Broemeling, A Marziali, M Wiggin, J Hocking, A Kalff, B Durie, A Spencer. *Circulating tumour DNA analysis demonstrates spatial mutational heterogeneity that coincides with disease relapse in myeloma*. Leukemia 2017; 31:1695-705

- Jay Hocking, Sridurga Mithraprabhu, Anna Kalff, Andrew Spencer. *Liquid biopsies for liquid tumours: emerging potential of circulating free nucleic acid evaluation for the management of hematologic malignancies*. Cancer Biol Med 2016 13(2):215-25

- *Targeting the RAS-MAPK in Multiple Myeloma with Small Molecule Inhibitors*. Jay Hocking, Tiffany Khong, Daniella Brasacchio, Sridurga Mithraprabhu, Jake Shortt, Andrew Spencer. Inaugural National Myeloma Workshop 2016, Plenary oral presentation

- *Targeting the RAS-MAPK in Multiple Myeloma with Small Molecule Inhibitors*. Jay Hocking, Tiffany Khong, Daniella Brasacchio, Sridurga Mithraprabhu, Jake Shortt, Andrew Spencer. Haematology Association of Australia 2015, poster presentation

LIST OF FIGURES & TABLES

ABBREVIATIONS

ºC	Degrees Celsius
ALL	Acute lymphoblastic leukaemia
AML	Acute myeloid leukaemia
AP1	Activator protein 1
APRIL	A proliferation-inducing ligand
ASCT	Autologous stem cell transplant
ATCC	American Type Culture Collection
ATM	Ataxia telangiectasia mutated
ATO	Arsenic tri-oxide
ATP	Adenosine triphosphate
ATR	Ataxia telangiectasia and Rad3-related protein
AVM	Arteriovenous malformation
BAFF	B-cell activating factor
BMMC	Bone marrow mononuclear cells
BMME	Bone marrow micro-environment
BMSC	Bone marrow stromal cells
BSA	Bovine serum albumin
CDA1	Cell division antigen 1
CHK1/2	Checkpoint kinase 1/2
CK2	Casein kinase 2
CKS1B	Cyclin dependent kinase regulatory subunit 1
CLL	Chronic lymphocytic leukaemia
CML	Chronic myeloid leukaemia
CNS	Central nervous system
CR	Complete response/remission
CRC	Colorectal carcinoma
CRS	Cytoplasmic retention sequence
CSR	Class switch recombination
ddPCR	Droplet digital polymerase chain reaction
DMSO	Dimethyl sulfoxide
DNMT	DNA methyltransferase
ECOG	Eastern co-operative oncology group

EDTA	Ethylenediaminetetraacetic acid
EGFR	Epithelial growth factor receptor
EMT	Epithelial-to-mesenchymal
ERK	Extracellular-regulated signal kinases
FBS	Foetal bovine serum
FFP	Farnesyl pyrophosphate
FGF/R	Fibroblast growth factor/receptor
FITC	Fluorescein isothiocyanate
FTi	Farnesyl-transferase inhibitor
GAP	GTPase activating protein
GEF	Guanine exchange factor
GEP	Gene expression profile
GFP	Green fluorescent protein
GGPP	Geranylgeranyl pyrophosphate
GI	Gastro-intestinal
GIST	Gastro-intestinal stromal tumour
GO	Gene ontology
Grb2	Growth factor receptor-bound protein 2
GSK3	Glycogen synthetase kinase 3
GTP	Guanosine triphosphate
HCC	Hepatocellular carcinoma
HCL	Hairy cell leukaemia
HLP	Hind-limb paralysis
HMCL	Human myeloma cell lines
HMG	Hydroxymethylglutarate
HPMC	Hydroxypropylmethylcellulose
HRP	Horseradish peroxidase
HSC	Haematopoietic stem cells
HSP	Heat shock protein
IHC	Immunohistochemistry
Ig	Immunoglobulin
IgH	Immunoglobulin heavy chain
IL-6	Interleukin-6
IMiDs	Immunomodulatory drugs

IMWG	International Myeloma Working Group
IP	Intra-peritoneal
IQGAP	IQ motif and GTPase activating protein
ISS	International staging system
IV	Intra-venous
JAK	Janus kinase
JNK	Jun N-terminal kinase
KSR	Kinase suppressor of RAS
LCH	Langerhans cell histiocytosis
LXN	Latexin
MAPK	Mitogen activated protein kinase
MDS	Myelodysplasia
MEK	Mitogen-activated protein kinase kinase
MEKi	MEK inhibitor
MGUS	Monoclonal gammopathy of undetermined significance
MIP1α	Macrophage inflammatory protein 1-alpha
μL	Microlitre
mL	Millilitre
MLL-AML	Mixed lineage leukaemia rearranged acute myeloid leukaemia
μM	Micromolar
mM	Millimolar
MM	Multiple myeloma
MMSET	Multiple myeloma SET domain
MPN	Myeloproliferative neoplasm
MR	Minor response
mTOR	Mammalian target of rapamycin
nCR	Near complete remission
NFkB	Nuclear factor kappa-light-chain-enhancer of activated B cells
nM	Nanomolar
ns	Non-significant
NSCLC	Non-small cell lung cancer
NSG	NOD scid gamma
OCT	Organic cation transporter

OG	Oral gavage
ORR	Overall response rate
OS	Overall survival
PAGE	Polyacrylamide gel electrophoresis
PBS	Phosphate buffered saline
PCL	Plasma cell leukaemia
PD	Progressive disease
PDGF/R	Platelet derived growth factor/receptor
PFA	Paraformaldehyde
PFS	Progression free survival
PI	Propidium Iodide
PI3K	Phosphatidylinositol 3-kinase
PLK	Polo-like kinase
PR	Partial response
PTEN	Phosphatase and tensin homolog
PVDF	Polyvinylidene difluoride
R/R	Relapsed/refractory
RAF	Gene name derived from “rapidly accelerated fibrosarcoma”
RAF^{M}	RAF mutated
RAS	Gene name derived from “rat sarcoma virus”
RAS^{M}	RAS mutated
Rb	Retinoblastoma
RBD	RAS binding domain
R-ISS	Revised international staging system
RPM	Revolutions per minute
R/R	Relapsed/refractory
RT-PCR	Reverse transcriptase polymerase chain reaction
RTK	Receptor tyrosine kinase
Scr	Scramble siRNA
SD	Stable disease
SDS	Sodium dodecyl sulfate
SEM	Standard error of the mean
SH2	Src homology domain 2
SHM	Somatic hypermutation

siRNA	Short interfering-RNA
SLC	Solute carrier family
SOS	Son of sevenless
STAT	Signal transducer and activator protein
TBP	TATA binding protein
TBS	Tris buffered saline
TTP	Time to progression
TNBC	Triple negative breast cancer
UT	Untreated
VEGF/R	Vascular endothelial growth factor/receptor
VGPR	Very good partial response
WB	Western blot
WES	Whole exome sequencing
WT	Wild type

1. INTRODUCTION

1.1 MULTIPLE MYELOMA

Multiple myeloma (MM) is a B-cell malignancy characterised by a clonal proliferation of malignant plasma cells in the bone marrow, a monoclonal protein of either intact immunoglobulin (Ig), light chains or both in the blood and often detected in the urine (described as Bence-Jones protein) with associated end-organ dysfunction[1]. It is the second most common haematologic malignancy and accounts for approximately 1% of all cancers. The median age of onset is 70 years. Despite many novel treatment options over the past two decades, MM remains incurable with a median survival of between 42 and over 100 months depending on disease risk[2].

Plasma cells are terminally differentiated, antibody-secreting B-lymphocytes. The generation of plasma cells occurs initially in response to T-cell antigen presentation, where B-cells receive an antigen-receptor dependent signal which leads to the rapid development of B-lymphoblasts. These lymphoblasts divide and may undergo class switch recombination (CSR), resulting in a change of antibody isotype. This results in short lived plasmablasts which secrete large amounts of antibody[3]. This antibody is typically low affinity due to limited somatic hyper-mutation (SMH). Subsequently, some of these activated B-cells re-enter the follicle, undergo SMH, and develop into long-lived plasma cells generating high affinity antibody, also capable of re-activation at times of repeat immune challenge[4,5]. This provides the long-term memory component to the human immune system. The processes of CSR and SMH both require double stand breaks in DNA at the immunoglobulin locus[6,7]. This very process which gives rise to an effective, high affinity immune response with memory, is thought to be the point at which MM arises, resulting in the clonal expansion of long-lived malignant plasma cells. Hence it is not surprising that the incidence of clonal expansion of plasma cells increases with age[8].

The pre-malignant condition, monoclonal gammopathy of undetermined significance (MGUS), is thought to precede almost all cases of MM[9-11]. MGUS is

defined as the presence of fewer than 10% clonal plasma cells in the bone marrow, <30g/L of monoclonal protein and the absence of end organ damage which defines MM. Where parameters exceed those of MGUS, but there is still absence of end organ damage, the condition is termed asymptomatic MM. The risk of progression to overt symptomatic MM increases with each of these parameters[12]. A subset of asymptomatic MM patients has been defined with a particularly high risk (>80% at two years) of progression to symptomatic MM[13-15]. Current recommendations from the International Myeloma Working Group (IMWG) suggest consideration for treatment of asymptomatic patients that fit the high-risk category[12].

Karyotypic abnormalities are thought to be present in the founder MGUS clones. Approximately 40% of the cytogenetic abnormalities involve the immunoglobulin heavy chain locus (IgH) on chromosome 14, and one of five partner chromosomes 4, 6, 11, 16 or 20. These are thought to arise during the process of CSR. Approximately 50% of cases are hyperdiploid, harbouring trisomies typically of the odd number chromosomes. An hyperdiploid karyotype portends a better prognosis[16]. Whereas, the genetic lesions, t(4;14), t(14;16) and deletion of the short arm of chromosome 17 (del(17p)), adversely impact on prognosis[17]. The presence of these has been incorporated into the revised international staging system (R-ISS) to better characterise relative risk and survival[2].

On the background of these cytogenetic abnormalities secondary oncogenic mutations occur leading to progression from MGUS, to asymptomatic MM and finally to the clinically apparent MM. The most common of these involve members of the *RAS* family genes, *KRAS* and *NRAS*. Confirming these as molecular markers of progression, mutations in *RAS* genes are almost never seen in MGUS. Further rates of mutation increase beyond 50% in later stages of disease[18]. Finally, dysregulation of *MYC* and mutations in *p53* are considered late stage processes and harbingers of accelerated disease[19-22].

1.2 THE RAS-MITOGEN ACTIVATED PROTEIN KINASE PATHWAY

The RAS-MAPK is a kinase pathway comprising the four kinases: RAS, RAF, MEK and its final effector ERK (Figure 1.1)[23,24]. It is not strictly a cascade, as the signal is not amplified at each step. The RAS-MAPK transduces extracellular signals from membrane bound receptors, most typically the receptor tyrosine kinases (RTKs) and is involved in proliferation, growth, migration, survival and anti-apoptosis[25].

Following stimulation of a receptor by its cognate ligand (mitogens, growth factors, cytokines), receptor dimerization occurs leading to activation and auto-phosphorylation of the intracellular domain. Once phosphorylated the adaptor protein "growth factor receptor bound protein 2" (GRB2) is recruited via its Src homology domain (SH2) along with "Son of Sevenless" (SOS). SOS is a "guanine nucleotide exchange factor" (GEF) that activates RAS by replacing GDP with GTP and thus propagates the signal to the pathway[26].

The RAS proteins are a family of small GTP-binding proteins, encoded by the *RAS* proto-oncogenes[27]. Three isoforms exist: KRAS (A and B), NRAS and HRAS, which share 85% sequence homology. Functional differences between the encoded proteins are not fully elucidated. However, highlighting differences, *KRAS* knockout mice die mid-gestation whilst *N* and *HRAS* knockout survive[28]. Post-transcription modifications of RAS take place affecting cellular localisation. The first step in trafficking to the cell membrane requires isoprenylation, the addition of a 15-carbon isoprenoid chain from farnesyl pyrophosphate (FPP) by farnesyltransferase (FTase). Alternatively, both K and NRAS can be isoprenylated by the 20-carbon chain geranylgeranyl pyrophosphate (GGPP) by geranylgeranyltransferase (GGTase). The mevalonic acid pathway generates both FPP and GGPP. Following isoprenylation, an endopeptidase removes three terminal amino acid residues, this is followed by methylation and the addition of two palmitoyl long chain fatty acids by palmitoyltransferase allows stabilisation at the plasma membrane. This final step is not required for KRAS as it has lysine residues at it carboxy terminus, which interacts with the negatively charged lipid bi-layer[29].

After RAS-GDP binds to SOS, GEF activity generating RAS-GTP is initially low, however once RAS-GTP is generated this allosterically enhances the activity of SOS 10-fold, rapidly generating RAS-GTP. This process is reversed by the GTPases (GAPs), which hydrolyse GTP to GDP, inactivating RAS once again. The activity of the GAPs are several fold higher than that of the GEFs leading to rapid inactivation of RAS providing fine control of pathway activity[30].

Targets of RAS include RAF leading to signalling via the MAPK pathway, PI3K resulting in activation of the PI3K/AKT pathway and phospholipase C. Why activity directed to any one pathway is preferred over another is not entirely clear[27].

The RAF family of serine/threonine protein kinases consist of ARAF, BRAF and CRAF (RAF-1)[31]. Each RAF kinase consists of CR1, 2 and 3 domains. The CR1 domain contains the RAS-binding domain (RBD), CR2 is a regulatory phosphorylation site and CR3 the active kinase domain. RAF is maintained inactive in the cytosol via the regulatory 14-3-3 protein binding to the CR2 domain[32]. Once RAF is recruited to RAS by the RBD, phosphorylation occurs resulting in the "dislocation" of the CR2 domain, RAF monomers form homo- and heterodimers now paradoxically enhanced through crosslinking by 14-3-3, resulting in activation of the CR3 kinase domain[33]. In contrast to RAS, RAF has few target substrates with MEK the only target of all three isoforms.

MEK1/2 are serine/threonine protein kinases[34]. They are dual specificity kinases which phosphorylate both serine and threonine residues on ERK1/2. Activation of MEK occurs once RAF has phosphorylated its two serine residues. The only known targets of MEK1/2 are ERK1/2[34], thus making MEK a "convergence" point of the MAPK pathway.

ERK1/2 are serine/threonine kinases[35]. ERK1 and ERK2 appear to have overlapping/redundant functions, with over 80% sequence homology. There is likely some distinction in their activity though, as only *ERK2* knockout in mice is embryonic lethal[36,37]. Functional differences remain to be dissected. ERK is activated via phosphorylation of a serine and threonine residue by MEK1/2. ERK is the final effector in the pathway with over 160 nuclear, cytoplasmic and

cytoskeletal substrates[25]. This results in the MAPK pathways involvement in such an extensive range of cellular processes including cell-cycle, proliferation, anti-apoptosis, migration, adhesion.

In addition to the kinase pathway itself, several influencers exist including scaffold proteins, positive and negative modulators, negative feedback loops and phosphatases. These proteins and enzymes serve to potentiate, dampen or turn off pathway activity.

Scaffold proteins provide “docking” points for the enzymes of the MAPK and in doing so co-localise the individual elements[38]. “Kinase suppressor of Ras1” (KSR1) is a misnamed multi-domain scaffold protein, which localises to the cell membrane, providing docking sites for RAF, MEK and ERK, co-localising and enhancing sequential activation. When not activated by RAS, KSR is maintained inactive in the cytoplasm by 14-3-3. IQGAP, originally thought to be a RAS-GAP, is another scaffold protein for RAF, MEK and ERK. IQGAP modulates the nature and duration of MAPK signalling particularly between MEK and ERK2[39,40]. MP1, SEF and PAXILLIN are also scaffold proteins that traffic ERK to specific locations in the cytosol. In redirecting ERK they prevent nuclear translocation limiting its effects to cytosolic and membrane proteins[41,42].

Positive modulators of the pathway “suppressor of ras-8” (SUR-8)[43] and “connector enhancer of KSR” (CNK)[44] both potentiate the interaction of RAS and RAF and the latter’s activation. Negative modulators of the pathway Erbin, Sprouty and “Raf-1 kinase inhibitor protein” (RKIP)[45] predominantly interfere with interactions of CRAF. Sprouty also binds to and sequesters Grb2/SOS inhibiting RAS activation[46,47].

Once activated ERK has negative feedback loops with SOS[48], CRAF[49] and MEK1[50] (Figure 1.2).

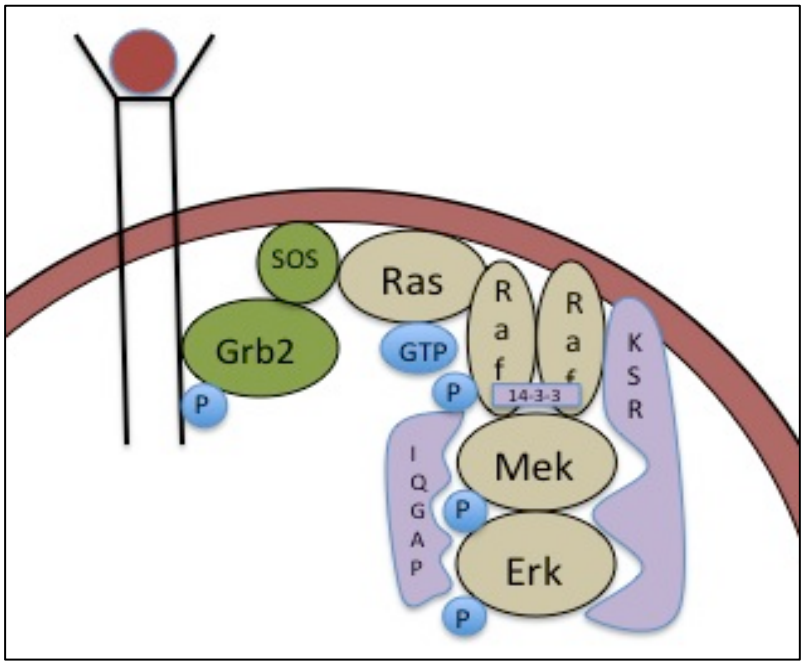

Figure 1.1: The RAS-MAPK in the active state

1.3 THE RAS-MAPK IN NON-MALIGNANT CONDITIONS

Mutational activation of the RAS-MAPK is not limited to malignant conditions. Investigations of non-malignant conditions, using highly sensitive techniques are identifying MAPK mutations.

Utilising droplet digital PCR (ddPCR), a study of sporadic arteriovenous malformations (AVM) in the brain identified activating *KRAS*^{M} in the endothelium in 45 of 72 cases[51]. Downstream analysis found preferential activation of ERK over either AKT or p38 and increased expression of genes associated with angiogenesis. MEK inhibition abrogated the angiogenesis gene signature.

In a similar study of endometrial tissue, using whole exome sequencing (WES) and ddPCR, three of 27 samples were identified to have *KRAS* mutation[52]. Endometriosis is considered a benign disease without malignant potential.

Both these studies are consistent with the known roles of the RAS-MAPK in growth and proliferation. Inhibition of the pathway appears to impact on AVM gene expression and might possibly offer a treatment option in recalcitrant endometriosis.

1.4 THE RAS-MAPK AND MALIGNANCY

Mutations within the MAPK pathway are among the most frequently observed in all malignancy[53]. First described in 1982[54-56], investigation continues, repeatedly identifying cancers with previously unknown pathway mutations.

RAS^{M} are observed in pancreatic adenocarcinoma (90%)[57,58], colorectal carcinoma (CRC) (45%)[59], papillary thyroid tumours (60%)[60,61] and non-small cell lung cancers (NSCLC) (35%)[62,63]. In solid tumours *RAS*^{M} do not appear to influence prognosis. Despite the frequency of these mutations, targeting these lesions has remained elusive and does not form part of standard clinical practice.

RAF^{M} are found in metastatic melanoma (60%)[64], papillary thyroid cancer (up to 70%)[65,66] and right sided colon cancer (10-15%)[67] conferring a poor prognosis in the latter. *RAS*^{M} or *RAF*^{M} in CRC result in resistance to the EGFR inhibitor cetuximab.

In haematologic malignancy *RAS*^{M} is present in chronic myelomonocytic leukaemia (CMML)(40%)[68], acute myeloid leukaemia (AML) (25%)[69] and relapsed childhood acute lymphoblastic leukaemia (ALL)(30%)[70]. It is likely the *RAS*^{M} in childhood ALL are present at diagnosis and may be enriched at relapse. The *BRAF*^{M}V600E (also seen in melanoma) is the diagnostic hallmark of hairy cell leukaemia (HCL)[71,72]. *BRAF*^{M} is present in Langerhans cell histiocytosis (LCH) (50%)[72]. In BRAF wild type, a *MEK* mutation is often present (25%)[73,74].

Currently the only disease in which targeted therapy is utilised is in *BRAF*^{M} melanoma, with the *BRAF*V600E specific inhibitor vemurafenib[75]. Monotherapy with vemurafenib has improved both progression free survival (PFS) and overall survival (OS), however resistance typically develops. Dual pathway inhibition with both vemurafenib and the MEKi trametinib[76,77] can forestall this resistance.

1.5 THE RAS-MAPK AND MULTIPLE MYELOMA

1.5.1 RAS: Mutations, Associations and Clinical Implications

Activating *RAS*^{M}, along with *p53*, *MYC* dysregulation, *Rb* disruption and mutations in DNA mismatch repair (*ATM, ATR*) are amongst the most common molecular mutations in MM[20,78]. As described in other malignancies, recurring sites of mutation involve both *NRAS* and *KRAS* at codons 12, 13 and 61. Interestingly *HRAS*^{M} are exceedingly rare[79]. Several studies have investigated the prevalence of *RAS*^{M} (Table 1.1) with rates quoted from "not observed"[80-82] to 100%[83]. Reasons for these apparent discrepancies include small study cohorts, the use of total bone marrow samples rather than enriching for tumour/plasma cells and the sensitivity of the platform used affecting detection of low variant allele frequency. Additionally, whilst some mutations are rare, not all studies included all known mutations. Further, racial differences have been suggested to affect mutation frequency[84,85]. Although mutations in *RAS* genes are thought to be mutually exclusive[86,87], sub-clonal populations harbouring multiple mutations have been described[78,88].

RAS^{M} operate as secondary oncogenic drivers, rather than initiating mutations[11,20]. Consistent with this, most studies support the absence of *RAS* mutations in MGUS (Table 1). However, two studies have reported *RAS* mutation in single MGUS patients[89,90]. In the first, a patient with MGUS for 14 years is described, prior to identification of an *NRAS*^{M}. At three years follow up the patient had not developed MM, eventually dying from unrelated illness. The second report had no clinical follow up details.

Supporting the theory that *RAS*^{M} operate as secondary oncogenic drivers, memory B-cells have been identified harbouring the same IgH translocations seen in plasma cells from patients with MGUS and MM, however the *KRAS* mutation detected in the same patients' plasma cells was not seen in the memory B-cell compartment[91]. This would suggest the acquisition of *RAS*^{M} leading to the clinical disease.

Endeavouring to recreate the malignant phenotype with *RAS*^{M}, *KRAS*^{92} and *NRAS*^{93} mutation have been introduced into murine germinal centre B-cells and plasma cells. However, in the case of *KRAS*^{M}, off-target Cre effects resulted in lung adenocarcinoma, T-cell lymphoma and sarcoma without evidence of MM. The *NRAS*^{M} model resulted in an accumulation of plasma cells in the peripheral blood and increased immunoglobulins but again not MM.

RAS mutations occur at a higher frequency depending upon the underlying cytogenetic abnormality. It is generally considered that *RAS*^{M} and t(4;14) MM are mutually exclusive given redundancy in pathway activation. Whereas t(11;14) disease is enriched for *RAS*^{M} with rates reported at 37 to 65%[78,87,89,90].

Taken together, these findings support *RAS*^{M} as a secondary oncogenic transforming event, enriched in t(11;14) disease and a potential molecular distinction between MGUS and MM.

The effect and correlation of *RAS*^{M} status on clinical parameters and outcomes has been investigated. The largest study by the Eastern Cooperative Oncology Group (ECOG) evaluated 439 patients with a new diagnosis of MM[89]. *RAS*^{M} correlated with more aggressive disease, specifically a higher bone marrow plasma cell load, higher β2-microglobulin levels, a greater rate of international staging system (ISS) stage II and III and lower haemoglobin levels. Overall, *RAS*^{M} was found to be an independent prognostic variable for OS. Patients with wild-type (WT) *RAS* had an OS of 44.3 months vs 35.5 months for those with *RAS*^{M}. The negative influence of *RAS*^{M} was only borne out by those with *KRAS*^{M}, where survival was worse at 19.9 months compared with 40 months for those with *NRAS*^{M}. In a second study it was similarly found that *KRAS*^{M} was associated with a higher disease burden and poorer OS of 24 months compared with 44 months for WT *KRAS*^{94}. No other group replicated the significant differences in disease or survival findings due to *RAS*^{M}.

NRAS^{M} has been implicated in inferior response and resistance to bortezomib[95]. Those with *NRAS*^{M} were found to have significantly lower response rates compared with WT (7% vs 53%; p=0.0016). This also resulted in shortened time

to progression (TTP) but did not impact on OS. The lack of effect on OS was attributed to *NRAS*^{M} cases being enriched for cyclinD1 overexpression/hyper-diploid cytogenetic subgroups, which typically have a better overall prognosis. Additionally, *NRAS*^{M} disease still responded to high dose dexamethasone salvage and as such OS may have been preserved due to response to subsequent therapies. Patients with *KRAS*^{M} disease have been reported to have significantly lower response rate to melphalan compared with *KRAS* WT (26.9% vs 58.3%; p=0.015)[96].

To better delineate the effects of *RAS*^{M}, both *N* and *KRAS*^{M} have been introduced into IL-6 dependent HMCLs[97-102]. *NRAS*^{M} achieves IL-6 independence, whilst *KRAS*^{M} achieves partial independence. Interestingly, in one case following introduction of RAS^{M} the HMCL acquired resistance to doxorubicin, dexamethasone and melphalan.

STUDY	n	NRAS (%)	KRAS (%)	Total RAS (%)	Comment
Mikulasova[103] 2017	33 MGUS	1 (3)	2 (6)	2 (6)	2 *RAS*^{M} in 1 pt
Mithraprabhu[18] 2017	15 NDMM 33 RRMM	6 (40) 15 (45)	8 (53) 19 (58)	11(73) 22 (67)	3 *BRAF*^{M} RR pts more likely to have multiple mutations 1 RR pt had 17 *RAS*^{M} detected
Xu[104] 2017	103 NDMM 77 RRMM	14 (14) 22 (28)	24 (23) 17 (22)	43 (42) 43 (56)	4 *BRAF*^{M}, 4 both *RAS*^{M} & *BRAF*^{M} 6 *BRAF*^{M}, 4 both *RAS*^{M} & *BRAF*^{M}
Kortum[105] 2016	50 RRMM	13 (26)	16 (32)	29 (58)	9 *BRAF*^{M}, 68% pts resistant to both PI and IMiD
Walker[106] 2015	463 NDMM	90 (19.4)	98 (21)	188 (41)	2% had both *K* & *NRAS*^{M}, 31 (6.7%) *BRAF*^{M} *RAS*^{M} had no impact on prognosis
Lionetti[107] 2015	132 MM 24 pPCL 11 sPCL	35 (27) 1 (4) 4 (36)	48 (33) 4 (17) 2 (18)	73 (55.3) 5 (21) 6 (55)	Total *BRAF*^{M} 20 (12%)
Bolli[108] 2014	67 (51 NDMM)			32 (48)	
Mulligan[95] 2014	133 MM	26 (20)	32 (24)	58 (44)	3 *BRAF*^{M}, no diff. in OS for *N* or *KRAS*^{M}
Mosca[109] 2013	23 pPCL	0	0	0	1 *BRAF*^{M} V600E
Hucthagowder[110] 2012	42 MM	0	4 (9.5)	4 (9.5)	Discovered new 9bp deletion
Walker[87] 2012	22 MM	4 (18)	7 (32)	11 (50)	
Chapman[111] 2011	38 MM	9 (24)	10 (26)	19 (50)	1 *BRAF*^{M} G469A
Chng[89] 2008	439 MM (ECOG) 60 new MM (MAYO) 22 relapsed MM (MAYO)	74 (17)	28 (6)	102 (23) 15 (25) 10 (45)	*KRAS*^{M} assoc. aggressive disease, shorter OS Suggestive of *RAS*^{M} assoc. with late disease

Tiedemann[112] 2008	39 sPCL 41 pPCL			6 (15) 11 (27)	
Intini[113] 2007	81 MM 13 sPCL	12 (15) 2 (15)	4 (5) 0	16 (20) 2 (15)	No significant lab/clinical correlation
Ortega[84] 2006	252 MM	7 (2.8)	46 (18.3)	53 (21)	Suggests lower incidence in Brazilian pts
Martin[82] 2005	13 MGUS 30 MM 1 sPCL	0 0 0	0 0 0	0 0 0	Only screened for *KRAS* 12 and 61 codons.
Rasmussen[90] 2005	20 MGUS 58 MM	1 (5) 7 (12)	0 11 (19)	1 (5) 18 (31)	0/14 t(4;14) pts showed RAS^M
Ng[85] 2003	31 MM 1 sPCL	1 (3)	3 (9)	4 (13)	Suggests lower incidence in Chinese pts
Bezieau[114] 2001	8 MGUS/SMM 33 MM 11 relapsed MM 10 pPCL	1 (12.5) 7/30 (23) 4/10 (40) 3 (30)	0 18 (54.5) 6 (54.5) 3 (30)	1 (12.5) (54.5) (81) 6 (60)	No data on whether mut pt MGUS or SMM Incomplete data due to insufficient samples
Kalakonda[83] 2001	34 MM	34 (100) 1 (3)		34 (100)	All pts had varying clonal freq. of $NRAS^M$
Liu[94] 1996	139 MM	40/129 (31)	23/139 (16.5)		Different denominators due to test protocol $KRAS^M$ significantly affects OS
Millar[80] 1995	18 MM	0	0	0	
Yasuga[81] 1995	45 MM	2 (4.4)	0	2 (4.4)	Only screened for *NRAS* 12 and 61 codons.
Corradini[115] 1993	30 MGUS 77 MM 8 Plasmacytoma 13 sPCL	0 2 (2.5) 0 4 (31)	0 5 (6.5) 0 0	0 7 (9) 0 4 (31)	
Portier[116] 1992	30 MM			14 (47)	

Tanaka[117] 1992	10 MM	5 (50)		5 (50)	
Matozaki[118] 1991	12 MM 3 Plasmacytoma	3 (25) 1 (33)		3 (25) 1 (33)	
Paquette[119] 1990	17 MM	2 (12)	0	2 (12)	
Neri[88] 1989	43 MM	11 (26)	2 (5)	13 (30)	2 pts had 2 muts. 1 pt had 3 muts.

Table 1: Summary of publications describing RAS mutations in MM MGUS-monoclonal gammopathy of undetermined significance, SMM-smouldering myeloma, MM-multiple myeloma, sPCL-secondary plasma cell leukaemia, pPCL-primary plasma cell leukaemia, OS-overall survival, pts-patient, muts-mutations

Whilst the in-vitro effects of introduced *RAS*^{M} echo some of the reported clinical pharmacologic resistance, given the frequency of *RAS*^{M} and the general good responses to initial therapy, it is difficult to believe that *RAS*^{M} alone confers this resistance.

1.5.2 Targeting RAS

To date the most frequently used approach to inhibition of RAS signalling in MM and in other malignancies[29], has been to target post-transcription modifications, specifically prenylation[120]. Three main approaches have been adopted: the first with farnesyltransferase inhibitors (FTi)[121], the second and third methods lead to substrate "starvation" through inhibition of the mevalonate pathway as a source of FPP with HMG-CoA-Reductase inhibitors[122] with either "statins" or bisphosphonates[123].

As mono-therapy the FTis R115777 (tipifarnib), manumycin and FTI-277 have all been shown to inhibition proliferation and induce apoptosis in both HMCLs and primary patient samples[124-128]. The studies conflict on the role of *RAS*^{M} affecting response. In primary patient samples the effect in both studies was independent of *RAS*^{M} [124,125]. Given several other cellular proteins are prenylated the effects of FTis are unlikely to be due solely to RAS processing[129].

In combination with icandronate (a bisphosphonate)[130], PD184352 (MEKi) and UCN-01 (CHK-1 inhibitor)[131], GGTase inhibitors and lovastatin (HMG-CoA-reductase inhibitor)[132] and bortezomib (proteasome inhibitor)[133], FTis have shown synergistic cytotoxicity. *RAS*^{M} status exerted no influence on the synergism. The addition of IL-6 or FGF-1 did not reduce either the inhibition of proliferation or apoptosis, suggesting the bone marrow micro-environment (BMME) might not afford protection against these effects.

Unfortunately, the in vitro promise of these agents has failed to translate successfully into the clinic. Two clinical trials have evaluated the use of tipifarnib in MM. The first, a phase II trial of 43 patients with relapsed/refractory (R/R) MM, with a median of four prior lines of therapy[134]. After two cycles of treatment, a

third of patients had progressed, whilst the remainder had stable disease (SD) as the best response. No patient achieved a partial response (PR). Correlative protein studies showed that whilst tipifarnib did indeed inhibit protein prenylation this was seen in several other proteins as well, not simply RAS. Further, decreased levels of phosphorylated AKT and STAT3, downstream of RAS were seen, however no change in phosphorylated ERK suggesting its effect was not mediated through inhibition of the MAPK. *RAS*^{M} status did not correlate with response to therapy. The second study investigated tipifarnib in a range of haematologic malignancies (CML, MDS and MM)[135]. Considering only those with MM, no patient achieved better than SD. These studies do not support the use of tipifarnib as monotherapy in MM and leave the role of *RAS*^{M} conferring sensitivity to prenylation inhibitors doubtful.

HMG-CoA-reductase inhibitors ("statins") have been investigated as single agents and in combination in HMCLs and primary patient samples. As mono-therapy and in combination with melphalan, dexamethasone, UCN-01, thalidomide, lenalidomide or bisphosphonates, statins can inhibit proliferation and induce apoptosis[122,136-141]. Their effect on prenylation of RAS has been confirmed through demonstration of loss of RAS at the cell membrane, loss of RAS phosphorylation and loss of ERK1/2 phosphorylation[122]. Following treatment, cells can be partly rescued by supplementation with FPP and completely rescued with either mevalonate or GGPP. The addition of simvastatin to either melphalan or dexamethasone lead to synergistic apoptosis[142].

A small number of clinical studies using statins have been undertaken, with conflicting results. The largest of these compared thalidomide and dexamethasone with or without lovastatin in patients with R/R MM[143]. Dosing of lovastatin was high at 2mg/kg days 1 to 5 and 8 to 12, followed by 0.5mg/kg days 15 through 28, well in excess of doses used for treatment of elevated cholesterol. Overall response rates (ORR) of PR or better were higher in the lovastatin group (44% vs 32%). Complete response (CR) and near complete response (nCR) rates were also higher (11% vs 5%). Both PFS and OS were longer (28.5 months vs 6 months; p=0.048, and 47.5 months vs 36.5 months; p=0.07). No data on *RAS*^{M} status were available.

The role of simvastatin to overcome apparent drug resistance was investigated in six patients with R/R MM all of whom had previously undergone autologous stem cell transplant (ASCT)[138]. Patients were treated with either bortezomib or bendamustine monotherapy. If after two cycles of therapy a PR was not achieved this was considered drug resistance and simvastatin 80mg daily was added for a planned two further cycles. The study was ceased after a total of four cycles. Four of the six patients had progressive disease after the first two cycles of therapy, whilst two had minor responses (MR). Following the addition of simvastatin five of the six patients had a reduction in paraprotein levels, none of which were clinically significant. Unfortunately, only historic controls were used, raising the possibility that on-going treatment was actually sufficient to achieve a response as opposed to the addition of simvastatin. Again, no comment was made on *RAS*^{M} status.

The role of simvastatin at 15mg/kg days 1-7 (a previously validated dosing schedule[144]) added to the combined chemotherapy regimen VAD (vincristine, doxorubicin, dexamethasone) has been investigated in 12 patients[145]. All patients had received two prior lines of therapy. A single patient achieved a PR, six had SD, the remaining five all progressed. The study was terminated early due to non-efficacy.

The effect of simvastatin on bone turnover markers in heavily pre-treated MM has been investigated[146]. In six patients, simvastatin was dosed at 15mg/kg in divided doses for seven days followed by a 21-day break. All patients had previously been treated with bisphosphonates, including two who were concurrently treated. Unsurprisingly, gastrointestinal (GI) side effects occurred in all six patients. Paradoxically, bone turnover markers increased during the period of simvastatin administration. No improvement in disease assessment was observed.

The pre-clinical potential of statins has failed to translate to clinical benefit. Whilst these patients were all pre-treated and no stratification with respect to *RAS*^{M} status was made, it is unlikely statins will find a place in the treatment of MM.

1.5.3 RAF: Expression, Mutations, Modifications and Clinical Implications

Overexpression of all RAF isoforms has been demonstrated in both HMCLs and primary patients' samples of MM, but not in MGUS[147]. The activity of RAF overexpression was confirmed, with the majority of HMCLs and patient samples showing both MEK and ERK phosphorylation. This could be inhibited either pharmacologically or with pan-RAF RNA-interference. Interestingly, RAF inhibition also resulted in abrogation of PI3K pathway activity, showing functional pathway cross-talk downstream of RAS.

Activating mutations in *RAF*, in contrast to *RAS*, are relatively uncommon at approximately 4-6%[87,111,148-150]. The only isoform found to be mutated in MM is *BRAF*. As in other malignancy, the most common mutation observed is the activating V600E[111,150]. Although much rarer, other activating mutations have been described[111,148]. Curiously, a rare mutation, G594N[148], has impaired kinase activity. What its true effects are on tumour genesis and progression are doubtful, but it is thought to act in concert with RAS^{M}.

Activating mutations in *BRAF* are thought to be mutually exclusive with *RAS*[78,87,111]. Similar to RAS^{M}, $BRAF^{M}$ are more frequently observed in t(11;14) MM[87]. Similar to *RAS*, RAF^{M} have not been observed in MGUS.

A unique mechanism of enhanced RAF kinase activity without mutation is through inactivation of the negative modulator "Raf-1 kinase inhibitor protein (RKIP)[151]. Whilst RKIP has been shown to be overexpressed in MM (in 20 patients samples and three HMCLs), it is maintained predominantly in its inactive phosphorylated state, leaving CRAF activity unopposed and as such effectively "up-regulated".

Similarly, a rare novel mechanism of RAF kinase activation by gene rearrangement/gene-fusion has been described (in 4 of 958 cases analysed)[152]. Again, this form of activation was mutually exclusive to clonal RAS^{M} RAF^{M}.

Clinically, *RAF* mutations occur late, signify a shift towards aggressive, frequently extra-medullary disease and portend a poor prognosis. In a case series of 379

MM patients, seven (2.8%) had a *BRAF*^{M}V600E mutation[150]. Four of those seven (57%) developed extra-medullary disease, as compared with only 17% of those with WT *BRAF*. OS was shorter for those with *BRAF*^{M} compared to those without (45 months vs 105; p=0.04). In that series a single patient was treated with the specific *BRAF*^{M}V600E inhibitor, vemurafenib.

Counter to those findings, a series of 209 MM patients, identified 11 (5.3%) with de novo *BRAF*^{M}V600E[149]. Timing of detection (whether new diagnosis or at relapse) was not reported. Not only did they report good response to broad agent therapy, but no adverse impact with respect to either PFS or OS was seen.

1.5.4 Targeting RAF

The use of RAF inhibitors in MM is limited to small phase I/II studies and a limited number of case reports.

Sorafenib (BAY43-9006) is a multi-targeted small molecule inhibitor of both receptor and non-receptor tyrosine kinases including vascular endothelial growth factor receptor (VEGFR), platelet derived growth factor receptor (PDGFR) and both B and CRAF irrespective of mutation status[153].

Given sorafenib's wide spectrum of targets it is unsurprising that it's effects are a modulated through a variety of cellular mechanisms. Two groups have shown sorafenib attenuated phosphorylation of AKT, STAT3 and MCL-1 in response to IL-6 and VEGF stimulation[154,155]. Similarly, consistent with RAF inhibition, there was a reduction in phosphorylated ERK. In both HMCLs and primary patient samples sorafenib induced apoptosis in both a caspase-dependent and independent manner. Sorafenib is effective against bortezomib resistant HMCLs and shows synergy with both bortezomib and dexamethasone. Treatment in combination with rapamycin results in synergistic cytotoxicity. In a xenograft mouse model of MM, sorafenib has been shown to reduce marrow homing[156].

There are three reported phase I/II clinical trials with sorafenib. The largest, a phase II trial of 11 patients with R/R MM, used single agent sorafenib[157]. A single

patient completed the intended 13 cycles, achieving a PR sustained for 24 months. One patient maintained SD, whilst the remainder all progressed. Median PFS was short at only 2.6 months. As seen in solid malignancy, rash correlated with sorafenib efficacy, the patient who achieved a PR experienced a grade 2 rash. No data were available regarding either *RAS*^{M} or *RAF*^{M} status. Another pilot study of three MM patients treated with single agent sorafenib resulted in SD in all three for durations of 2, 8 and 36 months.

A phase I study of sorafenib in combination with bortezomib has been used in a range of advanced malignancies including one patient with MM[158]. Following one cycle of therapy, SD was maintained. A phase I/II study of sorafenib and everolimus (NCT00474929) in patients with RR lymphoma or MM is on-going. Preliminary results are not yet available.

Similar to sorafenib, a novel multi-kinase inhibitor regorafenib has been tested in HMCLs and murine xenografts[159]. Regorafenib has a broad range of targets including VEGFR1-3, PDGFRβ, cKIT, RET, FGFR and RAF[160]. It is already FDA approved for use in metastatic CRC and inoperable gastrointestinal stromal tumours (GIST). In HMCLs regorafenib exhibited myriad actions including inhibition of proliferation, osteoclastogenesis, VEGF-induced microtubule formation, migration and in combination with dexamethasone and carfilzomib showed synergistic cytotoxicity. In a murine xenograft, tumour growth was delayed but did not significantly prolong survival. These effects are unsurprising given the broad range of targets of regorafenib.

There are burgeoning numbers of case reports describing the *BRAF*^{M}V600E in patients with multiply relapsed MM[150,161-163]. Typically, these are reported in patients with late stage disease, extra-medullary presentations and an aggressive phenotype. Most report vemurafenib achieving rapid but short-duration disease control. In two cases, there was sustained disease control beyond six months. One of these employed a discontinuous dosing strategy to forestall resistance[164]. However, a de novo *NRAS*^{M} arose resulting in loss of disease control at 10 months. Vemurafenib was ceased, disease control regained

through bortezomib with subsequent vemurafenib retreatment in combination employed.

A single case reports the use of combination *BRAF*^{M}V600E inhibition and MEK inhibition with cobimetinib (as is the practice in metastatic melanoma) in a heavily pre-treated patient with R/R MM[162]. A rapid disease response to a very good partial response (VGPR) was reported but follow up was limited to only three months.

These limited studies suggest there may be a small percentage of patients who may have an additional treatment option. Despite the success of vemurafenib in the first case report, it would appear unlikely that monotherapy will maintain extended disease control and that combinations may prove more effective.

1.5.5 MEK: Modulator & Clinical Implications

MEK mutations have not been described in MM. However, "cross-talk" from other signalling pathways, including HSP90[165], NFκB via TPL2[166], CKS1β[167] and AKT[168], as well as activating mutations of up-stream kinases all result in increased signalling via MEK and consequent ERK activation. As such MEK serves as convergence point and potentially an ideal target for inhibition.

As MEK is the only known activator of ERK, inhibition of MEK has provided insight into specific targets of ERK in MM. MAF is a transcription factor downstream of ERK, whose main target in MM has been identified as cyclin D2[169]. MAF plays a role in adherence to the marrow microenvironment and increased marrow expression of VEGF. MAF's overexpression occurs in both t(14;16) and t(4;14) MMs. In t(14;16) the IgH enhancer directly drives MAF transcription through regulatory elements. However, in t(4;14) the mechanism of MAF overexpression is not fully elucidated[170]. MAF overexpression portends a poor prognosis.

Inhibition of MEK with UO126, results in down regulation of the AP1 complex as well as MAF. In a study of 16 HMCLs treated with UO126, 10 responded, nine of which overexpressed MAF, suggesting MAF may be a biomarker for sensitivity

to MEK inhibition[170]. Demonstrating a further interaction between MEK and MAF, two groups have shown that MEK, through phosphorylation of GSK, results in MAF phosphorylation and stabilisation[171,172].

MM cells stimulate osteoclast maturation and activation through MAPK driven expression of MIP1α[173]. Again, MEK inhibition with UO126 resulted in loss of MIP1α and a reduced osteoclast formation[174]. Similarly, MEK inhibition with selumetinib inhibited osteoclast formation, and release of the survival factors B-cell activating factor (BAFF), a proliferation inducing ligand (APRIL), and MIP1α from osteoclasts themselves. This is further evidence of the role of the MAPK and the pathologic presentations of MM[175].

1.5.6 Targeting MEK

Several pre-clinical studies evaluating MEK inhibition in combination with traditional and novel agents have been undertaken. The early "laboratory" MEK inhibitors UO126 and PD098059 were unsuitable for clinical use due to their side effect profiles. Several clinically suitable compounds have since been developed.

UO126 has been investigated in combination with inhibitors of AKT[168,176] and STAT3[177]. In each instance the combination was synergistic and either inhibited proliferation or induced apoptosis.

PD098059 has been used in combination with the Checkpoint 1 (CHK1) inhibitor UCN-01[178,179]. UCN-01 on its own resulted in up-regulation of phosphorylated ERK, whilst in combination with either MEKi PD098059 or PD184352 there was enhanced apoptosis. Neither IL-6 nor FGF-1 limited apoptosis. Similarly, highlighting the role of combination therapy, PD098059 in combination with siRNA against STAT3 generated apoptosis not seen with either therapy alone[180]. This combination also overcame the protective effects of marrow stromal cells.

In combination with arsenic trioxide (ATO), MEK inhibition resulted in synergistic apoptosis in HMCLs and primary patient samples[181]. MEK inhibition alone resulted in up-regulation of BIM (a BH3 only pro-apoptotic protein) whilst ATO

down-regulated MCL-1 (a critical anti-apoptotic protein in MM), together enhancing PARP and caspase cleavage resulting in marked apoptosis. This combination appeared successful in both *p53* WT and mutant HMCLs, suggesting potential efficacy at later stages of disease.

The novel MEK1/2 inhibitor selumetinib (AZD6244) has demonstrated efficacy in HMCLs, primary patient samples and a murine model of MM[182]. In combination with dexamethasone, bortezomib, lenalidomide and perifosine it is synergistic. Similar to other MEKi, selumetinib also inhibits osteoclastogenesis.

The MEK inhibitor trametinib (GSK1120212) in combination with the AKT inhibitor afuresertib (GSK2110183) has been evaluated in both solid tumours and MM (ClinicalTrials.gov NCT01476137)[183]. Unfortunately, the combination was poorly tolerated, and SD was reported as the best response.

A phase II study of selumetinib monotherapy has been reported in 36 heavily pre-treated (median prior lines 5, range 2-11) patients with MM (ClinicalTrials.gov NCT01085214)[184]. Whilst the single agent was well tolerated, efficacy was poor with ORR of 5% and median response duration of <5 months.

A retrospective case series of 58 patients has shown the potential of trametinib in patients with R/R MM[185]. Fifty-one patients had activating mutations in either *RAS* or *RAF*, the remaining seven had gene expression profiles (GEP) consistent with MAPK pathway activation. In patients with biochemically measureable disease 16 of 40 (40%) achieved a PR or better. Twelve of these were in combination with other agents, most frequently pomalidomide or combination chemotherapy. On the back of these results, the authors have launched a prospective trial of trametinib in R/R MM.
These clinical data, along with the in-vitro studies, suggest that combination therapy will be required to maximise response to MEK inhibition. Careful selection of the partner agent is clearly required.

1.5.7 ERK

ERK mutations have not been described in MM. However, given the frequency of mutation of up-stream kinases and as the terminal kinase in MAPK pathway ERK is an attractive molecular target.

Analysis of relative levels of phosphorylated ERK by IHC (high, low or absent), in multivariate models with existing prognostic data, has identified phosphorylated ERK as an independent negative prognostic marker[186]. Whilst this is not equivalent to mutation, it is representative of MAPK pathway activation, and implies this activity as an adverse prognostic maker.

1.5.8 Targeting ERK

Inhibiting ERK and its interactions is limited to laboratory studies, with no clinical data.

The antimalarial artesunate has been shown to reduce VEGF expression in MM, as well as reduce levels of phosphorylated ERK in a RAS^{M} HMCL (RPMI-8226)[187]. In doing so artesunate reduced angiogenesis, migration and inhibited proliferation in a dose dependent manner.

A novel approach to ERK inhibition is targeting of the scaffold protein IQGAP. IQGAP overexpression has been demonstrated in both HMCLs and primary patient samples. Knockdown of IQGAP with shRNA resulted in reduced phosphorylated ERK and reduced proliferation[188]. The flavonoid, quercetin, recapitulated these findings, reducing IQGAP mRNA, phosphorylated ERK and proliferation[189]. This effect was observed in both HMCLs and primary patient samples. The effect of quercetin appears specific to the MAPK with no evidence of inhibition of AKT, STAT3, p38 or JNK pathways. A protein mimetic that interferes with the ERK/IQGAP interaction produces similar results[190].

1.6 RESISTANCE

Targeted kinase inhibitors are not a standard part of care in MM. As such there are no data regarding resistance mechanisms specific to MM. However, they are used in solid malignancies most notably *BRAF*^{M}V600E mutant melanoma. Molecularly MM has extensive clonal, spatial and temporal heterogeneity akin to that of solid malignancies and as such mechanisms of resistance to targeted therapies may well prove similar[78].

There are many and varied mechanisms by which tumours circumvent targeted therapy. Whilst prolonged exposure to therapy in vitro can generate resistant cell lines it is difficult to characterise a specific mechanism(s) belying this. Further, the influences and interactions of the micro-environment (cytokines, growth factors and immune effectors) are difficult to account for in vitro.

1.6.1 Resistance to RAF Inhibition

Despite the initial clinical success of targeted inhibition of the *BRAF*^{M}V600E in metastatic melanoma[191], resistance almost invariably develops, resulting in disease relapse and progression. Combination therapy with additional kinase inhibitors became standard and whilst this lead to further modest improvements in survival, again resistance emerges[76]. In addition to acquired resistance, not all patients are initially sensitive to targeted inhibition despite the presence of the *BRAF*^{M}V600E. The nature and causes of both initial and acquired resistance have been extensively investigated.

Upfront resistance to vemurafenib has been investigated by parallel whole exome sequencing (WES) of patients with primary refractory disease. This has identified gain of function in the oncogene RAC1 and loss of function in the transcription factor HOXD8 as causes of both upfront and acquired resistance to vemurafenib[192].

RAF signalling requires homo- or hetero-dimerization for signal propagation. However, *BRAF*^{M}V600E functions as a monomer, without requisite activation by RAS. As ERK is fully activated by this mechanism normal feedback inhibition is

present (Figure 1.2). This feedback inhibition is lost within 24 hours of vemurafenib mono-therapy resulting in restoration of ligand-receptor mediated RAS signalling[193]. This results in vemurafenib insensitive CRAF homodimers forming, recovery of normal MAPK signal propagation and reactivation of ERK. The addition of MEK inhibition to vemurafenib is able to maintain MAPK pathway inactivity[76,77].

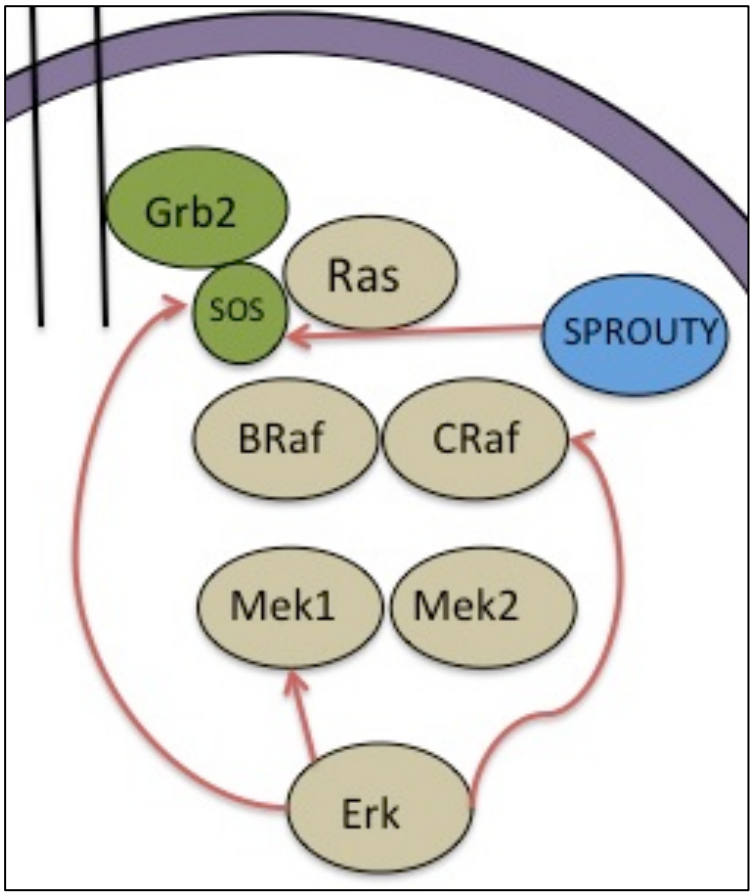

Figure 1.2: Negative feedback loops of the RAS-MAPK

An unusual mechanism of loss of efficacy of vemurafenib occurs when WT *RAF* is bound by drug. This leads to RAF activation via "conformational priming"[194] and trans-activation of RAF dimer partners[195] restoring MAPK signalling. These two mechanisms of resistance demonstrate that even in the absence of further mutations, normal cellular processes can lead to drug failure.

Acquired resistance to *RAF*^{M} inhibition can occur either upstream or downstream of RAF and intrinsically within RAF itself. Upstream of RAF, up-regulation of RTK

signalling (e.g. PDGFRβ)[196] and mutational activation of *N* and *KRAS* signalling[192] via WT *RAF* overcome inhibition.

Intrinsic changes to *BRAF*^{M}V600E have been implicated in acquired resistance. WES has identified mutant amplification of between 2- and 14-fold as sufficient to overcome targeted inhibition[197]. Splice variants of the *BRAF*^{M}V600E have been identified, whereby the RBD is lost allowing *BRAF*^{M} dimers to form even in the presence of inhibitor[198].

Downstream of *RAF*, activating mutations of *MEK1*[199] and *MEK2*[192] have been described. These mutations confer resistance to both RAF and MEK inhibition. Signalling from other kinase pathways via COT/TPL2[200] to MEK also leads to resistance downstream of RAF.

Addressing the development of resistance remains a challenge clinically. There are no rapid investigations available to guide changes in therapy. Increasing the dose of vemurafenib may be beneficial where mutant gene amplification is present, however this is likely to provide only short-term benefit. The addition of MEK inhibition can overcome modest *BRAF*^{M} amplification (of less than 15-fold amplification[201]), mutant splice variants, reactivation of MAPK signalling via loss of feedback inhibition and up-regulation of upstream receptors/kinases. Whilst the addition of MEK inhibition is employed clinically, the PFS and OS benefit is marginal at approximately three months.

An interesting approach to forestalling resistance is the use of a discontinuous dosing strategy. In a melanoma murine xenograft model, mice were treated with either continuous vemurafenib or a “4 weeks on, 2 weeks off” schedule[202]. After 100 days of treatment, mice on the continuous dosing regimen had all developed resistance, whilst no mouse on the discontinuous dosing schedule had developed resistance out to day 200. The dynamics of targeted therapy are clearly complex as some of the tumours that had become resistant demonstrated regression once vemurafenib was ceased suggesting tumour dependence upon vemurafenib. Currently vemurafenib is dosed continuously.

1.6.2 Resistance to MEK inhibition

There are fewer data investigating mechanisms of MEKi resistance than RAF inhibition.

Upstream of MEK, *KRAS* gene amplification results in MEKi resistance[203]. A threshold of 30 copies is sufficient to overcome inhibition.

Similar to targeted RAF inhibition, MEK inhibition leads to loss of negative feedback loops, resulting in pathway reactivation. In the presence of inhibitor, this reactivation causes the accumulation of phosphorylated MEK[204,205]. MEK inhibitor affinity for phosphorylated MEK is approximately one twentieth that for the un-phosphorylated form[206,207]. This results in drug dissociation and reactivation of ERK. As ERK negative feedback only inhibits MEK1, MEK2 effectively escapes inhibition.

Sequencing of *MEK* after acquired resistance to MEK inhibition in breast cancer cell lines, CRC cell lines and primary melanoma patient samples has revealed point mutations in the allosteric drug-binding pocket[208]. These mutations confer resistance to MEK inhibition and RAF inhibition, but in some instances lead to constitutive MEK activation[203,209].

Activation of alternative signalling pathways including overexpression and mutation in the PI3K/AKT pathway in NSCLC lines[210,211], and active WNT signalling even in the presence of $KRAS^{M}$ in CRC cell lines confers resistance to MEK inhibition upfront[212].

Genes signatures have been developed determining both sensitivity and resistance to MEK inhibition in melanoma cell lines[213]. The resistant gene signature is enriched for RAS effectors, which may effectively bypass inhibition.

1.7 CONCLUSION

Aberrant signalling through the RAS-MAPK pathway is frequently encountered in up to 70% of MM cases. Mutations in *KRAS* may impact on prognosis and

survival, whilst mutations in *RAF* heralds a more aggressive disease course. The pathway provides several potential drug targets using both novel inhibitors and several already clinically available. It is increasingly apparent, despite the initial promise in pre-clinical and cell lines studies, that targeted inhibition with monotherapy is destined to fail due to myriad mechanisms of both upfront and acquired resistance. Careful dosing strategies and combination therapy will likely be required to take maximal advantage of targeted therapy to counter resistance and improve patient outcomes.

The work described in this thesis investigates the use of MEK inhibition in MM. Targeted inhibitors or both RAS and RAF are also investigated. However, the specificity of the RAS inhibitor could not be confirmed, and the efficacy of the RAF inhibitors employed (chapter 3) is poor. Further, pragmatically the MEK inhibitor employed is already in use clinically, and as such is the focus of this body of work.

2. MATERIALS & METHODS

2.1 CELL LINES AND NORMAL CD138+ CELLS

2.1.1 Human Myeloma Cell Lines

MM1s, RPMI 8226, NCI H929, and U266 were obtained from the American Type Culture Collection (ATCC) (Manassas, Virginia, USA). Cell line validation was performed by the ATCC using short tandem repeat analysis. LP1, OPM2 and JJN3 were obtained from Deutsche SammLung von Mikroorganisemen and Zellkulturen (Branschweig, Germany). These cell lines were authenticated by the supplier using cytogenetics, DNA typing, immuno-phenotyping and cell line speciation. XG1 and ANBL6 were kind gifts from the Winthrop P Rockefeller Cancer Institute (Little Rock Arkansas, USA). KMS11, KMS12BM, KMS26, KMS34 and KMS28BM were kind gifts from Dr Takemi Otsuki of Kawasaki Medical School (Okayama, Japan). JIM1 was a kind gift from the Walter and Eliza Hall Institute (WEHI) (Melbourne, Australia). Cell lines were screened every three to six months for mycoplasma contamination using the VenorGeM Mycoplasma Detection Kit.

2.1.2 Normal CD138+ Cells

CD138+ plasma cells were obtained from healthy bone marrow donors with written and informed consent approval from the Alfred Hospital Research and Ethics committee. Bone marrow mononuclear cells (BMMC) were isolated with Ficoll-Paque Plus (Amersham Biosciences, Rydalmere, NSW, Australia), and washed with PBS. Red blood cells were lysed with NH_4Cl solution (8.29g/L ammonium chloride, 0.037g/L EDTA, 1g/L potassium bicarbonate) and washed with PBS again. Plasma cell percentage was quantified by CD45 and CD38 staining by flow cytometry.

2.2 CULTURE CONDITIONS

HMCLs were cultured in complete RPMI-1640 consisting of RPMI-1640 media (Gibco Invitrogen) supplemented with 10% heat inactivated foetal bovine serum

(FBS, Lonza Biowhittaker, Mt Waverly, Victoria, Australia), and 2mM L-glutamine (Gibco Invitrogen), in a humidified incubator at 37^{o}C with 5% CO_2.

Unless otherwise specified all experiments were performed using the same culture media and conditions.

IL-6 dependent HMCLs (ANBL6 and XG1) were cultured with 2-5ng/mL IL-6 as required.

All HMCLs were passaged 24 hours prior to experimental setup to ensure high viability (>85%) and consistent cycling.

2.3 CELL-BASED ASSAYS

2.3.1 Cell Viability Assays

Initial screening of MAPK inhibitor compounds was performed using the Promega CellTiter-Glo ® Luminescent Cell Viability Assay (Promega, Madison, Wisconsin, USA). Cells were plated in black 96-well plates at a density of $2x10^5$ cells/100µL/well with and without drug exposure for 24 and 72 hours. Plates were brought to room temperature prior to the addition of 100µL CellTiter-Glo® reagent (reconstituted as per manufacturer's instructions). Plates were incubated at room temperature for 10 minutes. Luminescence was measured using a FLUOstar OPTIMA (BMG Labtech, Mornington, Victoria, Australia). Each reaction was performed in triplicate. Results were expressed as a percentage ratio compared to untreated samples.

2.3.2 Cell Proliferation Assays

Proliferation of HMCLs with and without drug exposure was measured using trypan blue staining and haemocytometer count. Cells were seeded at $2x10^5$cells/mL in 10% FBS RPMI-1640, and counted at 24, 48 and 72-hour time points.

2.4 FLOW CYTOMETRY

2.4.1 Flow Cytometry Reagents

Antibody	Conjugate	Specificity	Cat. No.	Supplier
CXCR-3	FITC	C-X-C motif chemokine receptor 3	FAB160F-100	R&D Systems
IgG1κ	FITC	Mouse IgG1κ isotype control	555748	BD Pharmingen

Table 2.1: Flow cytometry antibodies. R&D Systems (Minneapolis, USA), BD Pharmingen (San Diego, California, USA)

2.4.2 Analysis of Cell Death in HMCLs

HMCLs were plated at $2x10^5$ cells/mL with specified treatments and harvested at specific time points. Cells were washed in annexin buffer and centrifuged at 1400RPM for 5 minutes at 4°C, and the supernatant discarded. The wash was repeated. Cells were then re-suspended in 62.5ng/mL propidium iodide (PI) in annexin buffer. Samples were immediately acquired by FACS. Analysed data represents the proportion of dead cells minus the untreated (UT) background proportion of cell death specific to that experiment. For drug combination studies interrogating synergy, Calcusyn (Ver 1) was used.

2.4.3 Analysis of Cell Cycling

HMCLs were plated at $2x10^5$ cells/mL with specified treatments and harvested at 24 hours. Cells were washed in PBS at 4°C, centrifuged at 1400RPM for 5 minutes at 4°C, and the supernatant discarded. The wash was repeated. Cells were re-suspended in 100µL of PBS at 4°C, then fixed in 1mL of 70% ethanol at -20°C and stored for a minimum of 30 minutes. Cells were washed again in 9mL of PBS at 4°C, centrifuged at 1600RPM for 10 minutes at 4°C with a slow brake, and the supernatant discarded. Cells were re-suspended in 300µL of neat RNase/PI solution (20mg/mL propidium iodide and 0.5µg RNase) (BD Biosciences, Franklin Lakes, New Jersey, USA) and incubated for 15 minutes in

the dark at room temperature. 10,000 events were collected for each sample with an event rate maintained at less than 150/second.

2.4.4 Surface Staining

Harvested cells were washed with PBS at 4°C, then re-suspended in FACS buffer (PBS, 1%FBS). Antibodies were then added to the cell suspension in pre-determined concentration (1:50 to 1:200) and incubated for 30 minutes in the dark at 4°C. Cells were washed again with PBS at 4°C, re-suspended in FACS buffer and immediately acquired on a flow cytometer. Isotype controls were used for all experiments.

2.4.5 Intracellular Staining

Cells were collected and washed in cold PBS, centrifuged at 1200RPM 4°C for 5 minutes and the supernatant discarded. Cells were re-suspended in cold PBS to $2x10^6$ cells/mL, which was then diluted 1:1 with 4% PFA in PBS to a final concentration of $1x10^6$ cells/mL in 2% PFA in PBS. This was incubated on ice for 15 minutes before cells were again washed in PBS, centrifuged at 1200RPM at 4°C for 5 minutes and the supernatant discarded.

2.4.6 Acquisition & Analysis

All flow cytometry samples were acquired on a FACSCalibur (BD) with Cell Quest software (BD) immediately after sample preparation. All analysis of flow cytometric data was performed using FlowJo v10.1 (Treestar, Ashland, Oregon, USA).

2.5 PROTEIN ANALYSIS BY WESTERN BLOTTING

2.5.1 Protein Lysates

Protein lysates were made using the Mammalian Protein Extraction Reagent lysis buffer (M-PER, ThermoFisher Scientific, Scoresby, Victoria, Australia) and protease inhibitor cocktails (Roche, Castle Hill, New South Wales, Australia). Samples were incubated on ice for 10-20 minutes then centrifuged at 10,000RPM for 10 minutes. The supernatant was collected and mixed with 4x-Laemmli buffer

(4% SDS, 20% glycerol, 10% β-mercaptoethanol, 1mM EDTA and bromophenol blue).

For detection of phosphorylated proteins, phosphatase inhibitor cocktail (Roche) was added to lysis buffer.

2.5.2 Cell Cytoplasmic & Nuclear Fractionation

For cell fractionation the NE-PER Nuclear and Cytoplasmic Extraction Reagents kit (ThermoFisher Scientific) was used as per manufacturer's instructions.

2.5.3 Protein Quantitation

Protein quantitation was performed using the Bio-Rad DC protein assay (Bio-Rad, Gladesville, New South Wales, Australia) as per the manufacturer's instructions using BSA in M-PER lysis buffer to generate a standard curve.

2.5.4 Protein Gel Electrophoresis & Blotting

For whole cell lysates 25-100μg of protein lysate was separated by SDS-PAGE (polyacrylamide gel electrophoresis). The gel percentage density was determined according to the MW of the protein being studied, between 7.5% and 15%. This was then blotted onto polyvinylidene fluoride (PVDF) (Immobilon-P) membranes using the Bio-Rad TransBlot Semi-Dry Transfer Cell.

For cytoplasmic/nuclear lysates 20-50μg of protein lysate was separated by SDS-PAGE. Gel percentage density was determined according to the MW of the protein being studied, between 7.5% and 15%. This was then blotted onto PVDF (Immobilon-P) membranes using the Bio-Rad TransBlot Semi-Dry Transfer Cell.

Membranes were blocked with either 5% BSA or skim milk powder in 0.1% Tween-20/Tris buffered saline (TBS) for 60 minutes at room temperature. Membranes were then incubated with primary antibodies (in 5% BSA, Tween-20/TBS) overnight at 4^{o}C. Blots were then washed three times for 15 minutes in 0.1% Tween-20/TBS at room temperature prior to being incubated with a secondary horseradish peroxidase (HRP) tagged antibody (in 5% skim milk

powder in 0.1% Tween-20/TBS) for 1-2 hours at room temperature. Membranes were washed again as above.

2.5.5 Western Blot Primary & Secondary Antibodies

Antibody	Specificity	Cat. No.	Supplier
BCL-2	B-cell Lymphoma 2	2872S	CST
P-BCL-2	Phospho-B-cell Lymphoma 2 (S70)	2827S	CST
CK2α	Casein Kinase 2α	2656S	CST
Cyclin B	Cyclin B	4135S	CST
DNMT3b	DNA Methyl Transferase 3β	67259S	CST
ERK 1/2	ERK 1/2	9102S	CST
P-ERK	Phospho-ERK 1/2 (T202/Y204)	9101S	CST
FGFR3	Fibroblast Growth Factor Receptor 3	4574S	CST
H3K36Me2	Di-Methyl Histone 3 Lysine 36	2901S	CST
H3K27Me3	Tri-Methyl Histone 3 Lysine 27	9733S	CST
LXN	Latexin	154744	Abcam
p27	Cyclin Dependent Kinase Inhibitor 1B	3686S	CST
SLC47A	Solute Carrier Family 47 Member 1	14550S	CST
α-Tubulin	α-Tubulin	T9026	Sigma Aldrich
β-Actin-HRP	β-Actin	12262S	CST
HDAC1	Histone Deacetylase 1	53091	Abcam
TBP	TATA Binding Protein	51841	Abcam
Swine anti-rabbit Ig HRP	Rabbit Ig	P0217	Dako
Rabbit anti-mouse Ig HRP	Mouse Ig	P0260	Dako

Table 2.2: Primary and secondary antibodies used for western blotting.

Abcam (Melbourne, Victoria, Australia), CST – Cell Signalling Technologies (Massachusetts, USA), Dako (Campbellfield, Victoria, Australia), Sigma-Aldrich (Darmstadt, Germany)

2.5.6 Western Blot Detection

The HRP secondary antibodies were detected using Pierce ECL (ThermoFisher Scientific). Membranes were incubated for five minutes in the dark. Chemiluminescent membranes were then exposed to medical X-ray film (AGFA, Scoresby, Victoria, Australia) and developed using a 100-Plus film developer (All-Pro Imaging, New York, USA). ImageJ® software was used for image density analysis.

2.6 RT-PCR

2.6.1 RNA Isolation, Reverse Transcription & PCR

Total RNA was isolated from HMCLs using the QIAGEN RNeasy mini kit (QIAGEN, Germantown, MD, USA). Any residual genomic DNA was removed using the Turbo-DNase I kit (AMBION, Austin TX, USA). The quality and quantity of RNA was assessed using the Nanodrop 2000 Spectrophotomer (Life Technologies) evaluating the 260/280 and 260/230 ratios; samples with a score below 1.9 were considered impure and discarded. Fewer than 1% of samples were discarded.

Synthesis of cDNA was performed using 500-1000ng of total RNA with 100U of Superscript III Reverse Transcriptase First Strand Synthesis System (Life Technologies) and random hexamers (Applied Biosystems, Foster City, California, USA) according to the manufacturer's instructions.

Quantitative RT-PCR was performed using 5μL Power-SYBR Green (Applied Biosystems), 2μL diluted 1:5 cDNA template and 500nM of each forward (F) and reverse (R) primers for target genes. Reactions were carried out on the LightCycler 480 instrument (Roche Diagnostics) at 95^{o}C for 10 minutes pre-warming, with 45 cycles of amplification at 95^{o}C for 15 seconds, 62^{o}C for 30 seconds, 72^{o}C for 30 seconds. Each reaction was performed in technical and

biological triplicate. Sample loading was normalised using the β-actin housekeeping gene: this has been found to have stable levels of mRNA across different HMCLs. To ensure specificity a water negative control was included for each primer pair. Amplified products were verified by melting curve analysis.

2.6.2 Data Analysis

C_T (Cycle threshold) values were exported from the LightCycler 480 software to Microsoft Excel (Microsoft, Redmond, Washington, USA) for analysis. Primer efficiency for each gene was determined using 10-fold dilutions of template cDNA from collated samples. C_T values were plotted and to determine "slope" and the following formula used to calculate efficiency:

$E = 10^{-1/slope}$

Relative gene expression was determined using the comparative threshold cycle method ($\Delta\Delta C_T$) using the Pfaffl Method and β-actin as the reference gene:

$$\text{Ratio} = \frac{(E_{target})^{\Delta C_T,\ target\ (calibrator\ -\ test)}}{(E_{ref})^{\Delta C_T,\ ref\ (calibrator\ -\ test)}}$$

2.6.3 Primer Sequences

Gene	HGNC ID	Forward Primer	Reverse Primer
AKR1C3	386	AGCCAGGTGAGGAACTTTCA	CCGGTTGAAATACGGATGAC
CXCL9	7098	GCAAGGAACCCCAGTAGTGA	TTTGGCTGACCTGTTTCTCC
CXCL10	10637	AGGAACCTCCAGTCTCAGCA	CAACACGTGGACAAAATTGG
CXCL12	10672	CCGTCAGCCTGAGCTACAGAT	CTTGTTTAAAGCTTTCTCCAGGT
CXCR3	4540	GCCCTCTACAGCCTCCTCTT	GTTCAGGTAGCGGTCAAAGC
FCRLA	18504	GCCACTGAGGACAACCAAGT	AGGCCCATCTGGTGATACAG
FGFR3	3690	See comment	
LEF1	6551	ACAGATCACCCCACCTCTTG	TGAGGCTTCACGTGCATTAG
LXN	13347	AAGGAACCGCTAGAAGCACA	TGCCAGAGAACTTGCATTTG
NLRP7	22947	AGCTGGGAGATGCAGAAGAA	CTGAGGTTGCAGTCTGTCCA
SLC47A	25588	AGCCTTCAGTGTCCTGCTGT	TGATGATCCCTGACCACAGA
SULF2	20392	GGGATGTCCTCAACCAGCTA	CTTCCCACAGTTGTCCCAGT
β-Actin	132	GACAGGATGCAAGAAGGAGATTACT	TGATCCACACATCTGCTGGAAGGT

Table 2.3: Oligonucleotide primer sequences used for RT-PCR. FGFR3 primers are Applied Biosystems TaqMan® Proprietary sequences Cat. 4331182 Hs00179829_m1

2.7 siRNA

For transient knockdown of Latexin, Ambion Silencer®Select siRNA was used (pooled siRNA, Ambion, cat. No. 4427037). For transient knockdown of DNMT3b, Ambion Silencer®Select siRNA (validated single siRNA, Ambion, cat. No. 4390824, s4221). For transient knockdown of CK2α Invitrogen Stealth RNAi^{TM} was used (pooled siRNA, Invitrogen, cat. No. 6475007). In each instance a control scramble siRNA was also used. Cells were plated in 6 well plates at a density of $5x10^5$ cells/well. For transfection Lipofectamine® RNA iMAX (Invitrogen, cat No. 13778150) was used as per the manufacturer's instructions for up to 72 hours. Cells were then harvested for downstream analysis with western blotting, proliferation and cell death analysis.

2.8 MURINE XENOGRAFT MODELS OF MM

Approval for murine studies was obtained from the Animal Ethics Committee of the Alfred Hospital, Melbourne Australia (E/1376/2013/M & E/1764/2017/A). The HMCLs U266, MM1s, LP1 and KMS12BM underwent lentiviral spinfection to introduce the FUL2-TGvector (a kind gift from Dr Marco Herold, WEHI, Melbourne, Australia) with luciferase2 and GFP under the constitutively active ubiquitin and IRES promoter respectively. Adult age-matched Cg-Prkdscid Il2rgtm1Wjl/SzJ mice (Jackson Laboratories, USA) were injected intravenously (IV) with 1-4x10^6 HMCLs. Tumour burden was measured weekly with in vivo imaging from the 2nd week onwards in respective experiments. Mice were injected intraperitoneally (IP) with 125mg/kg of luciferin, anaesthetised with inhalational isofluorane and imaged with Lumina III XR system (Perkin Elmer, Waltham, Massachusetts, USA). Acquisition and analysis were performed with the Living Image system. Upon reaching scientific end-points (i.e. hind limb paralysis, >20% weight loss) mice were humanely euthanized and relevant organs and tissues collected.

2.9 DRUGS/CHEMICALS

Drug/Chemical	Vehicle	Drug Type	Supplier
Azacitidine	DMSO 5% DMSO/PBS	Hypomethylating agent	Celgene
BGB-283	DMSO	RAF Dimer Inhibitor	BeiGene
BGB-3245	DMSO	RAF Dimer Inhibitor	BeiGene
Dexamethasone	DMSO 5% DMSO/PBS	Corticosteroid	SelleckChem
Nanaomycin A (NSC267461)	DMSO	DNMT3b inhibitor	NCI
Rigosertib (ON-01910)	DMSO PBS	RAS Inhibitor PLK1 Inhibitor	Onconova
Selumetinib (AZD6244)	DMSO	MEK Inhibitor	Array BioPharma
Silmitasertib (CX4945)	DMSO	Casein Kinase 2 Inhibitor	Senhwa Biosciences
Takeda-733	DMSO	MEK Inhibitor	Takeda
Trametinib (GSK1120212)	DMSO 5% DMSO/HPMC	MEK Inhibitor	GlaxoSmithKline
Venetoclax (ABT-199)	DMSO	BCL-2 Inhibitor	Abbvie

Table 2.4: List of drugs & chemicals. The first vehicle listed is that used for in vitro studies, where relevant the second vehicle is that used for murine studies. DMSO – Dimethyl sulfoxide, HPMC – Hydroxypropylmethyl cellulose, PBS – Phosphate buffered saline.

2.10 GENE ARRAYS

2.10.1 Illumina HT12 Microarray

Total RNA from HMCLs was prepared using RNeasy kit (QIAGEN, Doncaster, VIC, Australia) and any residual genomic DNA was removed utilizing the Turbo-DNase I kit (AMBION, Austin, TX, USA). The quality and quantity of the RNA obtained was assessed using Nanodrop 2000 Spectrophotometer and Quant-IT (Life Technologies), respectively. Samples were assessed on the Illumina HT-12 V2 platform. Raw signal intensity data from Illumina HT-12 slides was subjected to variance stabilization transformation including background correction. Each expression value below 50 was adjusted to 50, which was approximately 50% of the background noise level. Hereafter, signal intensities were log2 transformed and quantile normalized. Probes with variance smaller 0.5 were excluded from the subsequent analysis. Unsupervised clustering analysis was performed to identify differential expression between the categories (resistant and sensitive). Analysis of variance (ANOVA) analysis of normalized probe intensities values were performed in Partek Genomic SuiteTM software, version 6.5 (Partek Inc., St. Louis, MO, USA). ANOVA was used to calculate significance of variation in normalized expression values between sample groups; the fold change of gene expression was calculated as a mean ratio. Probes with an unadjusted *p*-value of 0.05 or less (no False Discovery Rate correction was applied) and an absolute fold change of 1.5 or more were defined as differentially expressed[214]. Bioinformatics were provided by Australian Genome Research Facility (AGRF, Victorian Comprehensive Cancer Centre, Melbourne, Victoria, Australia).

2.10.2 QIAGEN RT^2 Profiler PCR Array Human MAP Kinase

Total RNA from HMCLs pre- and post- specified drug treatments, was prepared and quantified as previously described. Synthesis of cDNA was performed using RT^2 First Strand Kit (QIAGEN) according to the manufacturer's instructions. Samples were prepared using 0.8μg RNA with the RT^2 SYBR Green Mastermix and plated onto the 384-well RT^2 Human MAP Kinase array plate, preloaded with validated proprietary primers, five housekeeping genes, a genomic DNA control, three reverse transcriptase controls and three positive PCR controls.

Real time PCR reactions were carried out on the LightCycler 480 instrument (Roche Diagnostics) at 95°C for 10 minutes pre-warming, with 40 cycles of amplification at 95°C for 15 seconds, 60°C for 1 minute.

Data was exported to Excel and analysed using the QIAGEN analysis platform at www.SABiosciences.com/pcrarraydataanalysis.php. The $\Delta\Delta C_T$ is the method employed.

2.10.3 RNA Sequencing Analysis

Total RNA was extracted from HMCLs using the RNeasy Mini Kit (QIAGEN) according to the manufacturer's protocol as previously described. The quantity of the RNA was measured using the Nanodrop 2000 Spectrophotomer. RNA (5-10μg) was then aliquoted into GenTegra tubes (Custom Science, Australia) which stabilizes RNA samples at ambient temperature. This was shipped to Novogene Technology Co. Ltd in Beijing to be sequenced. Each sample was eukaryotic RNA-seq (mRNA enrichment method) and sequenced 20M reads. Read lengths were paired-end 150bp.

Raw data generated by the sequencer were evaluated and quality controlled by FASTQC (v0.11.5, http://www.bioinformatics.babraham.ac.uk/projects/fastqc/). Low quality reads and contaminant reads (with adaptors or with "N" > 10% of the sequence) were removed by SOAPnuke (https://github.com/BGI-flexlab/SOAPnuke). Hisat2, a fast and sensitive alignment program, was used to align paired clean reads to the human genome and gene sequences. StringTie was used to profile the gene expression for each sample. FPKM (Fragments Per Kilobase of transcript per Million mapped reads) method was applied for normalization. Next, correlation heat map and PCA analyses were performed to evaluate the relationship between samples. Differential gene expression analysis, was undertaken to identify differentially expressed genes (DEGs) between groups (i.e. sensitive and resistant, treated and untreated). Numbers of up-regulated and down-regulated genes and the volcano plot of DEG were obtained. Functional analyses such as Gene Ontology annotation and KEGG pathway analysis were performed by the DAVID Bioinformatics Resources (http://david.abcc.ncifcrf.gov/) and the list of DEGs was used as the input.

3. EFFECTS OF MEK INHIBITION ON MULTIPLE MYELOMA

3.1 INTRODUCTION

The advent of Imatinib in the 90s, the first rationally designed tyrosine kinase inhibitor which targets the fusion product of the Philadelphia chromosome (t(9;22)) *BCR-ABL*, pathognomonic of chronic myeloid leukaemia (CML). heralded the era of rationally targeted therapy in cancer therapeutics[215]. This gave rise to the concept of "oncogene addiction", whereby mutation or overexpression of just a single gene can be critical for survival and growth of a tumour[216,217]. This concept has been refined in time, recognising that tumours are heterogeneous[8,78,218], often with several mutations/lesions present and evolving at different points in time[219]. Efforts to investigate various malignancies dependence upon targetable lesions using numerous gene arrays and sequencing platforms to interrogate mutations, amplification or overexpression of kinases, enzymes and receptors have become a major focus in improving treatment of malignancy[220,221]. Altogether, this gave rise to the premise of personalised medicine with the promise of both greater efficacy and less toxicity[222]. Dozens of kinase inhibitors continue to be approved for clinical use in all of the most common malignancies[223]. Additionally, hormonal therapy and immunotherapy (including monoclonal antibodies) add to the arsenal of targeted therapy.

Only recently has MM had a rationally designed targeted therapy approved for use, with the CD38 monoclonal antibody Daratumumab[224]. Whilst the proteasome inhibitors (bortezomib, carfilzomib) and IMiDs (thalidomide, lenalidomide, pomalidomide) can be considered targeted therapies, and have significantly improved the therapeutic landscape of MM, they cannot be considered truly rationally designed treatments based on addiction[225]. In the case of thalidomide, the lead IMiD compound, it was initially intended as a sedative/hypnotic and later (with disastrous consequences[226]) for the management of nausea and morning sickness in pregnancy[227]. There was no evidence that MM overexpressed or was reliant upon the IMiD target Cereblon, only hindsight has shown the relevance of this to response[228]. Similarly, for

proteasome inhibition, whilst it is oft quoted that MM cells have higher protein burdens in the context of immunoglobulin production, overexpression or mutation in the PSMB5 subunit is not recognised as a cause of sensitivity, rather it's mutation or overexpression has been identified as a marker of resistasnce[229,230].

Activation of the RAS-MAPK, through *RAS*^{M} [18,78,106], *RAF*^{M} and over-expression of RTKs in specific genetic subtypes (e.g. over-expression of FGFR3 in t(4;14)[20,21,87]), is a frequent event in MM, potentially affecting up to 70% of cases. The role of the RAS-MAPK in growth/proliferation, angiogenesis, survival and anti-apoptosis makes this an ideal target for clinical intervention and targeted therapy[25].

Efforts to target RAS have historically been unsuccessful[53]. As such, targeting downstream effectors of the MAPK (RAF, MEK and possibly even ERK) has been considered a better approach in malignancy, most notably in *BRAF*^{M} melanoma, where *BRAF*^{M}V600E inhibition with vemurafenib with or without the MEKi trametinib improves OS[76].

Trametinib is a type 3 allosteric inhibitor of MEK, it is ATP non-competitive, binding to a pocket adjacent to the ATP binding site[231]. Type 3 inhibitors are considered the most specific kinase inhibitors with little off-target inhibition[232]. However, a specific issue to some type 3 inhibitors (including MEKi) is priming. Priming is a process where in the presence of inhibitor, phosphorylated MEK accumulates resulting in reactivation of downstream ERK[206].

Here we investigate the effects and potential role of MEK inhibition in MM using trametinib.

3.2 STUDY RATIONALE & AIMS

The work described in this chapter aimed to:

- Assess proliferation, death and cell cycle changes in HMCLs treated with MEK inhibition
- Analyse the response in ERK activation and downstream signalling

- Analyse the use of MEK inhibition in combination with dexamethasone
- Evaluate the use of MEK inhibition in murine xenograft models of MM

3.3 RESULTS

3.3.1 Screening of MAPK inhibitors against a panel of HMCLs

We initially screened a panel of HMCLs using the Cell Titer-Glo® cell viability assay to assess cell viability when treated with several targeted inhibitors of the RAS-MAPK (Figure 3.1). HMCLs were selected to represent the cytogenetic and molecular heterogeneity present in MM (Table 3.1). As we expected that activation of the RAS-MAPK through *RAS*^{M} and t(4;14) would sensitise cells to targeted inhibition, the panel was enriched for these subtypes.

HMCL	Cytogenetics	RAS status	p53	Other
MM1s	t(14;16), t(8;14)	KRAS G12A	WT	
RPMI-8226	t(16;22), t(8;22)	KRAS G12A		
XG1	t(11;14)	NRAS G12R		IL-6-depend
NCI-H929	t(4;14)	NRAS G13D	WT	
U266	t(11;14)	*BRAF K601N		
KMS11	t(4;14), t(8;14), t(14;16)	WT		FGFR3 mut
KMS26	t(4;14)	WT		
OPM2	t(4;14)	WT		PTEN mut
LP1	t(4;14)	WT		
ANBL6	t(14;16)	WT		IL-6 depend
JJN3	t(14;16), t(8;14)	WT		
KMS12BM	t(11;14)	WT		

Table 3.1: HMCL characteristics. Cytogenetics and *p53* status have been obtained from keatslab.org and from available published data. *RAS*^{M} status has been confirmed in our laboratory using ddPCR.

The overexpression of FGFR3 in t(4;14) HMCLs was confirmed by both RT-PCR and WB (Figure 3.2A & B).

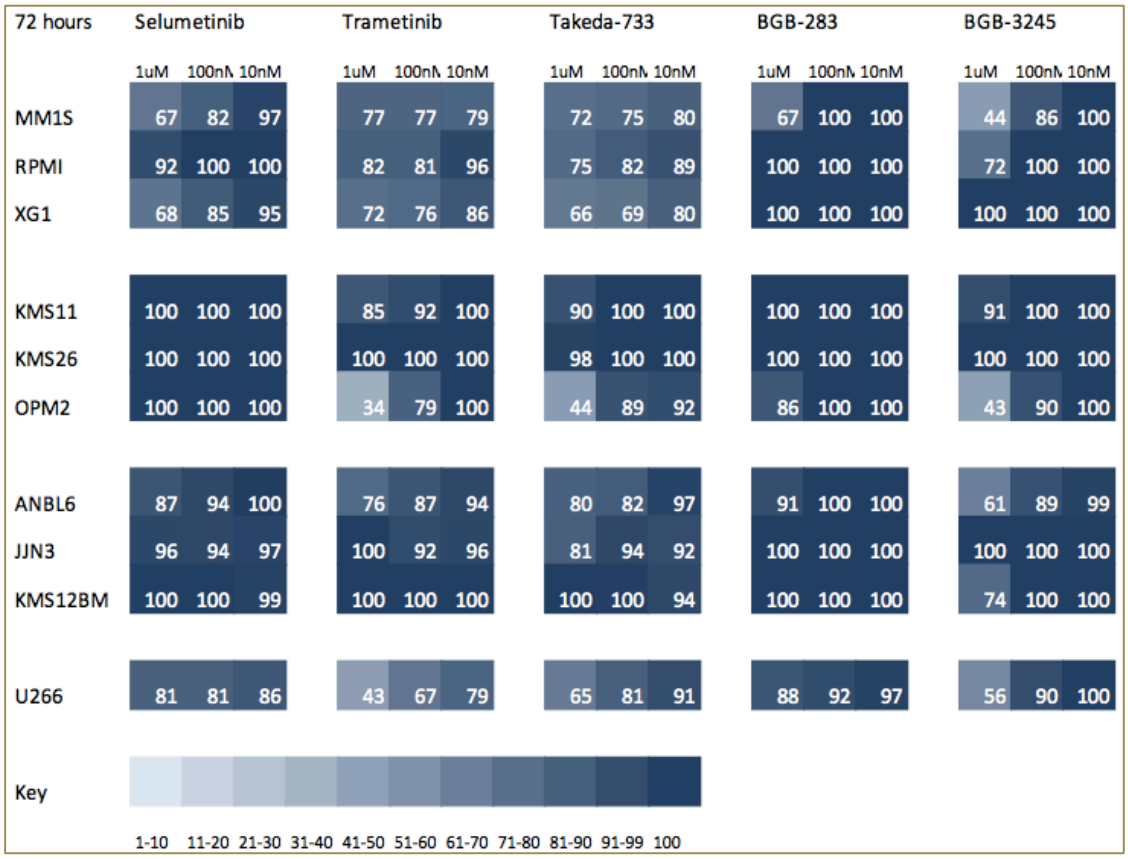

Figure 3.1: Heat map of ATP assays of HMCLs treated with MAPK pathway inhibitors. HMCLs were treated with three 10-fold concentrations of different MAPK pathway inhibitors for 72 hours. Results are expressed as the average percentage ratio of viable cells compared with an untreated sample (n=3).

Selumetinib (AZD6244), trametinib (GSK1120212) and takeda-733 are MEK inhibitors. BGB-283 and BGB-3245 are 1st and 2nd generation RAF-dimer inhibitors, reported to inhibit wildtype (WT) RAF rather than RAF^{M}. Given the superior results obtained with trametinib, and that it is already in clinical use, this inhibitor was used for all further studies.

In addition, a RAS inhibitor, rigosertib (ON-01910), was also evaluated (Supplementary Figure 9.1).

Both OPM2 and ANBL6 were used as part of the initial screen. OPM2 was removed due to its PTEN mutation, as this is an uncommon mutation in MM. ANBL6 was removed due poor sustained growth over time.

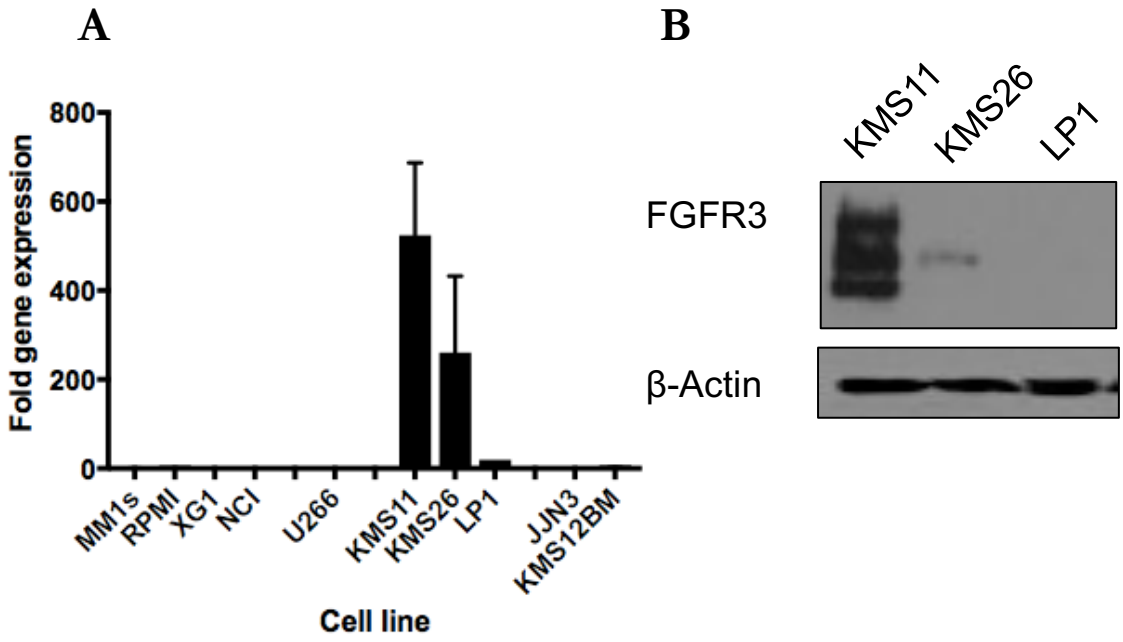

Figure 3.2: FGFR3 expression in t(4;14) HMCLs. (A) RT-PCR of relative gene expression of FGFR3 as a ratio against RPMI. (n=3, mean ± SEM). (**B)** Western blot of FGFR3 protein. β-Actin is the loading control.

3.3.2 Trametinib exerts an anti-proliferative effect with limited cytotoxicity

The anti-proliferative effect of trametinib observed in the Cell Titer-Glo® cell viability assay was confirmed by quantitation of viable cells using trypan blue staining, following treatment with trametinib at three 10-fold concentrations over 72 hours (Figure 3.3). The most pronounced effect of trametinib was observed in HMCLs which harbour a RAS^M then RAF^M. Minor activity was seen at the highest concentration in a single t(4;14) HMCL, KMS11, which expresses the highest amount of FGFR3 and also harbours a FGFR3 mutation[233]. Finally, no effect was observed in WT HMCLs (harbouring neither a RAS^M nor t(4;14)).

Cell death, investigated using flow cytometry with propidium iodide (PI) staining, was limited to essentially a single HMCL, NCI which has both a RAS^M and a t(4;14). Otherwise no overt cytotoxicity was observed at any dose (Figure 3.4).

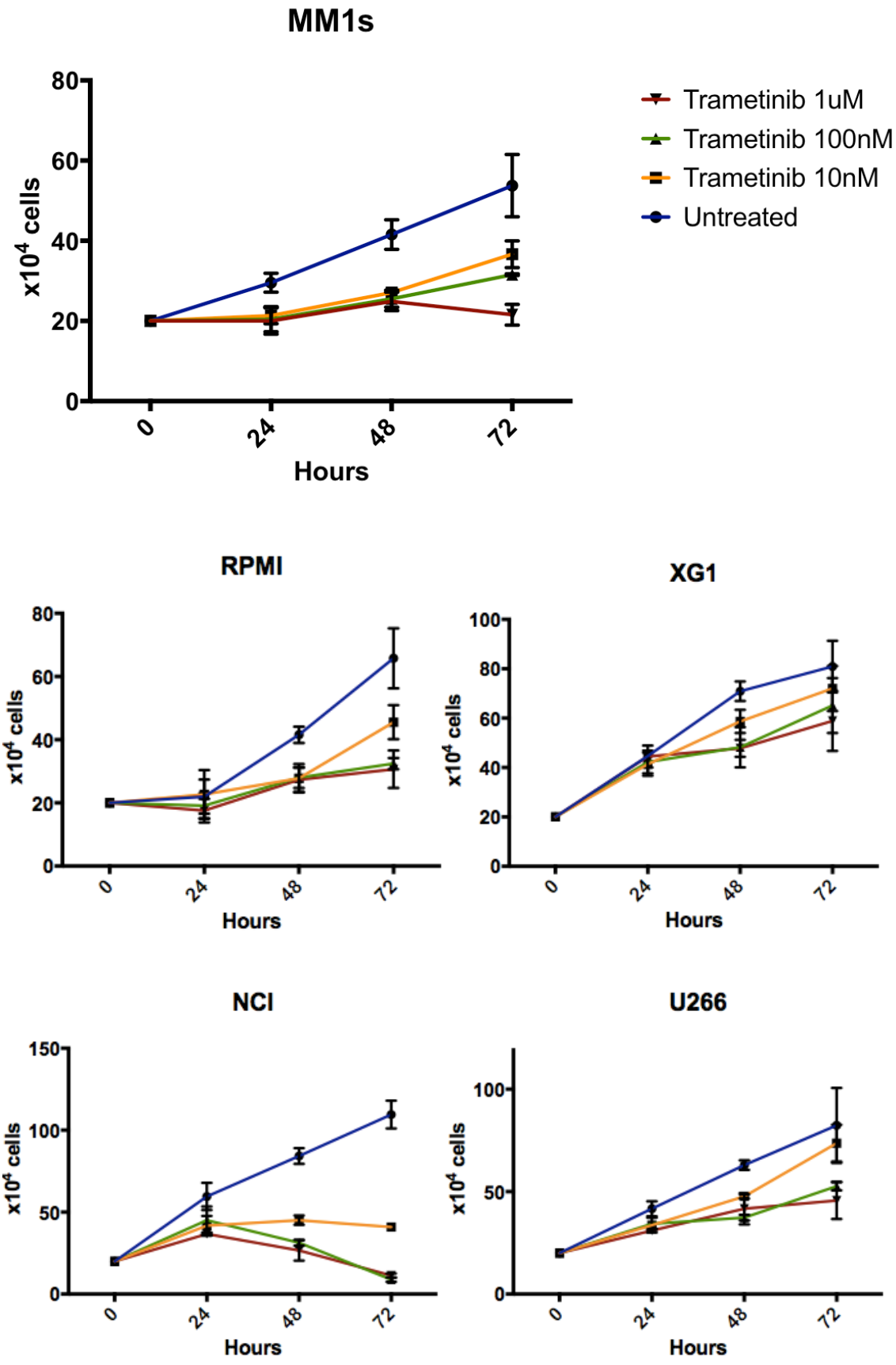
MM1s
Trametinib 1uM
Trametinib 100nM
Trametinib 10nM
Untreated
x10^4 cells
Hours
0
24
48
72
RPMI
XG1
NCI
U266

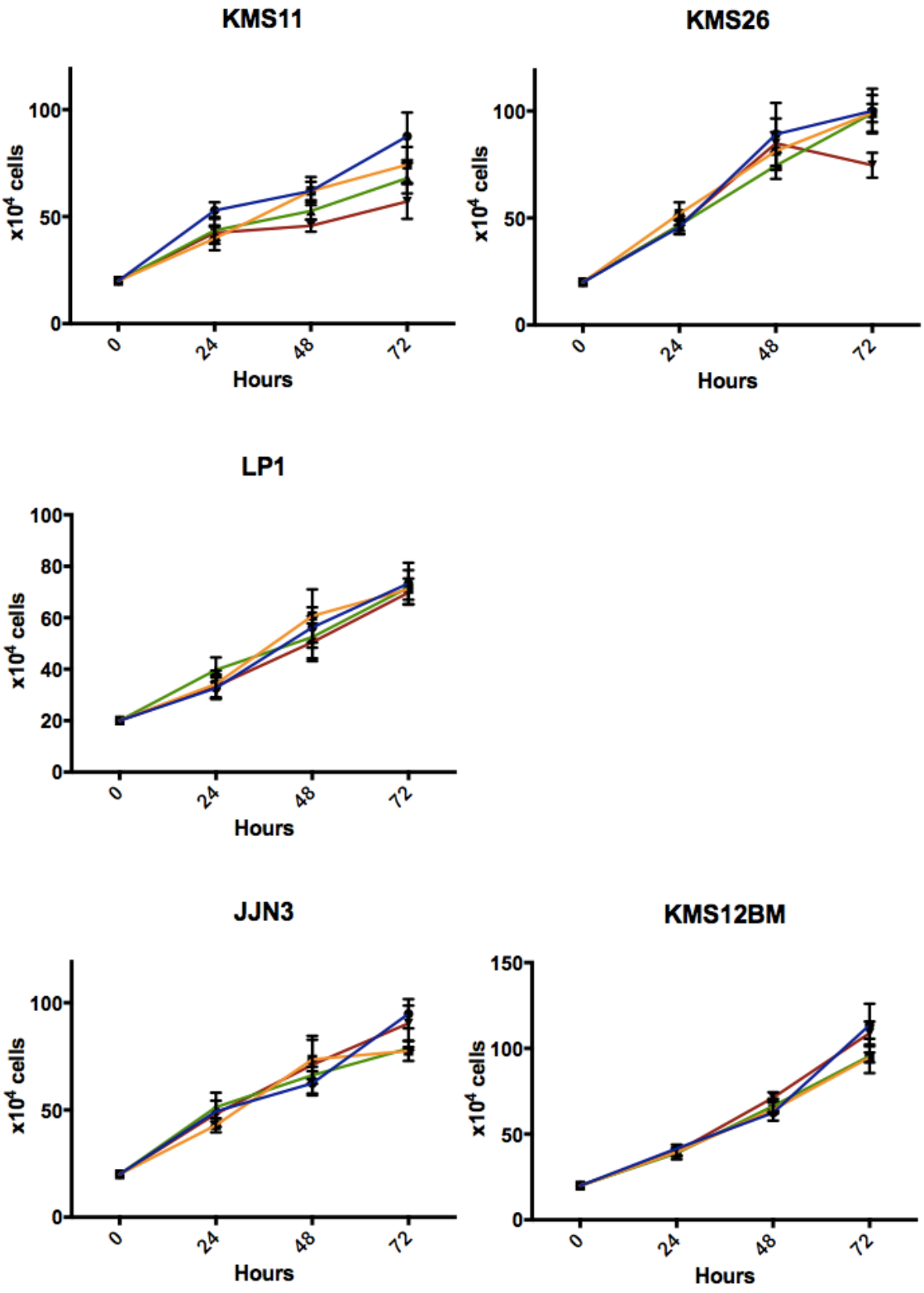

Figure 3.3: Cell proliferation. Absolute cell numbers as determined by haemocytometer, cultured untreated or with trametinib 10nM, 100nM and 1μM for 72 hours (n=3, mean ± SEM).

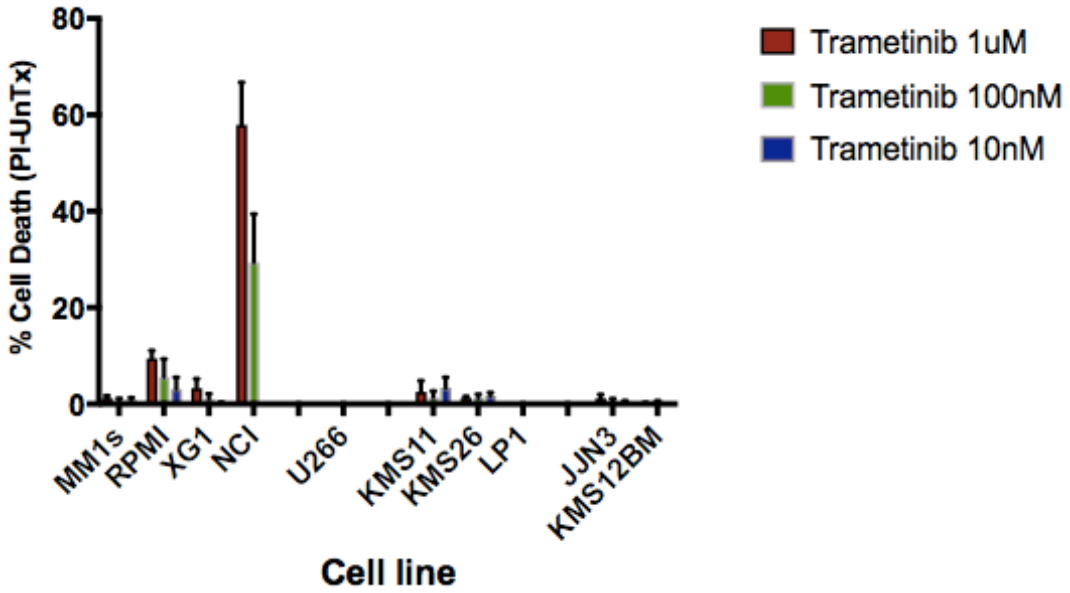

Figure 3.4: Cell death analysed by PI flow cytometry. Cell death was limited to <5% in HMCLs except for NCI. Results are expressed as the percentage cell death of the PI+ subtract the untreated sample (n=3, mean ± SEM).

On the basis of these data, for future studies, HMCLs were defined as sensitive with an IC_{50}<10nM (MM1s, RPMI-8226, NCI), intermediate with an IC_{50}<100nM (U266), or resistant.

3.3.3 MEK inhibition results in loss of phosphorylated ERK

ERK has several phosphorylation sites which modulate and modify its activity. MEK driven phosphorylation is the only known activator of ERK, phosphorylating threonine-202 and tyrosine-204. To confirm the activity of trametinib, we evaluated phosphorylated ERK in HMCLs pre- and post-treatment with trametinib (Figure 3.5 A-C).

All HMCLs, irrespective of their growth response to trametinib, showed complete loss of phosphorylated ERK at 24 hours. KMS12BM was the only HMCL not to express phosphorylated ERK at baseline (in culture), which would account for lack of response to treatment with trametinib.

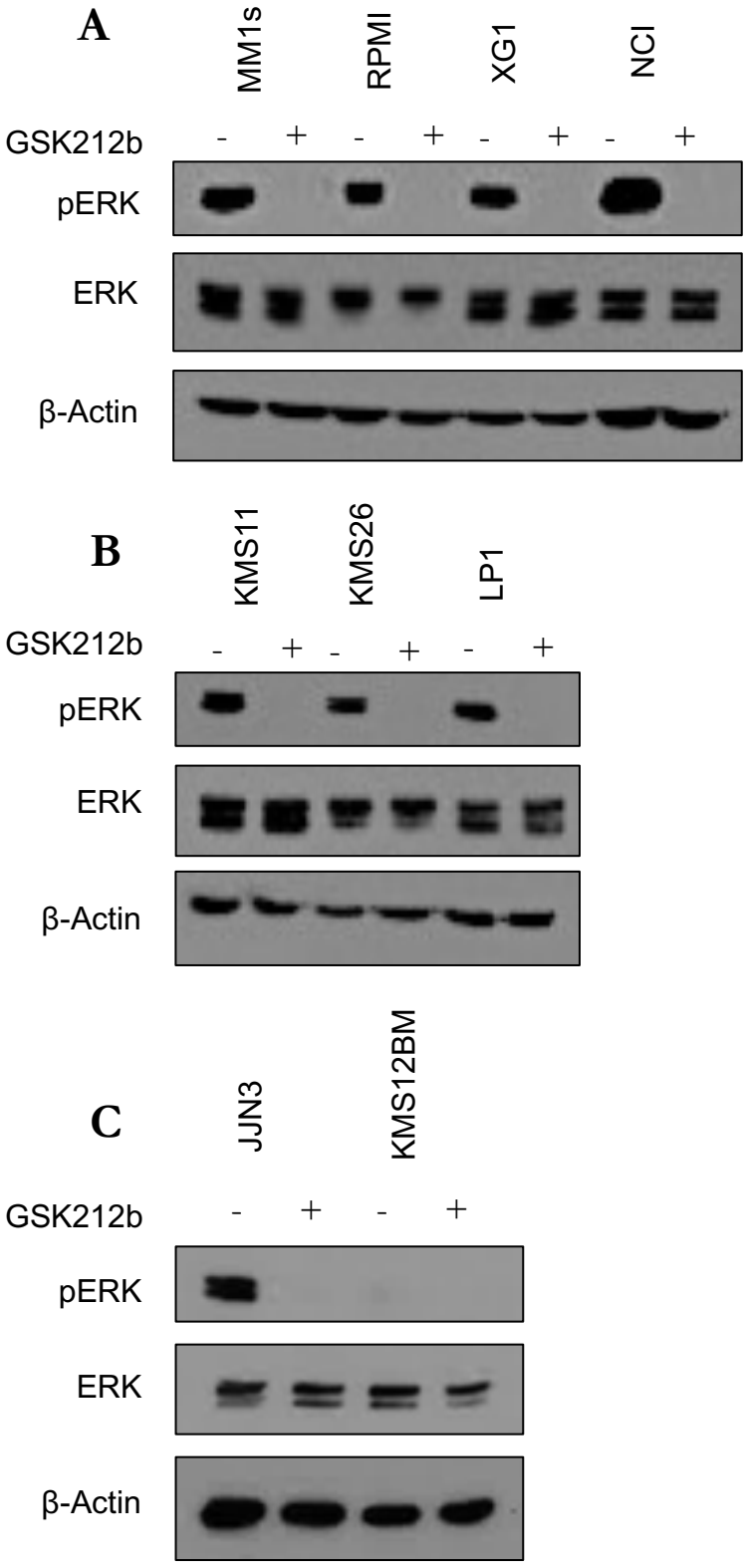

Figure 3.5: Phosphorylated & total ERK with & without trametinib 1μM at 24 hours. (A) RAS^{M} HMCLs. **(B)** t(4;14) HMCLs. **(C)** WT HMCLs. Irrespective of HMCL sensitivity to MEKi, all HMCLs lose phosphorylated ERK with no effect on total ERK when treated with trametinib for 24 hours. pERK – phosphorylated ERK. β-Actin is the loading control.

3.3.4 MEK inhibition results in $G_{0/1}$ arrest in HMCLs with WT *p53*

As trametinib inhibits cell proliferation we investigated its effects on cell cycling. In two HMCLs, MM1s and NCI, $G_{0/1}$ arrest occurs (Figure 3.6). Both MM1s and NCI have WT *p53*. This was not observed in any other HMCL irrespective of sensitivity.

Consistent with the induction of $G_{0/1}$ arrest, treatment with trametinib results in induction of p27 (Figure 3.7).

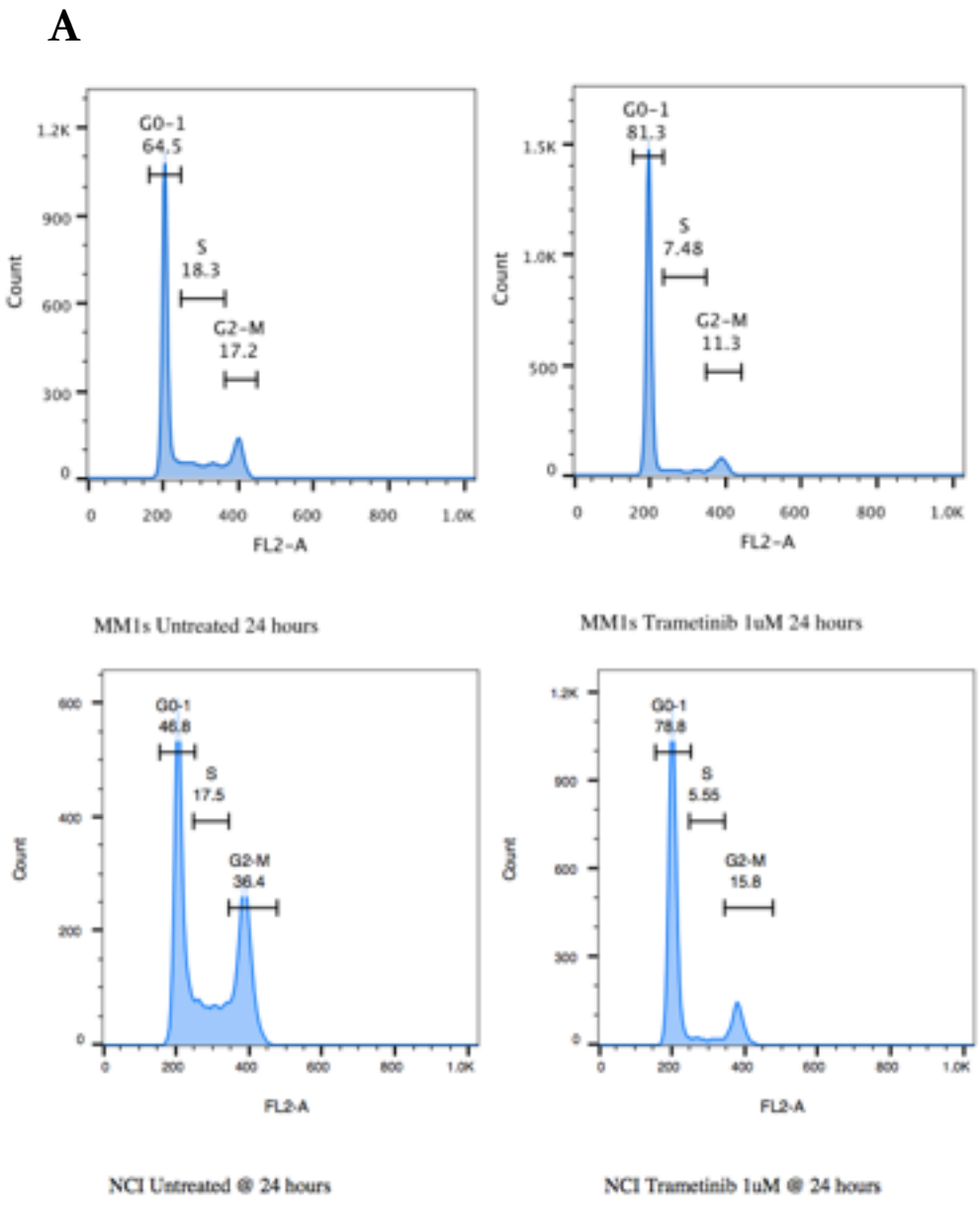

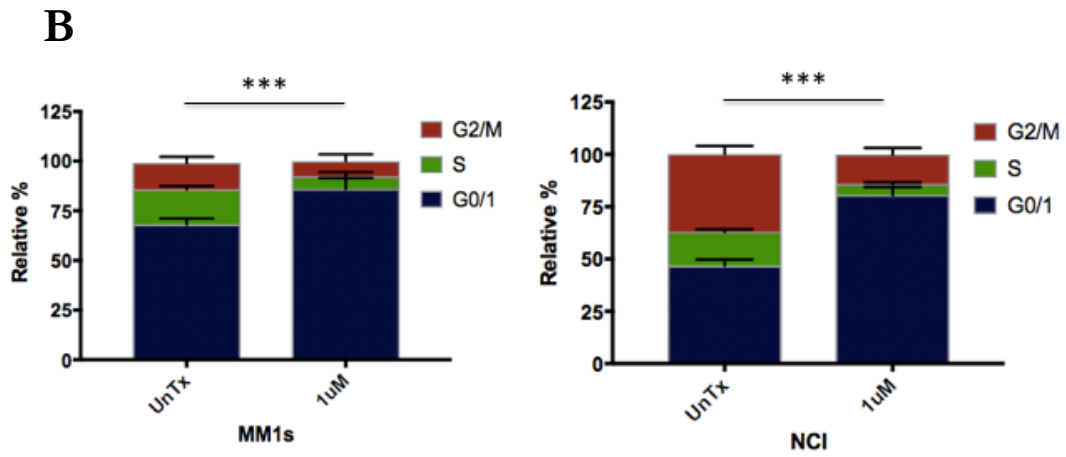

Figure 3.6: Cell cycle $G_{0/1}$ arrest in MM1s & NCI. (A) Representative cell cycle plots of MM1s and NCI treated with trametinib 1μM at 24 hours. **(B)** Relative percentages of cell cycle stages. (n=3, mean ±SEM).

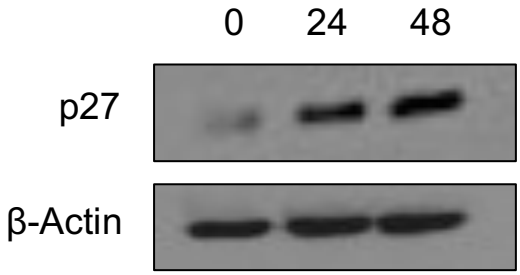

Figure 3.7: Induction of p27 in MM1s. p27 expression in MM1s treated with trametinib 1μM at baseline, 24 and 48 hours. β-Actin is the loading control.

3.3.5 MEK inhibition reduces cytosolic to nuclear translocation of ERK and Cyclin B

ERK plays a critical role in proliferation (including G_1/S transition) and nuclear transcription with over 100 nuclear targets. Localisation to the nucleus is necessary for these processes to occur and occurs rapidly upon ERK activation. The processes which control this transition are incompletely understood. However, activation by MEK is a necessary step in non-malignantly transformed cells.

We evaluated the ability of trametinib to inhibit nuclear localisation of ERK. Four HMCLs (MM1s, NCI, KMS26 and KMS12BM) were treated with trametinib 1μM

for 24 hours. In the two sensitive HMLCs (MM1s and NCI) treatment with trametinib resulted in a significant reduction in the presence of nuclear ERK, correlating with the reduction in proliferation previously observed. Whereas, in the two resistant HMCLs (KMS26 and KMS12BM) no difference in nuclear ERK was observed (Figure 3.8 A-D).

Cyclin B is the main cyclin required for transition at the G_2/M checkpoint and progression into mitosis. In quiescent cells, cyclin B is retained within the cytoplasm via its cytoplasmic retention sequence (CRS). The CRS consists of four sites, all of which require phosphorylation for nuclear localisation and progression to mitosis. Two of these sites are phosphorylated by ERK.

Similar to the analysis of nuclear localisation of ERK, we evaluated the effect of trametinib 1μM at 24 hours on the nuclear localisation of cyclin B. Again, in sensitive HMCLs a reduction in nuclear cyclin B was found. Whilst in resistant HMCLs, no reduction was observed. Unexpectedly, in KMS26 there was an increase in nuclear cyclin B following treatment (Figure 3.9 A-D).

3.3.6 MEK inhibition synergises with dexamethasone

Corticosteroids (dexamethasone and prednisolone) form the backbone of most combination therapies for MM. Trametinib in combination with dexamethasone resulted in marked synergistic cytotoxicity in five of eight HMCLs tested (Figure 3.10). HMCLs that had a cytostatic response to single agent trametinib typically showed the greatest response to the combination. KMS11 showed no response to either agent alone, but significant synergistic cytotoxicity was seen with the combination.

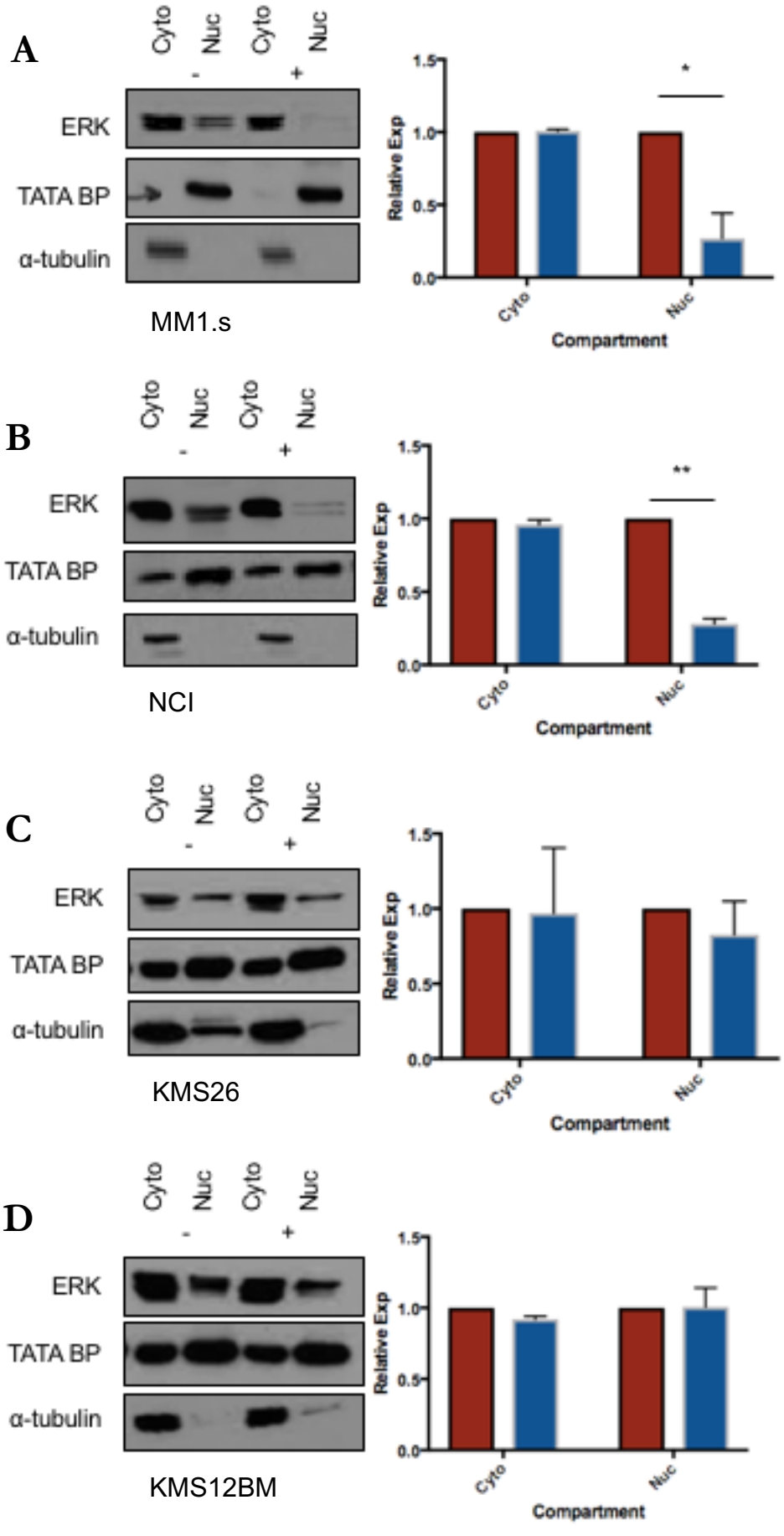
A
Cyto
Nuc
Cyto
Nuc
-
+
ERK
TATA BP
α-tubulin
MM1.s
Relative Exp
1.5
1.0
0.5
0.0
*
Cyto
Nuc
Compartment
B
Cyto
Nuc
Cyto
Nuc
-
+
ERK
TATA BP
α-tubulin
NCI
Relative Exp
1.5
1.0
0.5
0.0
**
Cyto
Nuc
Compartment
C
Cyto
Nuc
Cyto
Nuc
-
+
ERK
TATA BP
α-tubulin
KMS26
Relative Exp
1.5
1.0
0.5
0.0
Cyto
Nuc
Compartment
D
Cyto
Nuc
Cyto
Nuc
-
+
ERK
TATA BP
α-tubulin
KMS12BM
Relative Exp
1.5
1.0
0.5
0.0
Cyto
Nuc
Compartment

Figure 3.8: A-D Cytoplasmic to nuclear translocation of ERK, 24 hours treatment with trametinib 1μM. (A, B) MM1s and NCI show marked reduction of nuclear localisation of ERK (MM1s; p=0.05), (NCI: p=0.02). **(C, D)** KMS26 and KMS12BM show no significant change in nuclear localisation of ERK after treatment. (n=3, mean ±SEM, most representative blot is shown). Red bars are pre-treatment, blue bars are post-treatment. α-tubulin and TATA BP are the cytoplasmic and nuclear loading controls respectively. For contamination in the cytoplasmic compartment, ERK density was corrected for TATA BP density.

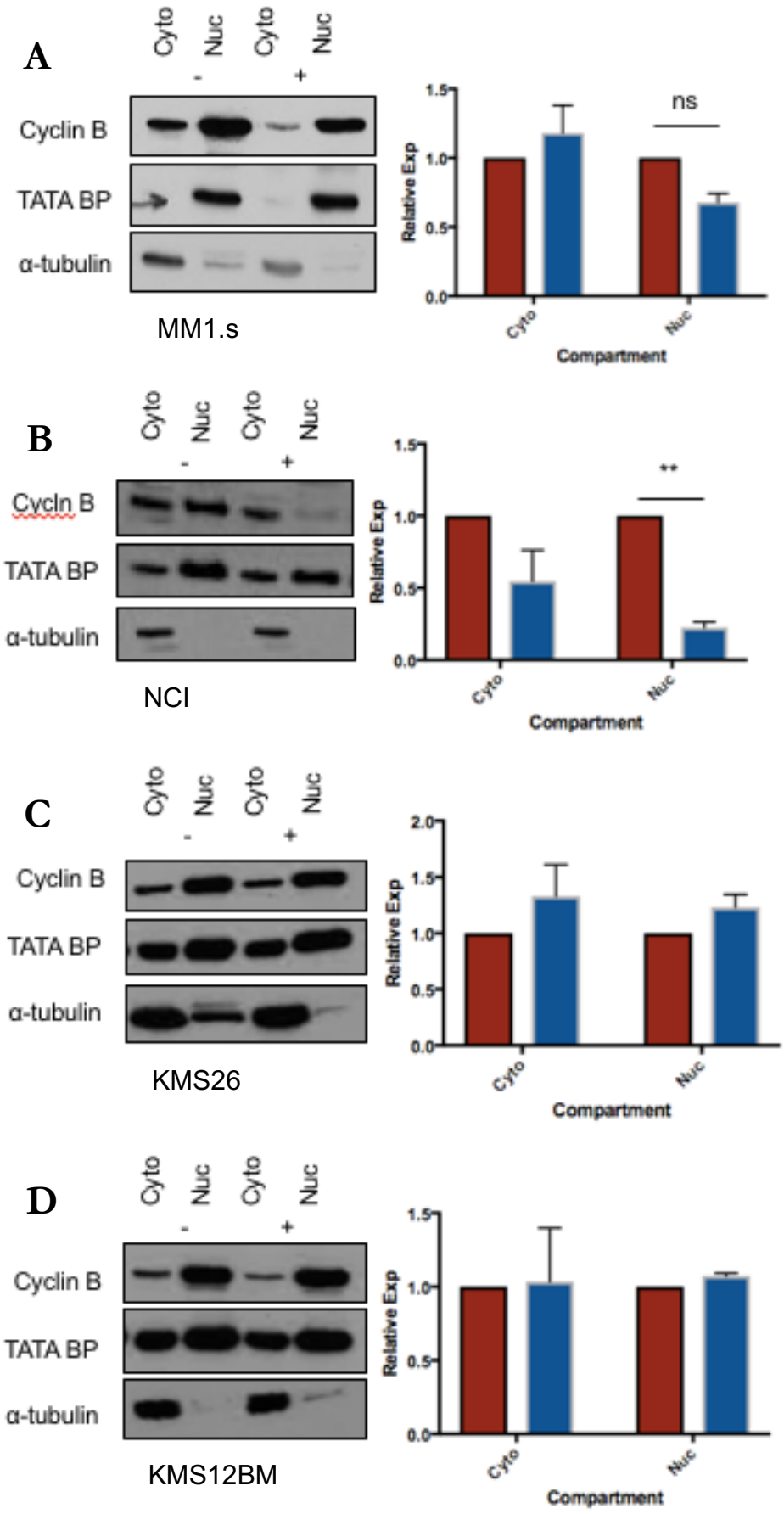
A
Cyto
Nuc
Cyto
Nuc
-
+
Cyclin B
TATA BP
α-tubulin
MM1.s
Relative Exp
1.5
1.0
0.5
0.0
ns
Cyto
Nuc
Compartment
B
Cyto
Nuc
Cyto
Nuc
-
+
Cycln B
TATA BP
α-tubulin
NCI
Relative Exp
1.5
1.0
0.5
0.0
**
Cyto
Nuc
Compartment
C
Cyto
Nuc
Cyto
Nuc
-
+
Cyclin B
TATA BP
α-tubulin
KMS26
Relative Exp
2.0
1.5
1.0
0.5
0.0
Cyto
Nuc
Compartment
D
Cyto
Nuc
Cyto
Nuc
-
+
Cyclin B
TATA BP
α-tubulin
KMS12BM
Relative Exp
1.5
1.0
0.5
0.0
Cyto
Nuc
Compartment

Figure 3.9: A-D Cytoplasmic to nuclear translocation of cyclin B, 24 hours treatment with trametinib 1μM. (A) MM1s shows a non-significant reduction of nuclear localisation of Cyclin B, (p=0.1). **(B)** NCI shows a significant reduction in nuclear localisation of Cyclin B (p=0.02). **(C, D)** KMS26 and KMS12BM show no change in nuclear localisation of Cyclin B. (n=3, mean ±SEM, most representative blot is shown). α-tubulin and TATA BP are the cytoplasmic and nuclear loading controls respectively. For contamination in the cytoplasmic compartment, cyclin B density was corrected for TATA BP density.

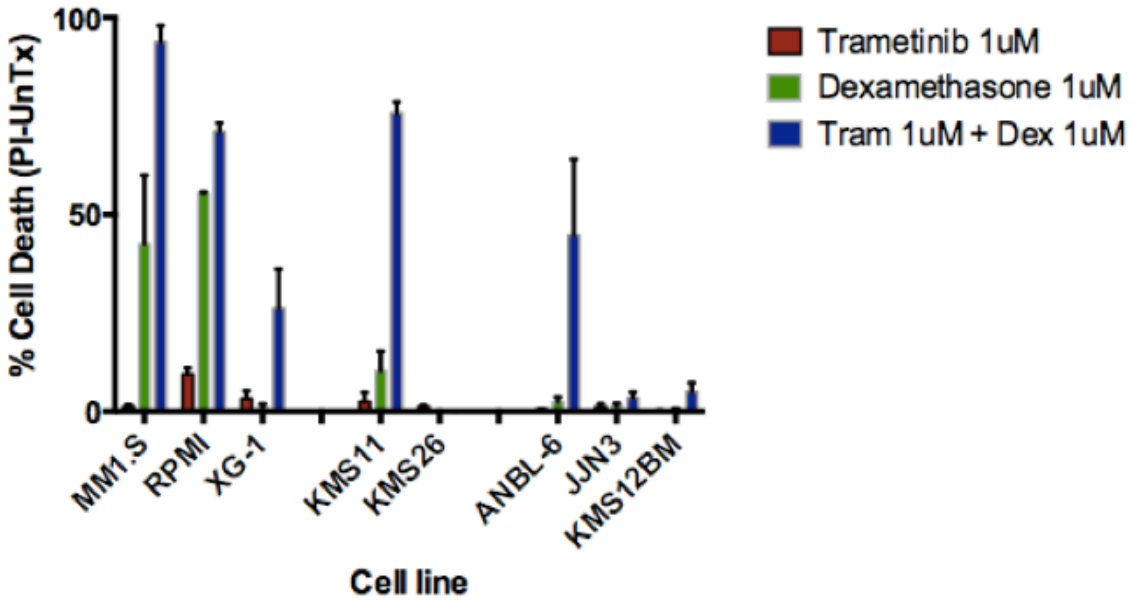

Figure 3.10: Combination of trametinib & dexamethasone at 72 hours. Determination of cell death by propidium iodide (PI) flow cytometry shows marked synergy in several HMCLs, including those that show no sensitivity to either agent alone. (n=3, mean ±SEM).

3.3.7 MEK inhibition in murine xenograft models of MM

We evaluated trametinib in two murine xenograft models of MM. The first recapitulates a *RAS*^{M} disease using the HMCL MM1s, the second recapitulates a *BRAF*^{M} disease using the HMCL U266. In both instances, NOD scid gamma (NSG) mice were transplanted (via IV tail vein injection) with 4x10^{6} MM1s or 2x10^{6} U266 cells stably expressing GFP and luciferase. In both models, disease established within two weeks. Tumour burden was monitored weekly using in vivo bioluminescence imaging using luciferin (IP) induced fluorescence measuring median flux as photons/sec of averaged dorsal and ventral views. Scientific end-points were high-limb paralysis (HLP) and/or >20% weight loss from baseline.

In the MM1s xenograft, mice were treated with vehicle alone, trametinib 1mg/kg (OG) or trametinib 3mg/kg daily, planned for 2 cycles of 3 weeks with a week break between cycles. The MM1s phenotype initially presents with pelvic disease with progression along the spine and to the long bones (Figure 3.11). Whilst both doses of trametinib slowed disease progression (Figure 3.12) neither resulted in

prolonged survival (Figure 3.13). No mouse reached the planned second cycle of therapy. All mice developed signs of HLP with no other toxicities observed.

In the U266 xenograft, mice were treated with vehicle alone, trametinib 3mg/kg alone daily, dexamethasone 1mg/kg alone daily or both trametinib 3mg/kg with dexamethasone 1mg/kg daily in combination. Treatment was continued for 2 cycles of 3 weeks with a single week break between cycles. The U266 phenotype initially localises to the spine and pelvis before progressing to involve the long bones (Figure 3.14). Whilst disease progression appeared to slow in both dexamethasone treated cohorts (Figure 3.15), no significant difference in survival was observed (Figure 3.16).

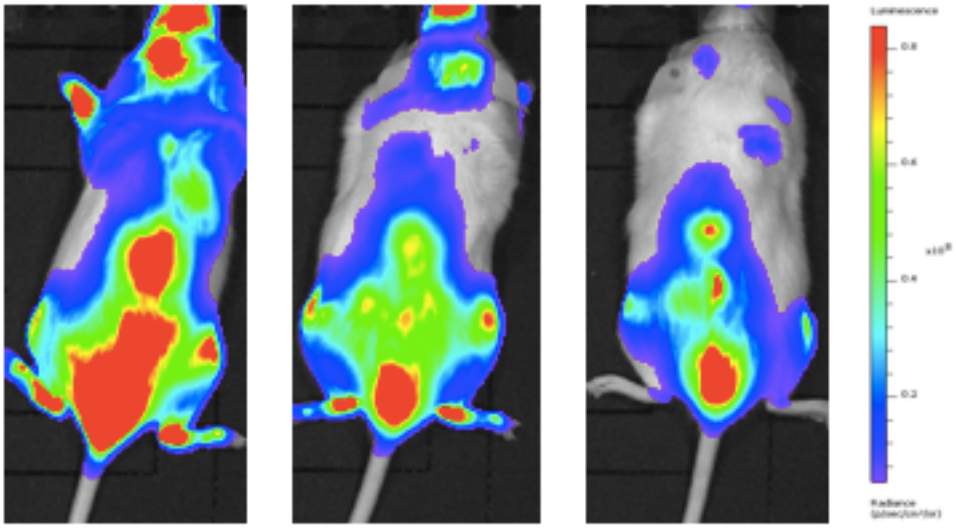

Figure 3.11: Disease pattern of MM1s murine xenograft. Images at four weeks. Disease initially presents in the pelvis, before extending to involve the spine, skull, and long bones. Treatment cohort is listed beneath each mouse.

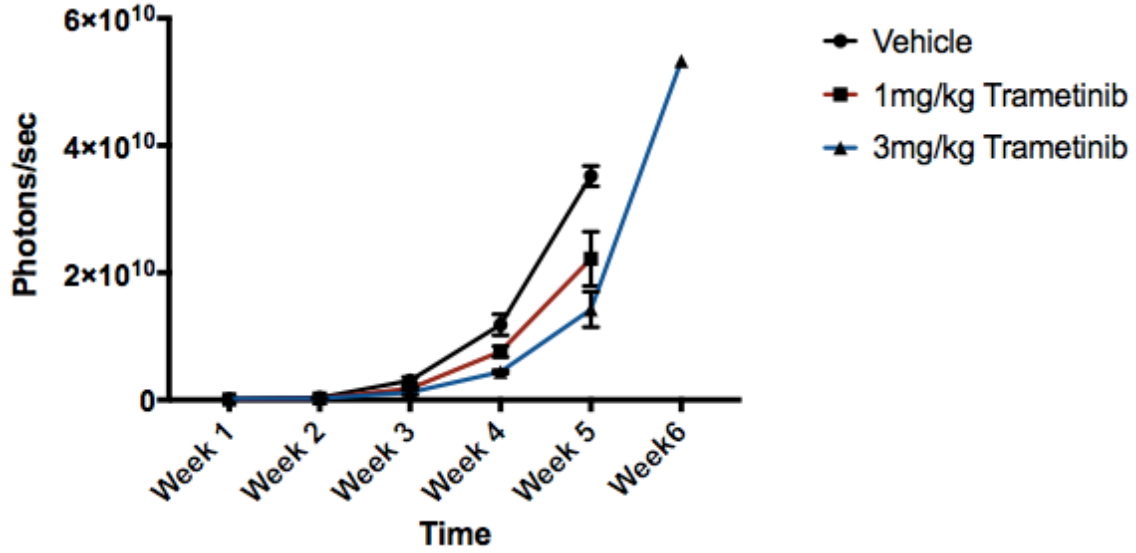

Figure 3.12: Disease bioluminescence measure over time in MM1s. Trametinib reduces disease burden and rate of progression at both 1mkg/kg and 3mg/kg doses. (n=5, mean ±SEM).

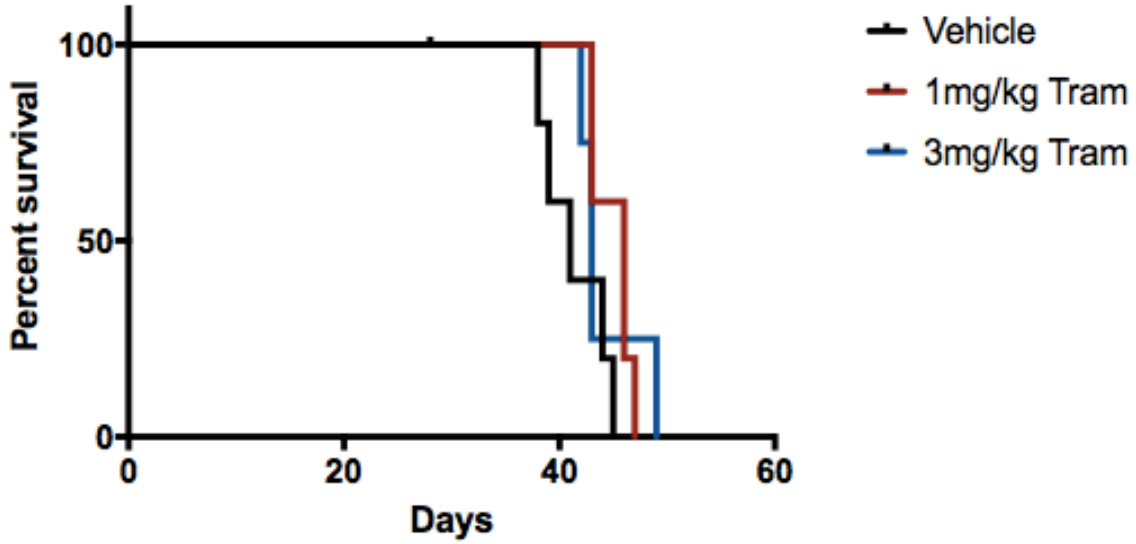

Figure 3.13: Survival curves of MM1s xenograft treated with trametinib. Despite slowing disease progression over time, there was no significant difference in median survival observed between groups. All mice succumbed to the scientific end-point of hind-limb paralysis (HLP). (n=5/cohort).

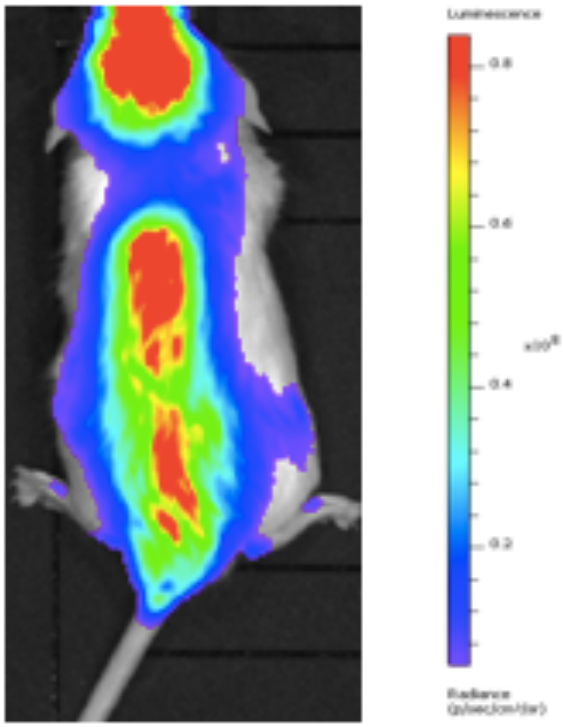

Figure 3.14: Disease pattern of U266 murine xenograft. Disease initially establishes in the pelvis but rapidly spreads to involve the entire spine and skull. Image is at 6 weeks of disease.

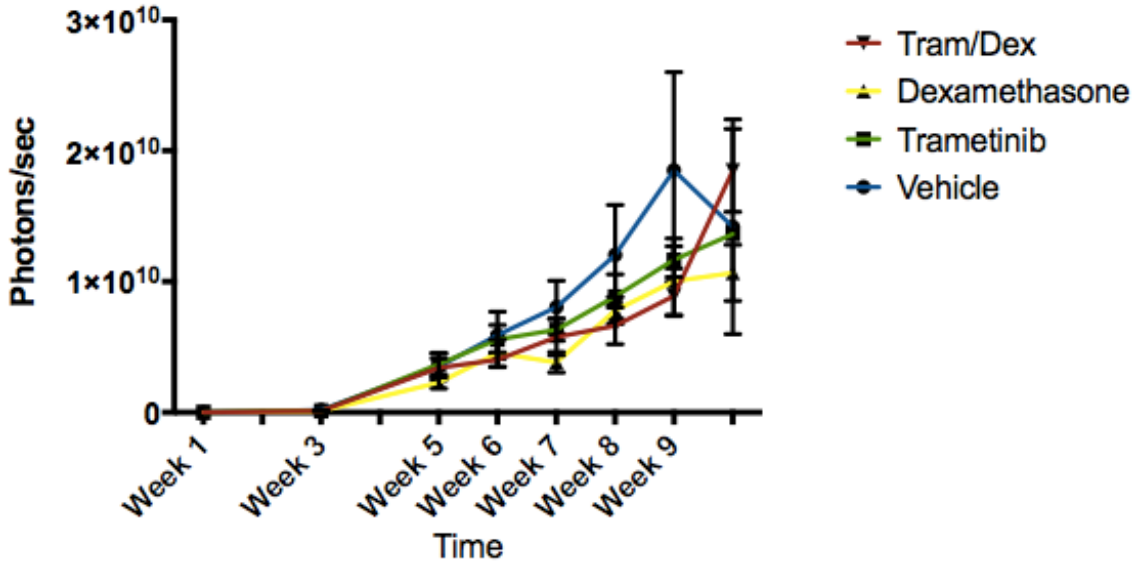

Figure 3.15: Disease bioluminescence measure over time in U266. No difference was observed in disease burden or progression in any treatment group. (n=5, mean ±SEM).

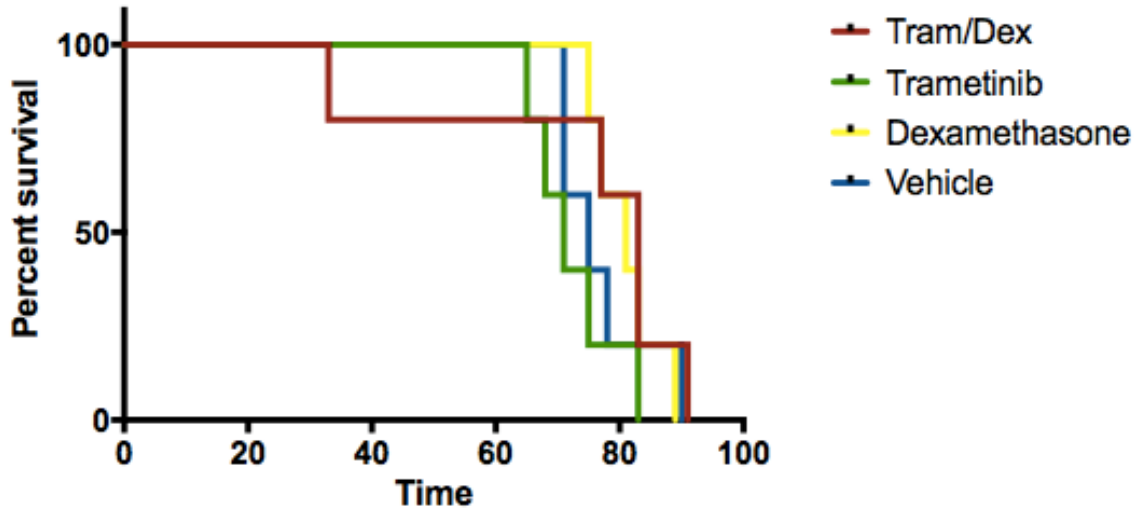

Figure 3.16: Survival curves of U266 xenograft with combination treatments. No significant difference in median survival was observed between any of the cohorts. (n=5/cohort).

3.4 DISCUSSION

Activation of the RAS-MAPK plays a fundamental role in the progression of MM[20] both through mutations in pathway effectors, dominated by *RAS*^{M}, as well as overexpression of RTKs in t(4;14) disease. The data presented here demonstrates inhibition of signalling through the RAS-MAPK can be achieved with the MEKi trametinib. With the exception of a single HMCL, KMS12BM[147] all HMCLs tested showed activation of the RAS-MAPK as demonstrated by phosphorylated-ERK. This phosphorylation was effectively inhibited in all HMCLs by trametinib. Treatment of HMCLs that harbour *RAS*^{M} with trametinib resulted in inhibition of proliferation, consistent with oncogenic addiction to *RAS*^{M} confirming a previous report[234]. Contrastingly, this effect was blunted in the HMCL harbouring a *RAF*^{M} (U266) which might suggest *RAF*^{M} signalling to pathways outside of the RAS-MAPK. Why this is not the case in *RAS*^{M} disease, given that RAS has several other known signalling pathways (PI3K/AKT, PLCγ) is not entirely clear. However, in the context of the mutations present in MM it *RAS*^{M} has a predilection for signalling via the MAPK. Minor activity was observed in a single t(4;14) HMCL, KMS11, which also harbours a FGFR3 mutation[233], whereas no effect was observed in any other t(4;14) HMLC, nor in any WT HMCL. With a single exception, MEK inhibition was cytostatic rather than cytotoxic.

Cytotoxicity was only observed in NCI, an HMCL which harbours both a *RAS*^{M} on a cytogenetic background of t(4;14). This may result in complete dependence on the RAS-MAPK to support its growth and survival.

In the presence of WT *p53*, MEK inhibition results in $G_{0/1}$ arrest and induction of p27. Mutations and loss of *p53* are generally regarded as late events in MM, whilst *RAS*^{M} is a relatively early oncogenic driver of disease. Thus, in early stage disease where most patients have WT *p53*, we postulate activity may be greater and more effective that were a MEKi used in later stage disease.

Once active, ERK has a broad range of functions in the cytoplasm, mitochondria and within the nucleus[25]. One of its most important nuclear roles is promoting progression from G_1 to S-phase. ERKs nuclear translocation is a complex active process, requiring activation by MEK driven phosphorylation, additional phosphorylation signals from casein kinase 2 (CK2) and specific nuclear pores for passage[235-238]. It has also been reported that ERK can passively diffuse into the nucleus[239,240] although this may not represent a significant mechanism. In sensitive HMCLs, we have shown MEK inhibition reduces nuclear localisation of ERK associated with cell cycle arrest. Despite the same loss of phosphorylated ERK in resistant HMCLs, there was either minimal (KMS26) or no reduction (KMS12BM) in nuclear localisation of ERK, consistent with no change in cell cycles state seen in these HMCLs. In resistant cells lines this might suggest the nuclear machinery may operate autonomously in the absence of ERK. KMS12BM harbours a t(11;14) translocation, which results in overexpression of cyclin D1[19,20], as such this may result in autonomous progression from G_1 in the absence of nuclear ERK. Finally, it is possible through the accumulation of phosphorylated MEK in the presence of inhibitor (as reported in type 3 allosteric kinase inhibitors), ERK activation is restored within the 24-hour window, permitting progression to S-phase and maintenance of proliferation.

Similar to the nuclear localisation of ERK, the critical cyclin for progression from G_2 to M-phase is cyclin B. Cyclin B has four phosphorylation targets termed the cytoplasmic retention sequence (CRS)[241-244]. Two of these sites are kinase targets of active ERK. One is a target for polo-like kinase (PLK), whilst the final

kinase remains undefined. Once all four sites are phosphorylated, cyclin B translocates to the nucleus allowing progression to mitosis. Again, in sensitive HMCLs, we demonstrate treatment with trametinib results in a trend towards reduced nuclear cyclin B in MM1s and significant loss of nuclear cyclin B in NCI. Whilst in the resistant HMCLs no meaningful reduction in nuclear cyclin B was observed. This may be due to cyclin B freely passing into the nucleus in the absence of ERK phosphorylation.

To optimise response to targeted therapy, treatment in combination with a broad acting agent or cytotoxic may optimise response. Here we show that MEK inhibition in combination with dexamethasone, which forms the backbone of most myeloma therapy, is synergistic in five of eight HMCLs tested. As ERK activity promotes survival and anti-apoptosis[245], loss of active ERK in cells that are dependent upon the RAS-MAPK may leave them open to a second hit to induce apoptosis. In effect, inhibition of MAPK signalling may be priming cells for death.

There is now increasing novel inhibitors targeting pro-survival proteins available. In MM it has been identified that cells harbouring t(11;14) show sensitivity to BCL-2 inhibition[246]. Leveraging this knowledge of disease sensitivity, in combination with MEK inhibition priming cells for death, would be a rational approach to identifying combination strategies. A murine study utilising a t(11;14) HMCL (ie U266) as a platform for the combination of MEK inhibitor and BCL-2 inhibitor could answer this question. Further, as other disease subsets sensitivity to target inhibition are identified, MEK inhibition could potentially provide a backbone for optimising responses.

Finally, trametinib was tested in two murine xenografts. In a *RAS*^{M} model of disease, trametinib slowed disease progression, but had no effect on OS. The lack of effect on survival is thought due to the ongoing accumulation of disease in the pelvis still resulting in symptomatic HLP (a scientific end-point) despite lower total disease burden. This may reflect effectively starting therapy too late, once disease is well established and potentially too aggressive for a cytostatic therapy to be effective. In the *RAF*^{M} model, no effect was observed either alone

or in combination with dexamethasone. This was perhaps unsurprising, as for this HMCL little in vitro activity had been observed. In neither case was drug toxicity observed with respect to haematologic counts or GI toxicity. Further optimisation of dosing including using higher doses (i.e. 5mg/kg), not interrupting therapy with a week between cycles and combining MEKi with dexamethasone in the RAS^{M} model might result in improvements in OS.

MEK inhibition has clear potential in inhibiting RAS^{M} driven disease. Its effect is predominantly cytostatic, but significant cell death can be induced with the addition of a second agent. Subsequent investigations in this work investigate defining optimal combination therapy.

4. KINOME REPROGRAMMING & RATIONAL COMBINATION THERAPY

4.1 INTRODUCTION

Kinase inhibition aims to target activated oncogenes in critical signalling pathways involved in growth and proliferation, migration and metastasis, survival and anti-apoptosis, metabolism and differentiation[219]. However, most of these kinase targets are often but one of several dysregulated signalling pathways, and rather than absolute dependence upon a single signalling pathway, mutated kinases serve as secondary oncogenic drivers, providing survival advantages[218]. The one exception, chronic myeloid leukaemia (CML), is perhaps the only monogenic driven disease. Thus, whilst single targeted kinase inhibition can slow progression and even reduce tumour burden, this is often only for a limited period of time, invariably any one of a number of resistance mechanisms (as previously discussed) can overcome single targeted kinase inhibition. Further, single agent therapy activity may be limited in its efficacy due to its very specificity in addressing only a single pathway and characteristic of a tumour phenotype. As such, combination therapy would be favoured over monotherapy to potentially broaden activity, deepen and prolong duration of response. A relatively novel approach is to interrogate the tumour response(s) to single agent inhibition and identify potential combination therapies through "dynamic kinome reprogramming"[247,248].

Dynamic kinome reprogramming describes the process whereby, in the face of targeted kinase inhibition, over the space of hours to days, alternative signalling pathways are either activated or up-regulated to address the loss of the inhibited oncogenic pathway[249]. There are over 500 human protein kinases involved in modifying up to a third of the human proteome[250]. Collectively these are referred to as the kinome, to which the members of the RAS-MAPK belong. Whilst changes in gene expression are extensively studied in malignancy, in response to specific stressors and therapy, this largely ignores the numerous influences and processes on RNA that results in the final protein product and its activity.

These include mRNA stability, translation, protein turnover, and post-translational modifications including phosphorylation which truly lead to the phenotype of specific gene expression.

Novel techniques in proteomics have permitted interrogation of the wider "kinome", such that extensive changes in protein phosphorylation can be measured within hours of cell manipulation or drug exposure[247,250-252]. This allows for comparison of kinase pathways in treated and untreated cells, malignant and non-malignant tissues, and investigation of mechanisms of resistance and the potential to identify additional targets for intervention.

This approach has been used in MM, to investigate different signalling pathways in malignant plasma cells compared to normal plasma cells[253]. This study identified increased signalling in mTOR-p70S6K and ERK1/2 pathways, suggesting both of these pathways could be therapeutic targets in MM sparing normal plasma cells.

Interrogation of kinome-wide changes in triple negative breast cancer (TNBC) in response to treatment with the MEKi selumetinib have been studied[254]. Whilst loss of phosphorylated ERK was initially observed, by 24 hours reactivation of MEK2 and partial phosphorylation of ERK was again seen, likely due to loss of negative feedback loops and possible inhibitor dissociation. The extended "kinome" response showed up-regulation of RTKs including VEGFR2 and PDGFRβ. Subsequent combination therapy targeting the adaptive response of upregulation of RTKs with sorafenib in addition to selumetinib resulted in synergistic cytotoxicity.

Similarly, in MLL rearranged AML, cell lines treated with the laboratory MEKi UO126 for five days, resulted in up-regulation of the RTK VEGFR2[255]. Combining UO126 with an anti-VEGFR2 antibody induced synergistic cytotoxicity in the cell line. This combination was used against primary AML patient samples resulting in synergistic cytotoxicity in three of eight. The limited efficacy in primary patient samples may reflect the use of an antibody treatment in the absence of immune effector cells, as such outcomes may be different in-vivo.

Here we interrogate dynamic kinome changes in HMCLs in response to MEK inhibition.

4.2.1 STUDY RATIONALE & AIMS

As MEK inhibition is predominantly cytostatic rather than cytotoxic and given our findings of synergy in combination with dexamethasone, we sought to rationally identify additional inhibitors to pair with trametinib through interrogation of dynamic kinome reprogramming in HMCLs.

The work described in this chapter aimed to:

- Evaluate the kinome response in both sensitive and resistant HMCLs treated with trametinib
- Identify and validate potential "drug-able" targets
- Utilise combination therapy to maximise cytotoxicity
- Identify predictors of sensitivity for combination therapy

4.2.2 KINOME ARRAY

The PepScan Kinome Array (PepCHIP) (Lelystad, Netherlands) is a glass slide with three replicated 32x32 grids. At each "spot" on the grid an 11-12 amino acid peptide is attached to the surface. At each spot the peptide is as densely loaded as possibly (>100 peptides per spot). These sequences represent critical phosphorylation site of given proteins with flanking amino acids that enhance kinase recognition and specificity. To the slide, cell lysates containing active kinases, γ-33-ATP and an activating reagent are applied and incubated at 37^{o}C for two hours. Slides are then washed, air dried and exposed to a phosphor-storage screen for 24 to 72 hours, before imaging with a phosphor-imager.

The resultant image is output to MattLab® software, spot pixel means, and medians are calculated and corrected for background. Kolmogorov Smirnov distance and probabilities are calculated, and background "noise spots" are eliminated. Positive and negative control spots are included for control and

normalisation. From triplicate slide data standard deviation and coefficient of variation are calculated and outliers eliminated.

The resultant data provides information on both the phosphorylated peptide sequences/protein target and the upstream kinase responsible for the phosphorylation, allowing identification of recurrently activated proteins and pathways.

As with any array platform there are limitations. Culturing cells in supplemented media can result in activation of many more pathways/kinases than might be the case in vivo. Thus, activity on the array may be overstated for many kinases. Cell lysate preparation stresses cells potentially activating kinases not otherwise active in the base state. Further, lysate preparation may result in loss or inactivation of kinases. Finally, whilst in vivo there is high specificity of cellular kinases, outside of the cell this specificity may be lost. Even in the presence of the flanking amino acids sequence, without the extended and complex protein-protein interactions specificity may be lost leading to false positivity.

4.2.3 STUDY DESIGN

We evaluated the kinome in four HMCLs, two sensitive *RAS*^{M} (MM1s & NCI) and two resistant t(4;14) HMCLs (KMS26 and LP1) at baseline and following 24 hours treatment with trametinib 1μM. We did not select WT HMCLs as KMS12BM did not express baseline phosphorylated ERK, which suggested there were unlikely to be any meaningful cellular responses to MEK inhibition. Further, as we had expected a response to MEK inhibition in t(4;14) HMCLs due to aberrant MAPK signalling but had not observed a response we anticipated kinome changes may play a role in this.

Combined analysis of both the two sensitive and two resistant HMCLs was undertaken to improve specificity in identifying differentially activated kinases in response to MEK inhibition, that might represent pathways of resistance and early dynamic kinome reprogramming.

4.3 RESULTS

4.3.1 Kinome array analysis identifies kinase targets & pathways of resistance to targeted kinase inhibition

We treated two sensitive and two resistant HMCLs with trametinib 1μM for 24 hours. Three consecutive cell passages were treated the same way, snap frozen on dry ice, then analysed as a single batch. Figure 4.1 shows typical PepCHIP® slide images from our experiments.

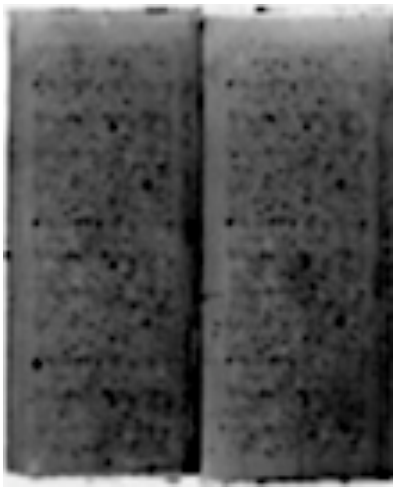

Figure 4.1: Representative PepCHIP® images.

As commented previously, to better identify general targets of resistance, rather than specifics to a single HMCL, the results from both sensitive and both resistant HMCLs were collated for comparison.

Differential kinome array analysis identified recurrent pathways and specific "drug-able" targets in resistant HMCLs that may confer resistance to MEK inhibition. Enriched pathways included PI3K/AKT, JNK/BCL-2 and CK2α (Figures 4.2 & 4.3). As AKT inhibition in combination with a MEKi has already been tested clinically and was poorly tolerated, limiting its utility, we did not investigate the combination further[183].

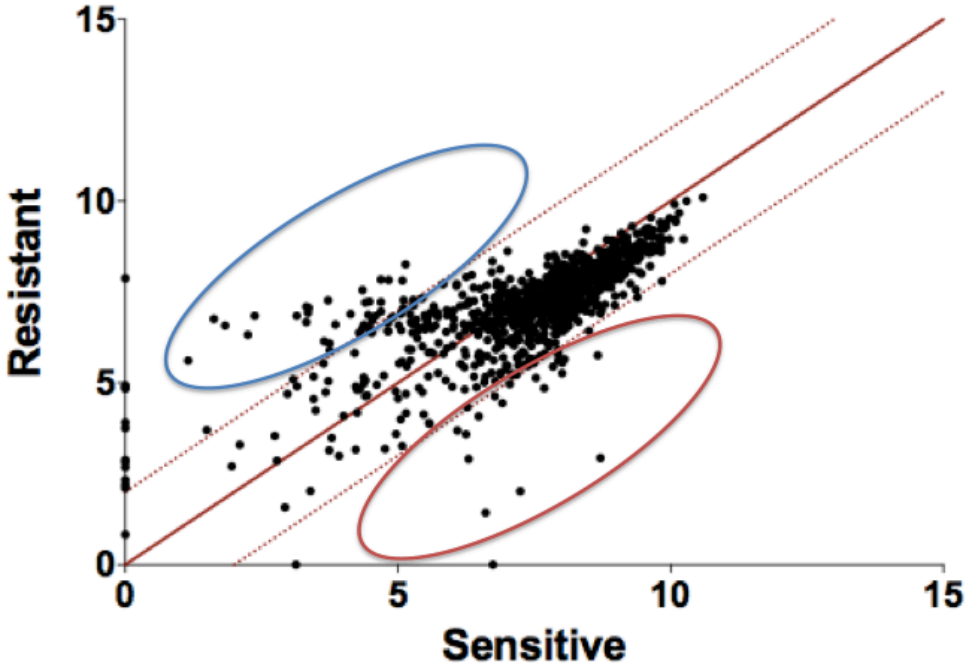

Figure 4.2: Dot plot comparing PepCHIP® data of sensitive & resistant HMCLs. Dotted lines represent ±2-fold difference in phosphorylation, considered a significant change in phosphorylation. Spots within the blue circle represent phosphorylation targets with increased phosphorylation in resistant HMCLs after treatment and are likely to represent changes associated with resistance. Spots within the red circle represent increased phosphorylation in sensitive HMCLs following treatment and are likely to represent changes associated with sensitivity. Dot intensity is the average of n=3 biologic replicates.

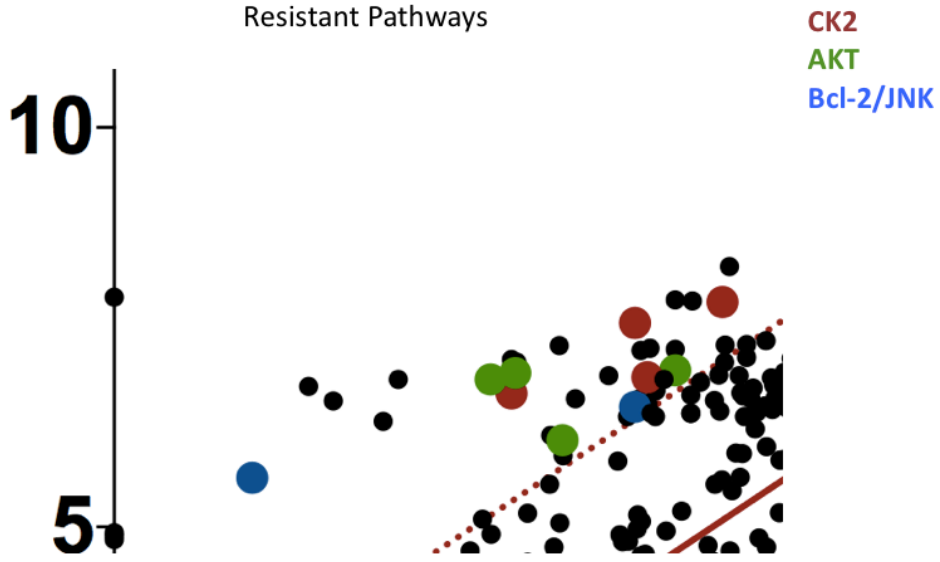

Figure 4.3: Peptide spots/pathways enriched in resistant HMCLs.

4.3.2 CK2α is overexpressed in HMCLs

Casein Kinase 2α (CK2α) is a ubiquitously expressed, constitutively active kinase which plays a supporting or enhancing role in many normal and malignant cellular processes. These include proliferation, growth, survival and resisting apoptosis. Specific to the MAPK, CK2α is known to phosphorylate activated ERK facilitating cytoplasmic nuclear translocation.

We validated the expression of CK2α as a target in HMCLs. In all cells tested, CK2α expression is greater than normal CD138+ (Figure 4.4).

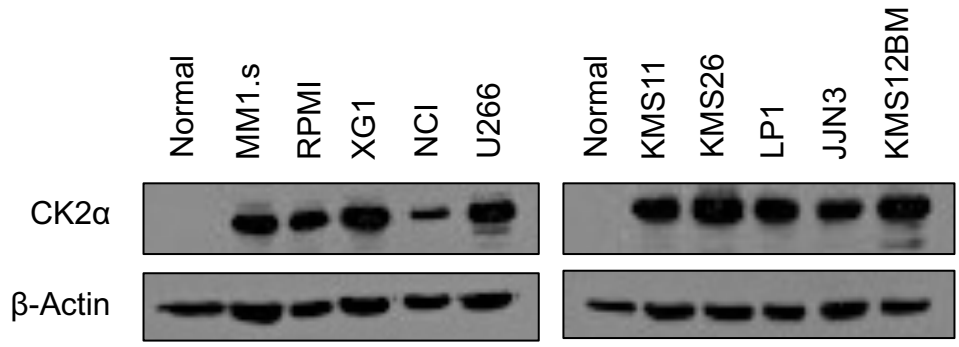

Figure 4.4: CK2α is overexpressed in HMCLs compared with normal CD138+ cells. All HMCLs overexpress CK2α compared to normal CD138+ cells.

4.3.3 Combined MEK & CK2α inhibition results in synergistic cytotoxicity in HMCLs

CX-4945 (silmitasertib) is an orally bioavailable ATP competitive inhibitor of CK2α[256]. Trametinib in combination with silmitasertib resulted in synergistic cytotoxicity in all *RAS*^{M} and t(4;14) HMCLs. No activity was observed in WT HMCLs (Figure 4.5). Whilst the combination was synergistic in t(4;14) HMCLs, the percentage of cell death was modest, cell proliferation was markedly reduced (Figure 4.6).

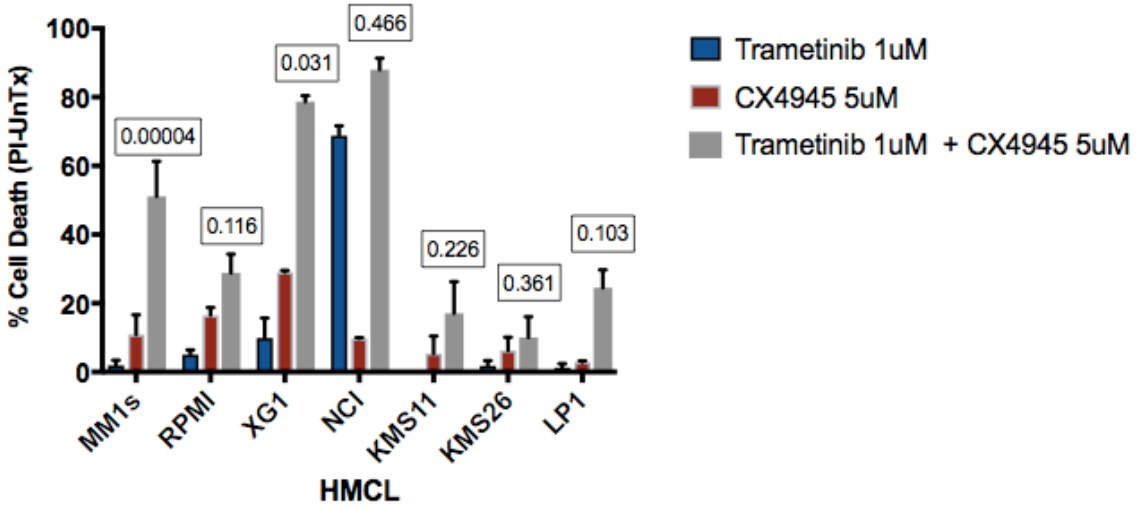

Figure 4.5: Synergistic cell death in HMCLs treated with trametinib & silmitasertib. The combination of silmitasertib and trametinib is synergistic in both *RAS*^{M} and t(4;14) HMCLs. Synergy was not observed in WT HMCLs. The CI of NCI and KMS26 are closer to additive rather than synergistic. Further, in KMS26 the cell death in combination fails to reach 20%. The box above each HMCL is the combination index, values of <1 are considered synergistic. (n=3, mean ±SEM).

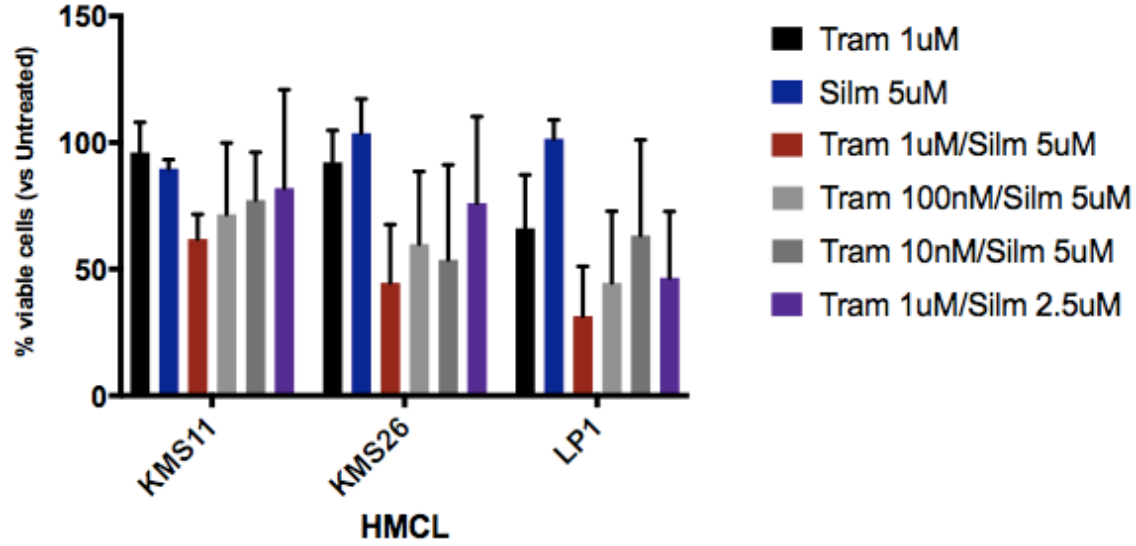

Figure 4.6: Cell counts of combination trametinib & silmitasertib t(4;14) HMCLs. Combinations of trametinib and silmitasertib result in reduced proliferation at 72 hours in t(4;14) HMCLs. Tram = trametinib, Silm=silmitasertib. (n=3, mean ±SEM).

We knocked down CK2α using siRNA to test loss of CK2α in combination with trametinib. Whilst knockdown was successful (Figure 4.7) subsequent treatment with trametinib failed to achieve the same cytotoxicity of CX-4945.

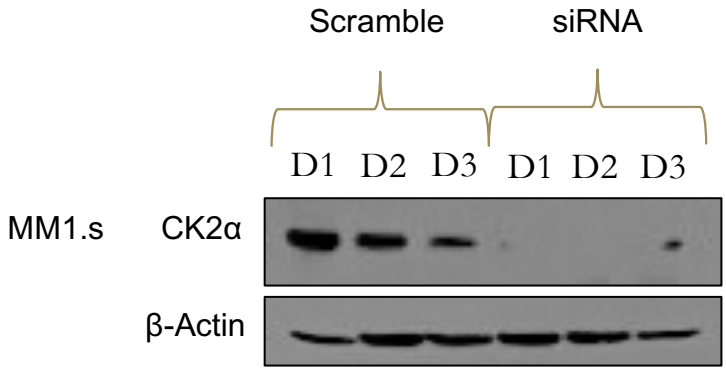

Figure 4.7: siRNA of CK2α. Successful knockdown of CK2α within 2 days

4.3.4 Phosphorylated BCL-2 is expressed in a subset of HMCLs & predicts for sensitivity to combined MEK & BCL-2 inhibition

Next, we investigated the expression of phosphorylated and total BCL-2 in HMCLs. BCL-2 is expressed in a limited number of HMLCs (Figure 4.8, A-C). *KRAS*^{M} HMCLs expressed phosphorylated BCL-2 at baseline, whilst *NRAS*^{M} did not. As previously described, we also found KMS12BM (a t(11;14)) also expressed phosphorylated BCL-2. All HMCLs that expressed BCL-2 also expressed the phosphorylated form.

ABT-199 (venetoclax) is a specific, orally bioavailable inhibitor of BCL-2[257]. As monotherapy, venetoclax had almost no effect against any HMCL except the WT HCMLs JJN3 and KMS12BM. The kinome array reported an increase in phosphorylated BCL-2 after treatment with trametinib, which was seen in LP-1 whilst the reverse was seen in WT HMCLs. Treatment with venetoclax in combination with trametinib, in *RAS*^{M} and t(4;14) HMCLS with baseline phosphorylated BCL-2 (Figure 4.8), resulted in synergistic cytotoxicity, with modest percentages of cell death (Figure 4.9).

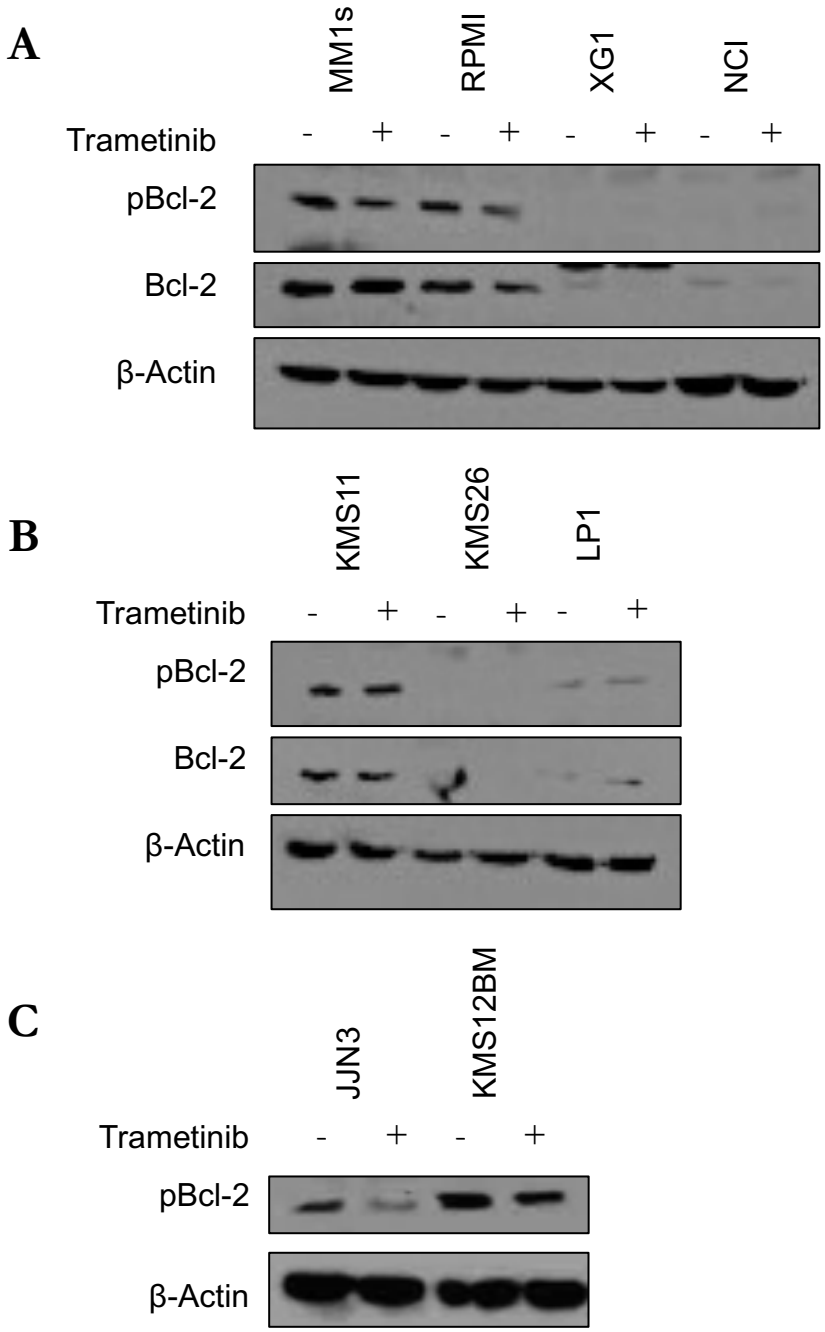

Figure 4.8: Total BCL-2 & phosphorylated BCL-2 in HMCLs. (A) *KRAS*^{M} HMCLs expressed BCL-2, whilst *NRAS*^{M} did not. The higher molecular weight band seen in XG1 is thought to be BCL_{XL} non-specific binding of the antibody. **(B)** Only one of three t(4;14) HMCLs expressed BCL-2. Whilst increased expression of BCL-2/phosphorylated-BCL-1 was seen in LP1 following treatment with trametinib. **(C)** Both WT HMCLs expressed phosphorylated BCL-2.

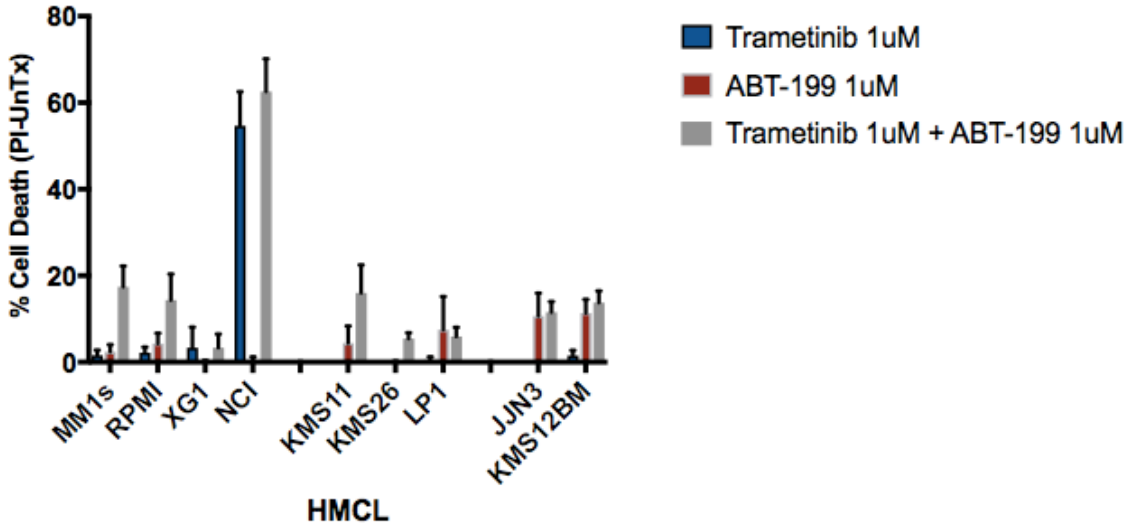

Figure 4.9: Cell death in HMCLs treated with the combination trametinib & venetoclax. Modest levels of cell death were observed following treatment with trametinib and venetoclax in *RAS*^{M} and t(4;14) HMCLs that expressed phosphorylated BCL-2 at baseline. (n=2, mean ±SEM).

4.3.5 Kinome array analysis identifies kinases & proteins that may confer sensitivity to targeted kinase inhibition

Table 4.1 lists the recurrent phosphorylated peptides whose phosphorylation change may confer sensitivity.

Peptide Target	Upstream Kinase
CHK2	ATM
ATM	
CDA1/TSPYL2	CDK2
H2AX	

Table 4.1: List of recurrently phosphorylated targets & respective kinases in sensitive HMCLs.

Consistent with our findings from chapter 3, many of the recurrent protein targets and kinases identified in sensitive HMCLs are involved in cell cycle regulation, at both the $G_{0/1}$ and G_2/M checkpoints, on a background of WT *p53*. Whilst these are not "targetable" kinases per se, they are suggestive of mechanism(s) potentially responsible for sensitivity to MEK inhibition. Secondly, proteins

involved in the DNA damage response/DNA double strand break are recurrently identified. This is an effect previously observed in solid tumours.

4.4 DISCUSSION

Evaluation of the extended kinome responses to targeted MEK inhibition rationally identified targetable kinases for combination therapy, that resulted in synergistic cytotoxicity. We identified and validated two targets, one protein target and one kinase, whose activities limit the efficacy of MEK inhibition. The first of these, CK2, is a constitutively active kinase involved in several cellular processes. The second, BCL-2, a mitochondrial protein involved in resisting apoptosis. Where others groups identified up-regulation of RTKs[254,255], whose activity would likely overcome that of MAPK inhibition, we have identified a kinase intimately involved in enhancing supporting of the MAPK and a mechanism to resist apoptosis.

Casein kinase 2 (CK2) is a ubiquitously expressed, constitutively active kinase with over 500 protein and kinases targets identified[258-260]. It is a tetramer, composed of two catalytic α (or α') subunits and two regulatory β subunits[261]. Its many roles include potentiating, enhancing and sustaining signalling pathways, resisting apoptosis and inhibiting tumour suppressors. Specific to the MAPK, it phosphorylates two additional sites on active ERK marking it for and enhancing nuclear translocation[236]. Activating mutations of CK2 have not been identified, but it has been found to be overexpressed in many malignancies, including MM, leading to the concept of non-oncogene addiction[217,262-264].

Similar to previously published results, we confirmed CK2α overexpression in MM compared with normal plasma cells[262,264]. This makes it an attractive target for inhibition, likely sparing normal plasma cells. In combination with trametinib, the CK2α inhibitor silmitasertib, induced marked synergistic apoptosis in *RAS*^{M} HMCLs. In t(4;14) HMCLs cell death was limited but synergistic, with marked inhibition of proliferation. Whereas in WT HMCLs no significant effect of either agent alone or in combination was seen. Silmitasertib is an orally active inhibitor,

currently undergoing investigation in several haematologic malignancies in combination with other inhibitors[265].

Targeting CK2α in combination with trametinib, represents a broad targeting agent with a wide reach number of pathways affected by its activity. Similar to our previous findings of trametinib in combination with dexamethasone, the addition of an inhibitor with a broad reach of many targets, may be an ideal partner agent to the very specific targeted MEKi to optimise cytotoxic effects and potentially delay resistance.

Knockdown of CK2α with siRNA was achievable for up to 72 hours in MM1s. Despite this successful knockdown, no appreciable cell death was observed with subsequent treatment with trametinib. This incongruent response between silmitasertib and siRNA knockdown may be due to the specificity of the siRNA for the α-subunit, as it is possible CK2α' may still be active and functional[261]. Further, siRNA knockdown may not be sufficiently prolonged or complete (despite the WB findings, Figure 4.7) to reproduce the effect of the chemical inhibitor. Alternatively, silmitasertib as an ATP-competitive inhibitor may have off-target effects[232].

The second target identified by kinome analysis was BCL-2, a mitochondrial protein involved in resisting apoptosis[266]. Several of the BCL-2 family members have been identified to play a role in plasma cell survival[267,268]. We demonstrated BCL-2 expression in *KRAS*^{M} but not *NRAS*^{M} HCMLs, two of three t(4;14) HMCLs (KMS11 and LP1), JJN3 and, as previously described, the t(11;14)[246] HMCL KMS12BM.

ABT-199 (venetoclax) is an orally active small molecule inhibitor of BCL2[257] with profound efficacy in CLL[269]. We recapitulated the single agent cytotoxic effects of venetoclax against the t(11;14) HMCL KMS12BM[246]. However, there was very limited cytotoxicity otherwise in any HMCL treated with venetoclax alone. In RAS^{M} and t(4;14) HMCLs with baseline expression of phosphorylated BCL-2, treatment with the combination of trametinib and venetoclax resulted in

synergistic cytotoxicity, albeit with modest rates of cells death. Unsurprisingly the combination did not further enhance the cytotoxic effect observed in KMS12BM. Venetoclax is currently under extensive investigation for combination treatment in MM[270,271].

In both instances, the most profound effects with the addition of a second inhibitor were observed in HMCLs already considered sensitive to trametinib monotherapy. Similar effects, although to a lesser extent, were observed in the t(4;14) HMCLs. Essentially no meaningful responses were observed for combination therapy in WT HMCLs. This is despite the kinome array analysis being intended to identify mechanisms of resistance. This may be due to several reasons:

First, the initial cell selection for the platform. As described in the study design we chose two *RAS*^{M} and two t(4;14) HMCLs. As such, we have not interrogated the effects of trametinib on the kinome response of WT HMCLs. To better assess this, the addition of WT HMCLs to the platform, that are known to express phosphorylated ERK would be required.

And second, a more marked response in sensitive HMCLs may be seen due to potentially greater reliance on CK2 activity in *RAS*^{M} lines once MEK is inhibited. It is likely given the oncogene addiction to RAS-MAPK signalling that support to the pathway from CK2 is of significant importance. Whilst CK2α inhibition had a modest effect in t(4;14) lines, their dependence up the RAS-MAPK and its partner kinases might be somewhat less than *RAS*^{M} lines.

The kinome array also identified cellular responses that might predict for sensitivity. Our kinome array findings were consistent with those reported in Chapter 3, that MEK inhibition can prevent cell cycle progression, particularly arresting *p53* WT cells at $G_{0/1}$. The kinome array recurrently identified kinases and their targets responsible for these effects. Whilst these are not “target-able” per se, they provide insight to the machinery required and might suggest other

mechanisms of resistance should these kinases and/or targets be absent, dysfunctional or mutated.

Additionally, the array identified a DNA damage response to MEK inhibition, previously observed in solid tumours[272,273]. This response gives insight to the potential priming effects and synergism observed in combination therapy.

Platform kinome interrogation can rationally identify combination targets to optimise response to MEK inhibition. Targeting the overexpressed kinase CK2α with silmitasertib in addition to trametinib results in either synergistic cytotoxicity or growth inhibition, where it was not previously seen. Phosphorylated BCL-2 is a biomarker of sensitivity for the combination venetoclax and trametinib, in both *KRAS*^{M} and t(4;14) disease.

5. IDENTIFYING MARKERS OF SENSITIVITY & RESISTANCE

5.1 INTRODUCTION

The presence of specific mutations within critical signalling pathways, overexpression of surface receptors or specific hormones/enzymes is the standard for identifying patients who might benefit from targeted therapy. However, experience from *BRAV^{M}* V600E melanoma has shown that simply having activating mutations does not guarantee sensitivity to targeted therapy[192]. Additional mutations within the RAS-MAPK, activation of parallel signalling pathways (PI3K/ATK) and their mutations (i.e. PTEN mutations), mutations in activators of protein kinases (RAC1) as well genes/proteins with seemingly unrelated or distinct actions (HOXD8) all potentially confer upfront or rapid acquisition of resistance to targeted therapy. Similarly, in CRC, concomitant mutation within the MAPK-pathway results in resistance to EGFR targeted therapy[274]. In both instances either there is no response to initial therapy or disease progression occurs rapidly after therapy is commenced.

Defining markers of sensitivity to targeted therapy should better help predict which patients will most likely benefit, reduce unnecessary treatment where failure is likely and in doing so reduce both unwanted toxicity and costs. Alternatively, identifying mechanisms of resistance to targeted therapy might also provide insight to better combination therapies.

Our data shows, that whilst activating *RAS^{M}* to confer sensitivity to MEK inhibition there are discrepant responses HMCLs harbouring similar *RAS^{M}*. Further, HMCLs with *RAF^{M}* do not exhibit the same degree of sensitivity to MEK inhibition as do the *RAS^{M}* lines. Additionally, HMCLs that do not harbour MAPK pathway mutations can exhibit some sensitivity to inhibition. This suggests that similar to the descriptions in melanoma, other genes and pathways are modifying response to targeted MEK inhibition.

A large-scale screening study in both solid and haematologic cancer cells lines investigated potential predictive markers of sensitivity and resistance to

trametinib[275]. As expected, *RAS*^{M} and *RAF*^{M} were the biggest predictors or sensitivity to trametinib. Concurrent mutations in *PI3K/PTEN* reduced the response from cytotoxic to cytostatic. In the presence of *KRAS*^{M}, a gene expression profile consistent with an "epithelial-to-mesenchymal" (EMT) phenotype exhibited less sensitivity. Whilst expression of DUSP6, a dual specificity phosphatase which inactivates phosphorylated ERK2, was associated with sensitivity.

Investigation of gene transcription signatures, independent of *RAS*^{M} or *RAF*^{M}, that reflect MAPK pathway activation might better predict disease phenotypes that respond to MEK inhibition. Studies in gastric cancer[276], CRC[277] and NSCLC[278] have recurrently identified genes that confer sensitivity to MAPK-pathways inhibition. These gene signatures would foreseeably identify more cases that would respond to targeted therapy rather than just those selected on mutation alone. Additionally, response signatures might better account for influences outside of the MAPK that might abrogate response to targeted inhibition. Consistent with this, a MEK-signature study in gastric cancer patients revealed that *PIK3CA* mutations were mutually exclusive from the signature consistent with previous reports that this mutation can mediate resistance to MEK inhibition[279].

Here we investigate gene expression to identify mechanisms of sensitivity and resistance to trametinib in HMCLs.

5.2 STUDY RATIONALE & AIMS

Given the different responses observed to targeted MEK inhibition in various HMCL subsets, we sought to identify genes and proteins responsible of sensitivity or resistance.

The work described in this chapter aimed to:

- Identify genes and their proteins that might confer sensitivity or resistance
- Corroborate differential gene expression signatures of sensitivity
- Validate these genes/expression signatures in a broader set of HMCLs

- Identify specific gene changes with the MAPK in response to treatment with trametinib

HMCLs that show >50% reduction in proliferation in response to trametinib at 10nM doses were considered sensitive for these studies.

Sensitive HMCLs	Intermediate HMCLs	Resistant HMCLs
MM1s	XG1	KMS11
RPMI	U266	KMS26
NCI		LP1
ANBL6		JJN3
		KMS12BM

Table 5.1: List of sensitive, intermediate and resistant HMCLs.

5.3 RESULTS

5.3.1 Illumina HT-12 gene array identified a small set of differentially expressed genes

Using existing gene expression data from the Illumina-HT12 platform we analysed differential gene expression in a panel of sensitive and resistant HMCLs.

Sensitive Genes			Resistant Genes
AKR1C3	ILDR1		LEF1
CD68	LGMN		SLC47A1
CD86	LXN		TMEM2
CRYBB1	NLRP7		
CXCL10	PACSIN1		
DMRT2	PLAC8		
FCRLA	SIRPA		
GNG10	SNCAIP		
GSDMC	SULF2		

Table 5.2: List of genes with increased expression in either sensitive or resistant HMCLs.

5.3.2 PCR validation identifies LXN as a marker of sensitivity

The gene expression results had a number of limitations, (i) it was across two different platforms in time, (ii) the results were approximately five years old and (iii) surprisingly few genes were found to be differentially expressed. From this we selected a number of genes based on degree of differential expression and biologic plausibility for further validation with PCR in a larger validation set of HMCLs.

PCR of an initial panel of genes from the gene array in a broader set of HMCLs did not correlate with sensitivity to treatment with trametinib (Figure 5.1).

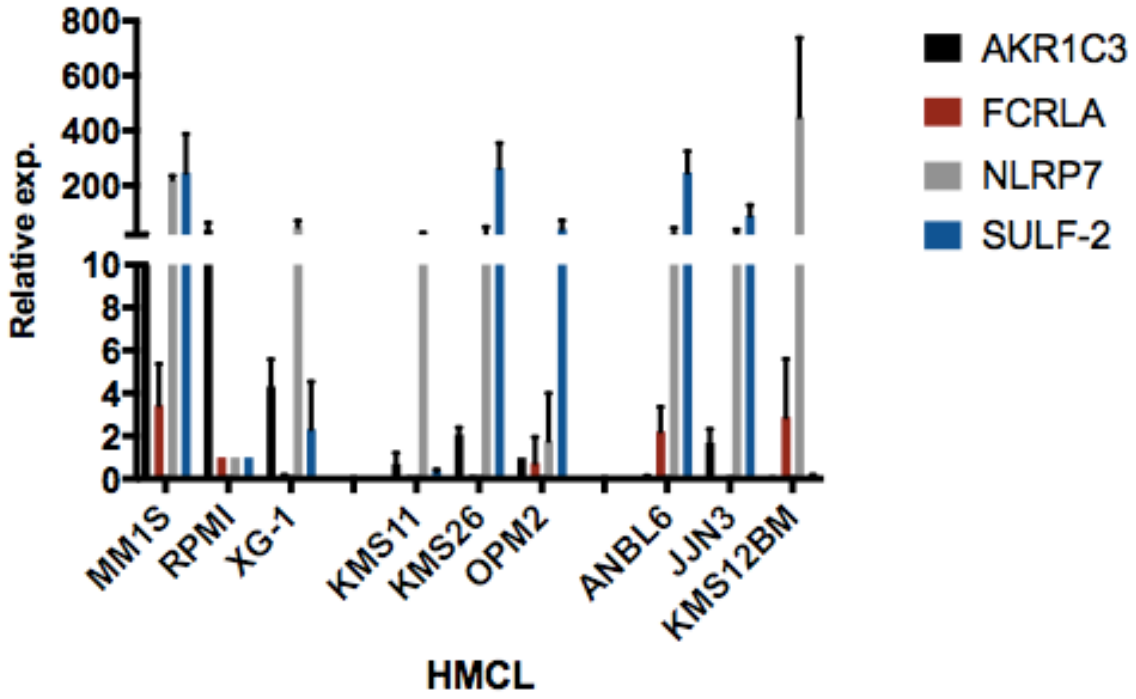

Figure 5.1: RT-PCR gene expression of 4 genes: AKR1C3, FCRLA, NLRP7, SULF-2. Relative gene expression (to RPMI) of 4 genes identified by gene expression profiling, showed no correlation with sensitivity of HMCLs. (n=3, mean ±SEM).

Next, we investigated the expression of latexin (*LXN*). Its expression was confined to sensitive HMCLs only, with no expression observed in any of the resistance HMCLs. Protein expression was confirmed by WB. (Figure 5.2 A, B)

5.3.3 siRNA knockdown of LXN does not affect the sensitivity of MM1s

To confirm the role of LXN in conferring sensitivity, we performed siRNA knockdown in MM1s with subsequent treatment with trametinib. Whilst knockdown was successfully achieved out to 48 hours, re-expression occurred at 72 hours (Figure 5.3). MM1s retained its sensitivity to trametinib despite knockdown of LXN.

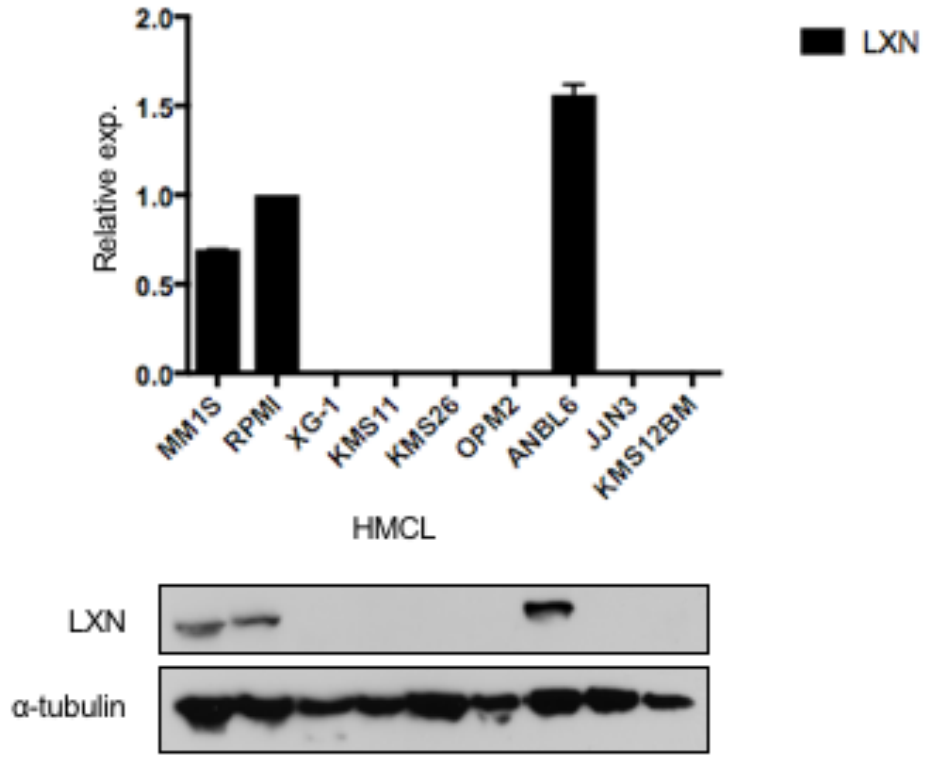

Figure 5.2: Latexin (LXN) expression by RT-PCR & WB. LXN expression was confined to sensitive HMCLs only, with no expression observed in resistant HMCLs. α-tubulin is the loading control. (PCR n=3, mean ±SEM).

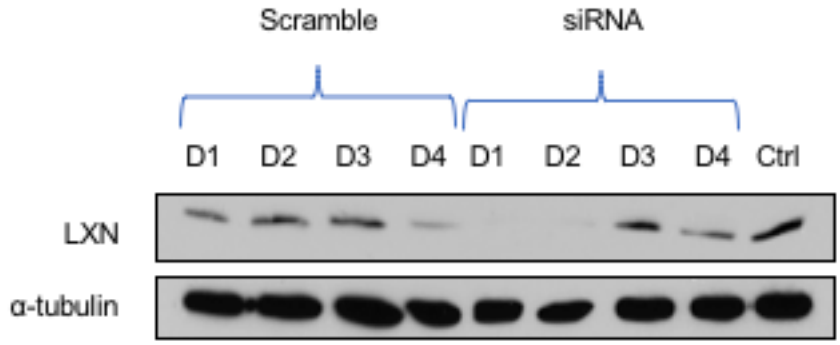

Figure 5.3: siRNA knockdown of LXN in MM1s. Knockdown of LXN was achieved for 48 hours before re-expression. Treatment of MM1s with trametinib after siRNA knockdown did not result in loss of sensitivity. α-tubulin is the loading control.

5.3.4 LXN is hyper-methylated in resistant HMLCs and its expression can be induced by azacitidine

It has previously been described that *LXN* is hyper-methylated in many malignancies. We confirmed these findings in the resistant HMCLs KMS11, KMS26, JJN3, and KMS12BM using bisulfite sequencing. This revealed methylation of 15 CpG sites proximal to the start codon. Treatment for five consecutive days with azacitidine 1μM resulted in gene and protein re-expression of LXN (Figure 5.4 A, B).

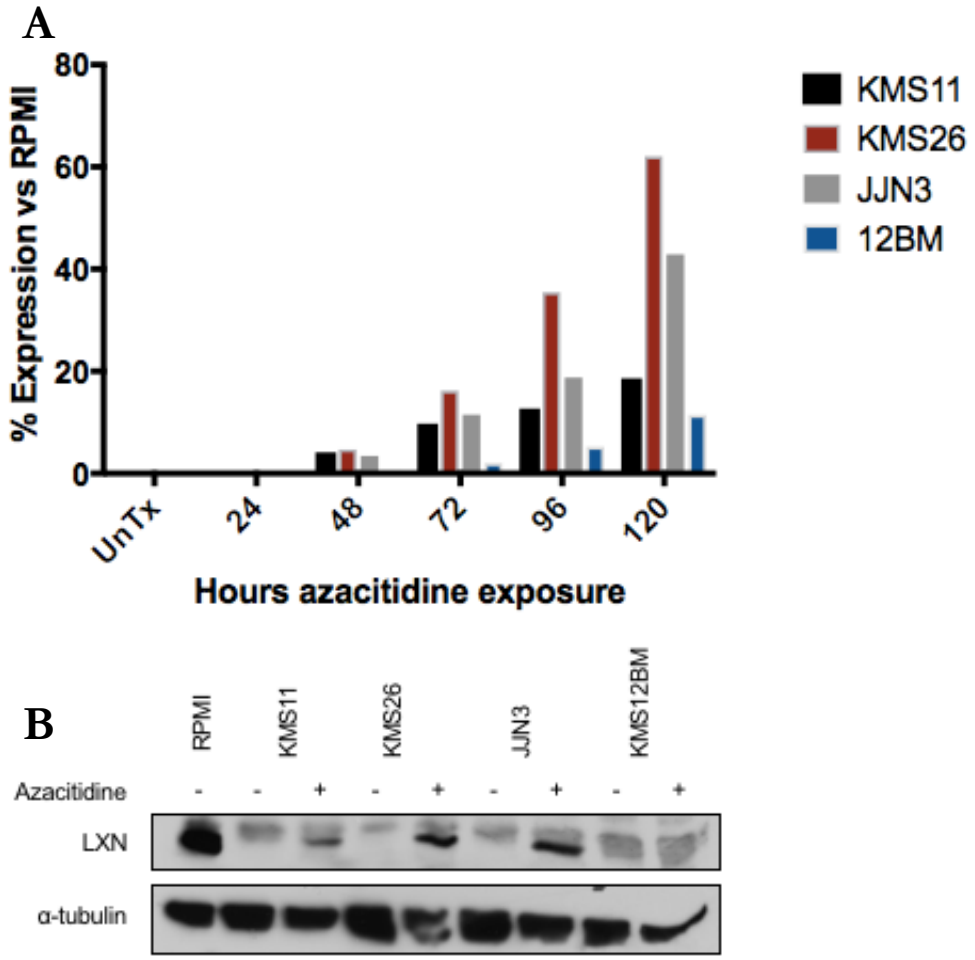

Figure 5.4: Re-expression of LXN following azacitidine 1μM. (A) *LXN* gene expression by RT-PCR increases progressively with azacitidine 1μM for 120 hours. (Reported as percentage gene expression vs RPMI). **(B)** LXN protein expression with and without azacitidine 1μM at 120 hours. Re-expression variably occurs in KMS11, KMS26 and JJN3, but not KMS12BM. α-tubulin is the loading control. RPMI is the positive control.

Trametinib treatment after azacitidine 1μM for five days resulted in significant cytotoxicity in resistant HMCLs. However, azacitidine doses of 1μM are clinically unachievable, and would likely result in several affects rather than just gene re-expression. As such we tested resistant HMCLs with clinically achievable, sub-lethal doses of azacitidine followed by treatment with trametinib. These results are reported in chapter 6.

5.3.5 SLC47A1 expression does not correlate with resistance

We investigated whether SLC47A1 correlated with resistance to trametinib. SLC47A1 (MATE-1, a multidrug and toxin extrusion protein-1) is a known drug and ion transporter[280] typically involved in renal excretion. We postulated that SLC47A1 may be a mechanism of drug efflux from the cell, and thus a cause of resistance. However, SLC47A1 is variably expressed in most HMCLs irrespective of sensitivity to trametinib (Figure 5.5.). Further, as we have previously shown, treatment with trametinib results in loss of phosphorylated ERK in all HMCLs, suggesting that trametinib is not extruded from the cell and is not a mechanism of resistance.

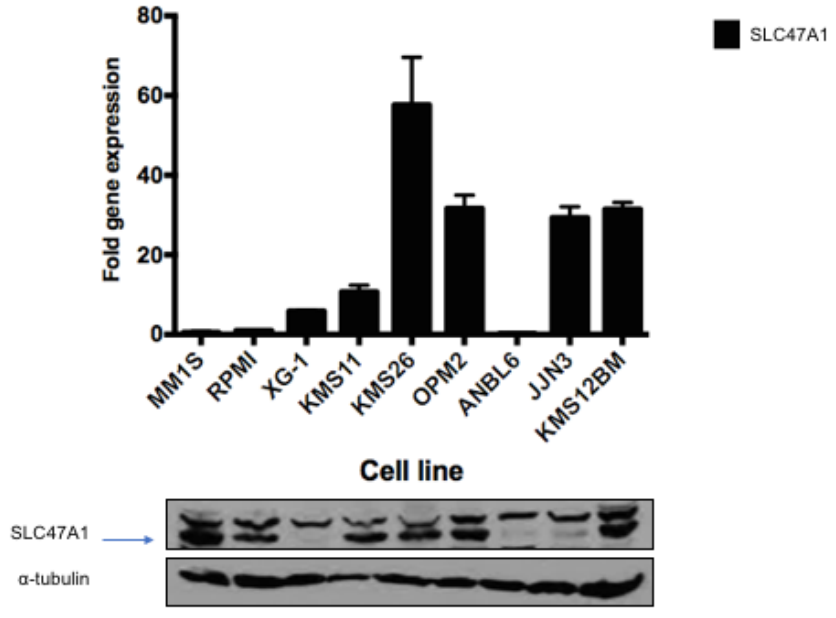

Figure 5.5: SLC47A1 expression by RT-PCR and WB. SLC47A1 was variably expressed at both the gene and protein level in most HMCLs tested and did not correlate with resistance. SLC47A1 is the lower band on the WB, as marked by the blue arrow. α-tubulin is the loading control. (PCR n=3, mean ±SEM).

5.3.6 MAPK gene expression does not change after treatment with trametinib

We next investigated changes in gene expression specific to the RAS-MAPK and downstream effectors. This was performed using the QIAGEN RT^2 RAS-MAPK array in two sensitive and two resistant HMCLs both pre- and post-treatment. In none of the HMCLs were any significant changes in MAPK gene expression observed. Thus, we excluded dynamic changes in gene expression as the cause of sensitivity or resistance to trametinib. (Data is presented in Supplementary Figure 9.3)

5.3.7 RNA-sequencing recapitulates the MEK-sensitivity gene signature

We expanded the selection of HMCLs and performed RNA-sequencing to identify genes and pathways potentially associated with trametinib sensitivity. Averaged expression for sensitive and resistant genes identified 5994 differentially expressed genes. When considering genes that either were expressed in all sensitive or all resistant HMCLs the number of differentially expressed genes was 485 (Figure 5.6). In neither of these panels did mapping to GO or KEGG pathways identify any significantly over represented pathways.

Analysis of RNA-seq data for previously reported MEK-sensitivity gene signatures, confirmed four of six genes to be overexpressed in sensitive HMCLs (Table 5.2).

5.3.8 CXCR-3 & its ligands, CXCL9 & CXCL10, correlate with sensitivity

The most significantly differentially expressed gene identified by RNA-seq was *CXCR3*. The ligands of CXCR3, CXCL9 and CXCL10 were also found to be significantly overexpressed. These were validated by RT-PCR in a wider set of HMCLs (Figure 5.7). Despite the greater gene expression, MM1s was the only HMCL that expressed surface CXCR3 as per flow cytometry (Supplementary Figure 9.4). CXCR3 has previously been described on HMCLs and MM cells, but its functional role remains unclear[281-283].

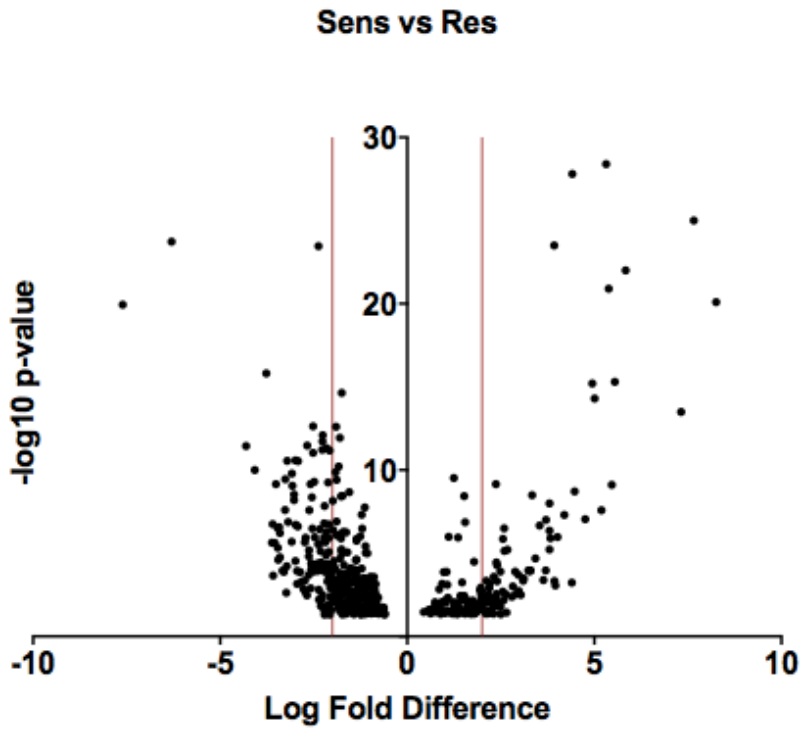

Figure 5.6: RNA-seq volcano plot of significantly differentially expressed genes. RNA-seq identified 485 differentially expressed genes. Red lines represent 2-log_2 fold difference.

Gene	log2 Fold Difference	P-vale
DUSP4	3.2775	$5.32x10^{-6}$
DUSP6	3.2412	$4.84x10^{-6}$
ETV4	2.285	0.0002
ETV5	3.8277	$2.52x10^{-8}$
PHLDA1	Not detected	
SPRY2	Not detected	

Table 5.3: RNA-sequencing genes consistent with a MEK-sensitive signature. RNA-seq of differentially expressed genes recapitulated four of six previously described genes found to confer sensitivity to MEK inhibition. These were identified in MM1s, RPMI, NCI and ANBL6.

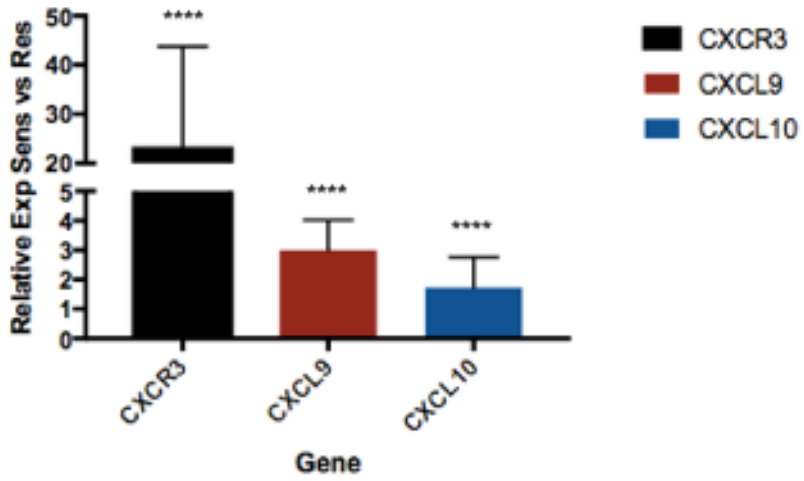

Figure 5.7: CXCR3, CXCL9 & 10 expression in sensitive HMCLs. CXCR3 and its ligands are all significantly overexpressed in sensitive HMCLs compared to resistant. *CXCR3* p=8.8x10^{-8}, *CXCL9* p=0.0005, *CXCL10* p=3.65x10^{-5}.

5.4 DISCUSSION

Targeting oncogene addiction relies on identification of the presence of a mutant or overexpressed target. However, often just the presence of this target does not guarantee efficacy of the targeted therapy. Predictive biomarkers, beyond single gene mutation, may better identify patients with disease that is likely to respond to targeted therapy. We have found *RAS*^{M} to predict sensitivity to MEK inhibition. However, there is heterogeneity in response between *RAS*^{M} HMCLs. Further, a small number of HMCLs that do not harbour a *RAS*^{M} also exhibit sensitivity to MEK inhibition. As has been reported in *BRAF*^{M} V600E melanoma[192], EGFR expressing CRC[274] and *HER2* amplified breast cancer[284], these simple markers do not universally predict for sensitivity to the targeted therapy. This in turn has led to the development of targeted therapy sensitivity gene-signatures[276-278].

Our gene array data identified relatively few differentially expressed genes between sensitive and resistant cell lines. Validation of these genes in an expanded set of HMCLs with both RT-PCR and WB, found only a single gene, *LXN* as a correlate of sensitivity. *LXN* is a putative tumour suppressor gene, whose expression has been found to confer a better prognosis in hepatocellular[285], gastric[286] and pancreatic[287] cancers and melanoma[288]. Further, in B-cell lymphomas, its expression is down regulated by hyper-methylation, with

re-expression leading to inhibition of lymphoma growth[289]. We also identified *LXN* to be methylated MM and successfully re-induced its expression in trametinib resistant HMCLs using azacitidine 1μM for five days. Pre-treatment with azacitidine resulted in profound sensitisation to subsequent treatment with trametinib and universal cell death in these resistant lines. At this clinically unachievable dose of azacitidine, undoubtedly numerous genes are re-expressed, and the specificity of this effect is low. Further, the effect of azacitidine alone as the cause of loss of viability is highly likely. However, the sensitisation of resistant HCMLs to trametinib suggested possible re-expression of silenced tumour suppressors. We further investigate the role of azacitidine inducing sensitivity in chapter 6.

We investigated whether drug efflux from resistant cell lines via the multidrug and toxin extrusion-1 transporter (MATE-1/SLC47A1), caused resistance in HCMLs, similar to the role of OCT1 (SLC22A1) affecting sensitivity to imatinib in CML[290]. However, SLC47A1 expression was present on both resistant and sensitive HMCLs. Further, loss of phosphorylated ERK in resistant HMCLs would suggest that cellular drug efflux does not mediate resistance to inhibitor. As such, mechanistically, SLC47A1 does not appear to be implicated in drug resistance in MM.

We analysed gene expression specific to the RAS-MAPK and its changes in response to MEK inhibition. No significant changes were observed in any of the genes of the RAS-MAPK in either sensitive or resistant HMCLs, that would affect their sensitivity to MEK inhibition.

We next utilised RNA-sequencing of HMCLs which identified over 5000 differentially expressed genes between sensitive and resistant HCMLs. However, recurrent pathway analysis failed to identify significantly enriched pathways associated with sensitivity. The most significantly differentially expressed gene, *CXCR3*, was confirmed to be overexpressed in sensitive lines, along with its known ligands *CXCL9* and *CXCL10*. Interestingly the surface expression of *CXCR3* by flow cytometry, was only confirmed in MM1s, with no other sensitive

HMLC demonstrating receptor expression. As such, whilst gene expression may identify sensitivity to trametinib, the utility of this marker in immunohistochemistry to identify sensitivity would be limited.

Our RNA-sequencing data recapitulated previously published RAS/MEK inhibitor sensitivity gene signatures[276-278]. Four out of six genes from these panels were similarly overexpressed in sensitive HMCLs suggesting the same gene signatures could be utilised in MM. Potentially the addition of *CXCR3* gene expression could further refine the panel specific to MM.

MM is a molecularly heterogeneous disease, and despite RAS^{M} serving as a marker of sensitivity to MEK inhibition, using two different gene interrogation approaches we could not identify any specific gene or enriched pathway that better identified or predicted HMCLs as sensitive or resistant. Gene array data identified LXN as a possible mechanism of sensitivity, and its methylation induced repression as a possible mechanism of resistance, raising the possibility that other tumour suppressors may be limiting response to MEK inhibition, warranting further investigation.

6. DEMETHYLATION SENSITISES t(4;14) MM TO MEK INHIBITION

6.1 INTRODUCTION

Epigenetic aberrations, including histone modifications and DNA methylation, play a significant role in virtually all malignant diseases[291,292]. DNA methylation results in changes in gene expression, most typically gene silencing due to promoter hyper-methylation[293,294]. In MM, the translocation t(4;14) results in juxtaposition of the MMSET/FGFR3 locus on chromosome 4 with the IgH locus on chromosome 14. This results in overexpression of MMSET, a histone methyltransferase in all cases, a mechanism of epigenetic modification in MM[295-298]. The t(4;14) is an adverse prognostic factor, associated with shortened overall survival[2]. Further, DNA methylation induced silencing of tumour suppressor genes[299] and cell cycle regulators[300] also adversely affects prognosis. Increasing aberrations in epigenetic modification have been described at relapse and later stages of disease[301,302].

The histone deacetylase inhibitors (HDACi), vorinostat and panobinostat are approved for use in R/R MM[303,304](in the US and Europe). Whilst the DNA hypomethylating agent, azacitidine, does not have an approved role in treatment. Despite this, azacitidine has been shown to be effective against HMCLs[305] and both gene[306] and methylation[307] scoring systems have been developed as predictive biomarkers for determining response to hypomethylating agents. The use of azacitidine has been reported in two clinical trials. The first, investigated oral azacitidine in re-sensitising patients to lenalidomide who had previously progressed on lenalidomide (Kalff, ASH abstract 2016). The second evaluated subcutaneous azacitidine twice weekly with lenalidomide (Reu, ASCO abstract 2015). Both demonstrated clinical benefit with response rates above 20%. A third study has investigated up-regulation of the immunogenic cancer testis antigen (CTA) in response to azacitidine therapy post ASCT to generate T-cell responses[308]. This approach has been effective in three of 14 patients reported to date.

In solid tumours, azacitidine has been shown to sensitise or reverse resistance to conventional chemotherapy[309-314], sensitise to targeted inhibitors[315,316] and hormonal therapy[317] or function as a radiation sensitiser[318]. In haematologic malignancy, demethylation in combination with conventional chemotherapy in lymphoma[319], with panobinostat in AML[320], and with bortezomib in MM[321] enhanced response in each case.

Here we investigate the potential of pre-treatment with azacitidine followed by trametinib.

6.2 STUDY RATIONALE & AIMS

Based on our findings described in the previous chapter, of tumour suppressor genes potential role in MEKi sensitivity, which can be induced with azacitidine, in concert we previous descriptions of tumour suppressor silencing through DNA methylation, we sought to evaluate the effects of azacitidine pre-treatment on HMCLs prior to MEK inhibition. Further, given the role of MMSET as an epigenetic modifier, we postulated in t(4;14) HMCLs, azacitidine may address the effects of MMSET, whilst MEK inhibition would address FGFR3 signalling through the RAS-MAPK.

The work described in this chapter aimed to:

- Evaluate the effect of azacitidine pre-treatment on sensitivity to MEK inhibition with trametinib
- Identify changes in gene expression induced by azacitidine that may be associated with or confer sensitivity to MEK inhibition
- Assess changes in histone methylations marks in response to azacitidine
- Knockdown a known target of azacitidine to recreate the effects observed
- Test the combination in murine xenografts of MM

6.3 RESULTS

6.3.1 Pre-treatment with azacitidine sensitises t(4;14) HMCLs to MEK inhibition

We treated two groups of HMCLs, t(4;14) and WT, with azacitidine 200nM for seven days followed by trametinib (10nM, 100nM and 1μM) for three days. Proliferation, cell viability and cell cycle were evaluated. This particular dose of azacitidine was sub-lethal, with <10% cell death (by PI flow cytometry) after seven days of treatment, is a clinically relevant and achievable dose.

Pre-treatment with azacitidine resulted in marked sensitisation of t(4;14) HMCLs whilst almost no effect was seen in WT HMCLs (Figure 6.1 A-C). In two of three t(4;14) HMCLs (KMS11 and LP1) growth was completely arrested at the highest trametinib dose of 1μM, whilst at the lowest dose (10nM) growth was reduced by >50%. In KMS26, the highest dose lead to greater than 50% growth reduction. Conversely, in WT HMCLs no significant reduction in growth was observed.

Whilst azacitidine alone had no significant impact on cell survival, in t(4;14) HMCLs initial cell growth was slowed, however this effect was not a sustained (Figure 6.1A).

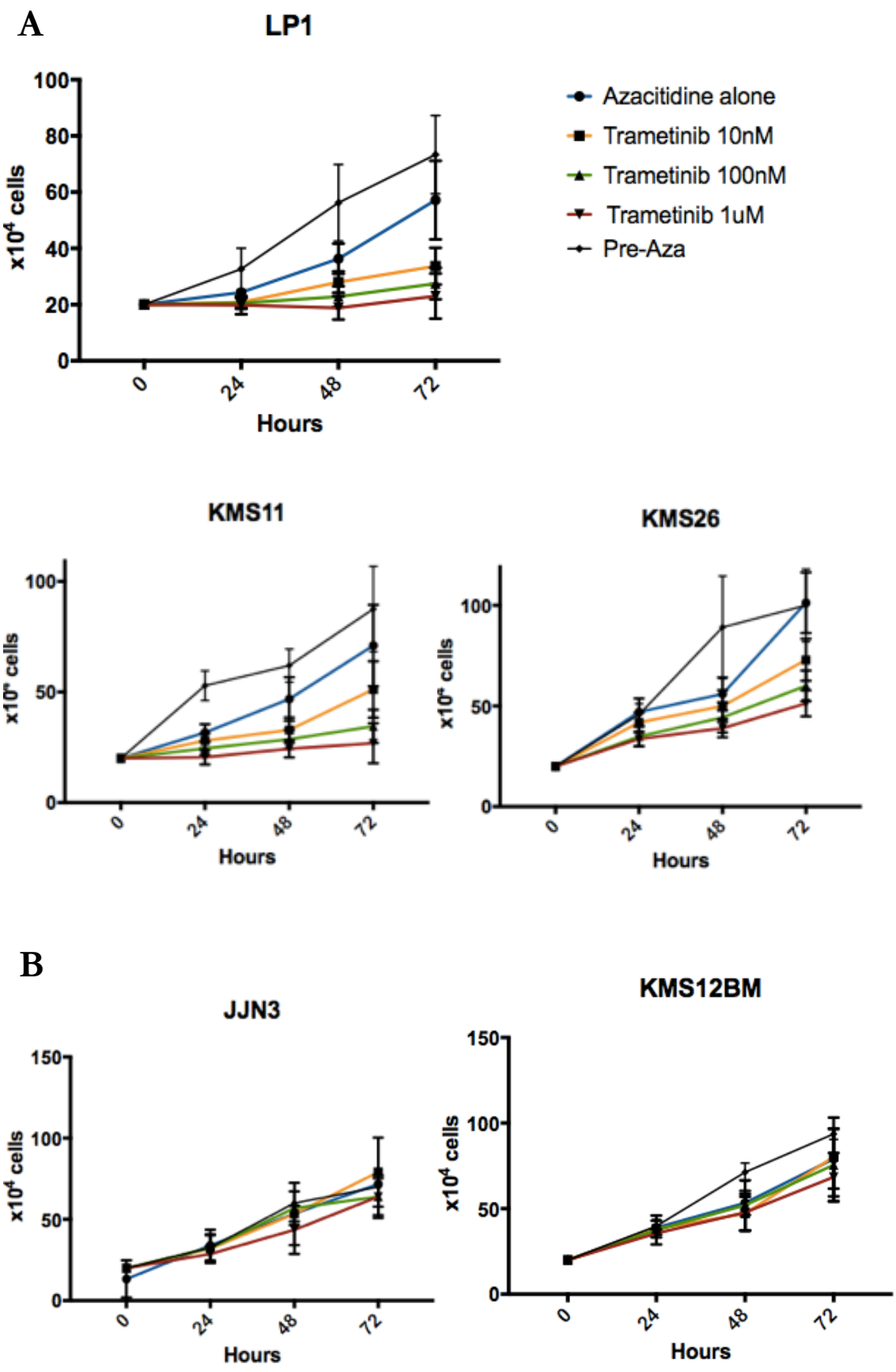
A
LP1
Azacitidine alone
Trametinib 10nM
Trametinib 100nM
Trametinib 1uM
Pre-Aza
x10⁴ cells
Hours
KMS11
KMS26
B
JJN3
KMS12BM

C

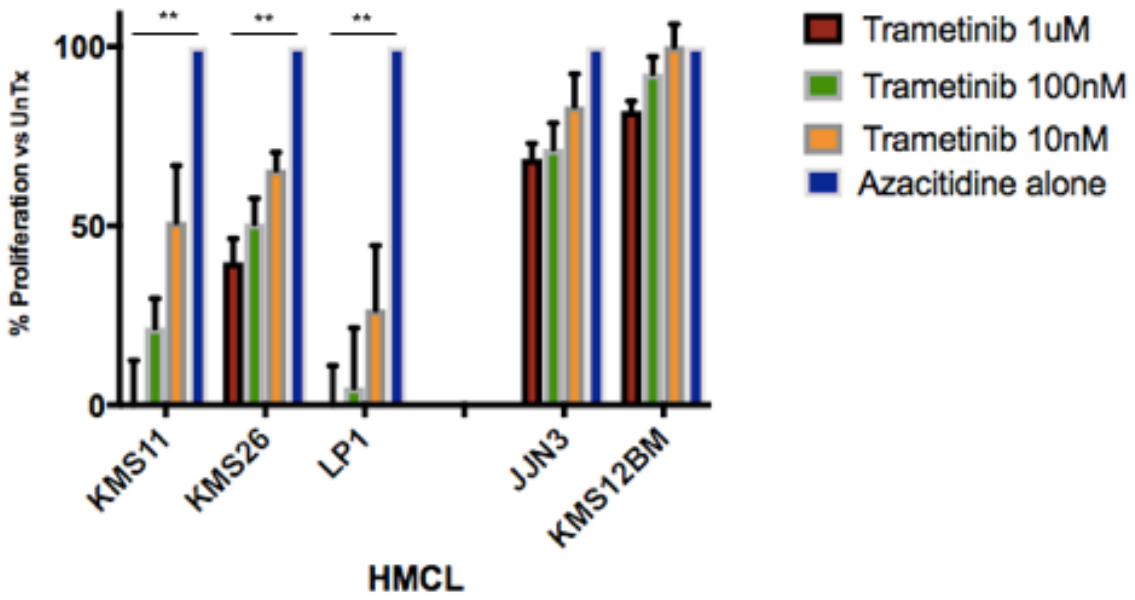

Figure 6.1: A-C. (A, B) t(4;14) & WT HMCL growth curves with azacitidine pre-treatment followed by trametinib. Growth arrest is seen in two of three t(4;14) HMCLs (KMS11, LP1) with significant growth inhibition in a third (KMS26). The pre-azacitidine curve for comparison, is trametinib 1μM alone (without azacitidine). **(C)** Normalised ratios of HMLCs growth curves. t(4;14) show a significant reduction in growth in response to trametinib treatment at all doses with azacitidine pre-treatment ($p<0.002$) (n=3, mean ±SEM).

To validate this effect three further t(4;14) HMCLs were similarly treated with azacitidine and trametinib (Figure 5.2). These three HCMLs recapitulated the original findings.

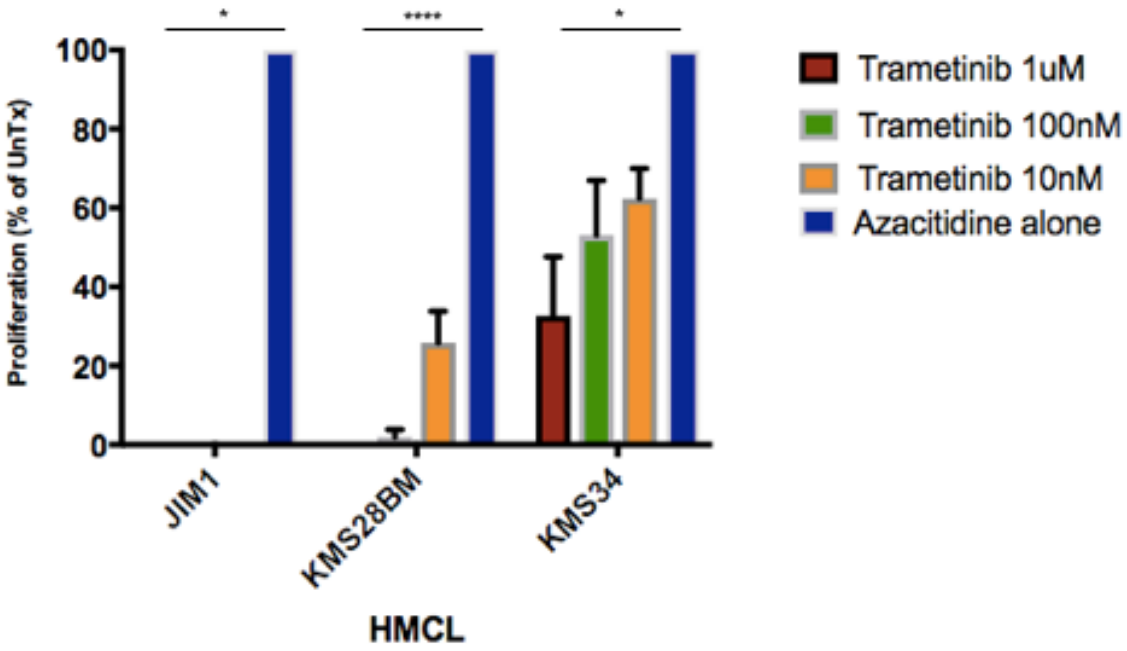

Figure 6.2: Validation set of t(4;14) HMCLs pre-treated with azacitidine then trametinib. Normalised ratios of growth curves of a validation set of t(4;14) HMCLs pre-treated with azacitidine then trametinib against azacitidine alone. In JIM1 all doses of Trametinib resulted in complete cell death. (JIM1 p=0.03, KMS28BM p<0.0001, KMS34 p=0.012), (n=3, mean ±SEM).

Treatment of *RAS*^{M} *p53* WT HMCLs results in $G_{0/1}$ arrest. This effect is not seen in t(4;14) or WT HMCLs. Azacitidine pre-treatment of t(4;14) but not WT HMCL resulted in trametinib-induced cell cycle shift to pre-G_0. (Figure 6.3 A-C).

A

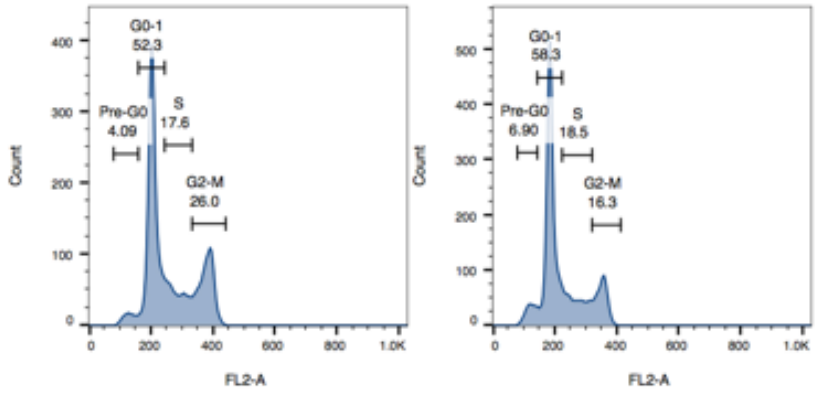

KMS11 Untreated 24 hours

KMS11 Trametinib 1μM 24 hours

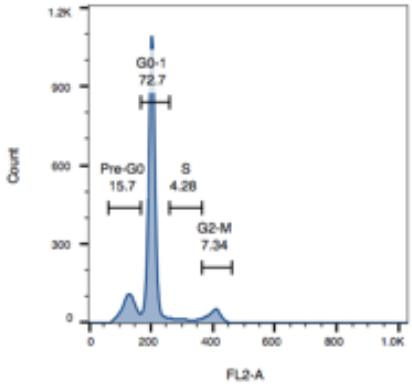

KMS11 Post Azacitidine 24 hours
Untreated

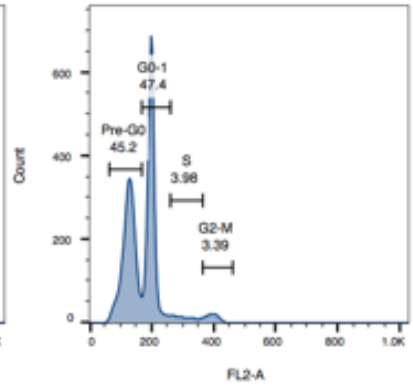

KMS11 Post Azacitidine 24 hours
Trametinib 1μM

B

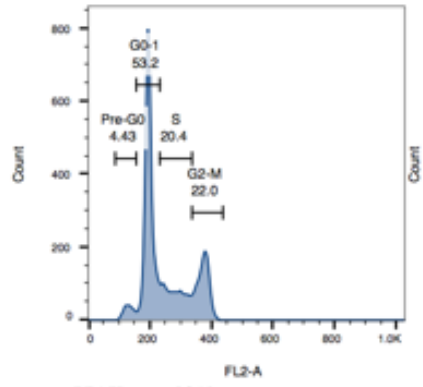

LP1 Untreated 24 hours

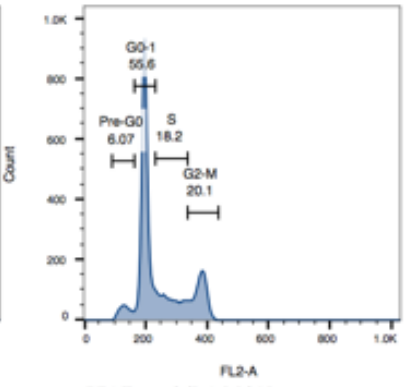

LP1 Trametinib 1μM 24 hours

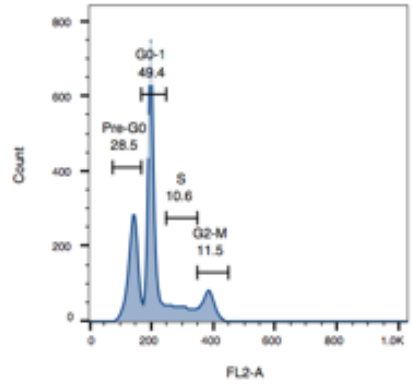

LP1 Post Azacitidine 24 hours
Untreated

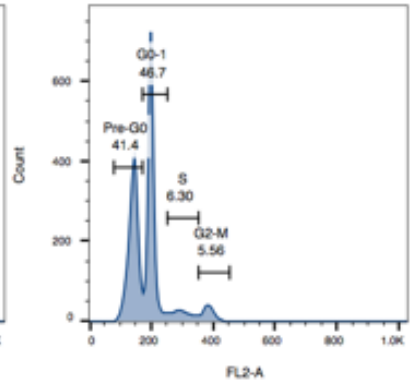

LP1 Post Azacitidine 24 hours
Trametinib 1μM

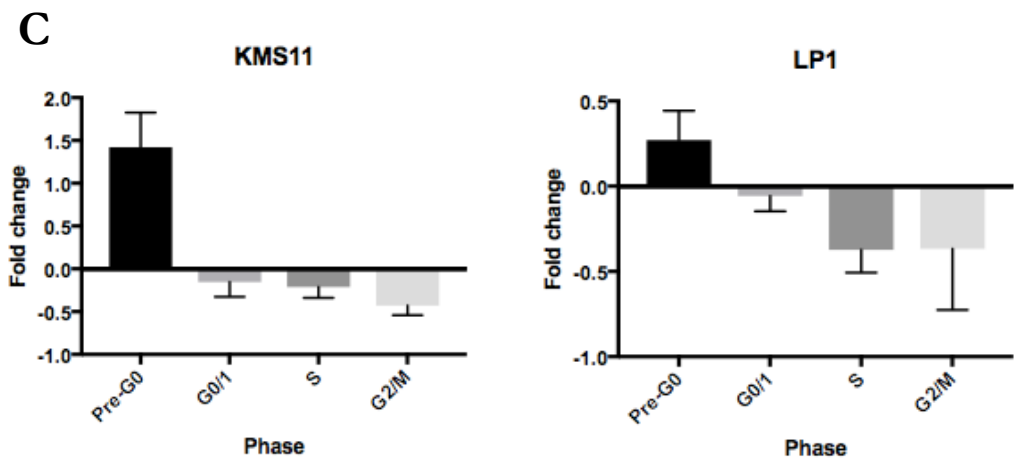

Figure 6.3: Cell cycle plots with & without azacitidine pre-treatment followed by trametinib. (A) KMS11. **(B)** LP1. **(C)** Relative phases of cell cycle.

6.3.2 DNMT3b, but not DNMT3a is overexpressed in t(4;14) HMCLs and correlates with response to azacitidine then trametinib

To determine the potential mechanisms of azacitidine induced sensitivity, we evaluated expression of the known targets of azacitidine, DNA methyltransferases 3 alpha (DNMT3a) and beta (DNMT3b). Using RNA-sequencing data we found in t(4;14) HMCLs DNMT3b was significantly over-expressed compared with WT HMCLs, whilst no difference was observed in the expression of DNMT3a (Figure 6.4). This held true for an expanded set of HMCLs (Figure 6.5).

DNMT3b was expressed at the protein level in all t(4;14) HMCLs. A reduction in DNMT3b expression was seen following treatment with azacitidine in LP1, that was not observed in the other t(4;14) HMCLs (Figure 6.6).

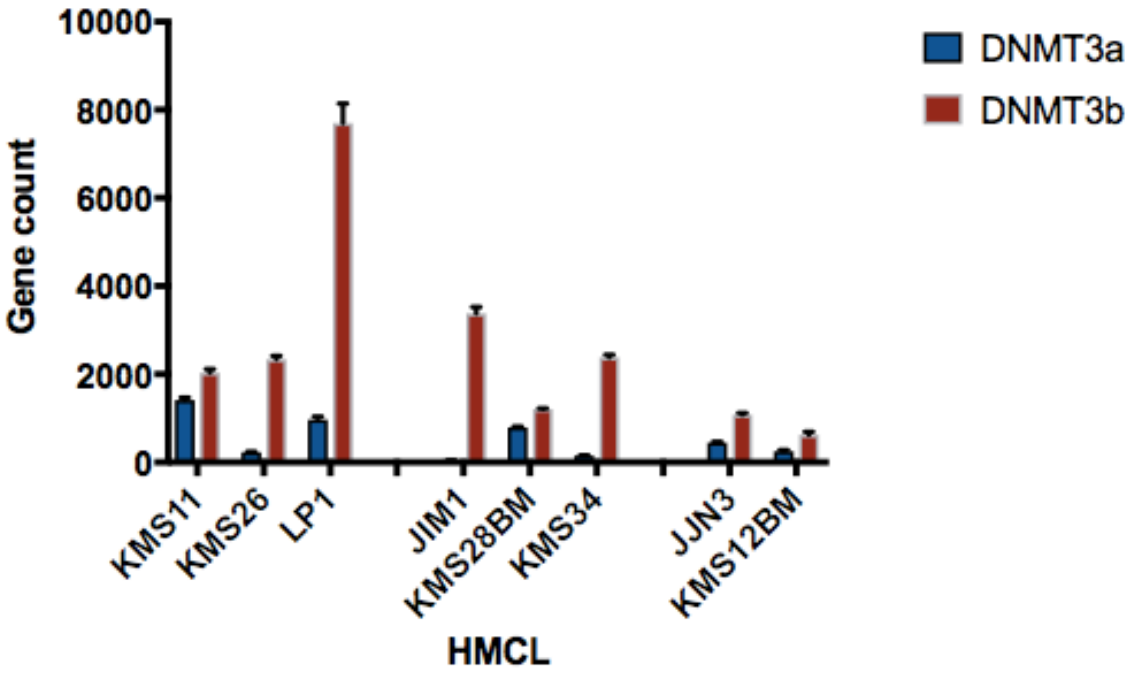

Figure 6.4: DNMT3a & b RNA-seq expression. DNMT3b is significantly over-expressed in all t(4;14) HMCLs compared to expression of DNMT3a ($p<0.0001$). Expression of DNMT3b is significantly greater in t(4;14) HMCLs compared to WT ($p=0.0003$). (n=3, mean ±SEM).

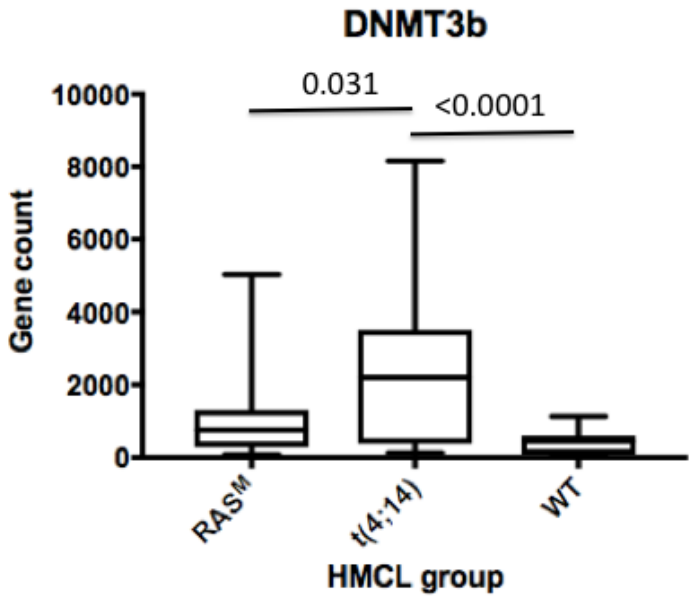

Figure 6.5: DNMT3b RNA-seq expression in 30 HMCLs by molecular & cytogenetic type. DNMT3b is significantly over-expressed in t(4;14) compared with both *RAS*^{M} ($p=0.031$) and WT ($p<0.0001$). DNMT3b expression in *RAS*^{M} is significantly greater that WT ($p=0.003$).

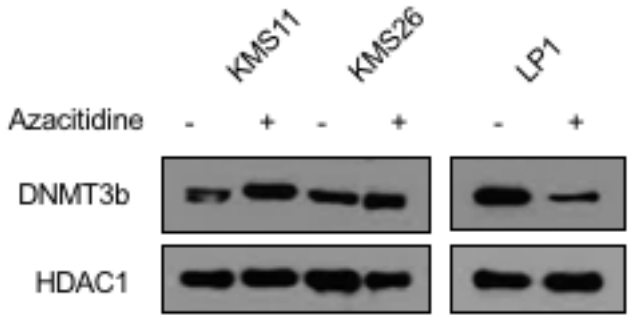

Figure 6.6: DNMT3b expression pre & post-treatment with azacitidine. LP1 demonstrated a reduction of DNMT3b after treatment with azacitidine, this was not observed in the other two t(4;14) HMCLs. HDAC1 is the nuclear loading control.

To investigate the role of DNMT3b as the target of azacitidine sensitization in t(4;14) HMCLs to trametinib, we undertook both siRNA knockdown (Figure 6.7), and treatment with a chemical inhibitor of DNMT3b, nanaomycin A. Whilst siRNA achieved partial knockdown this did not confer sensitivity to treatment trametinib.

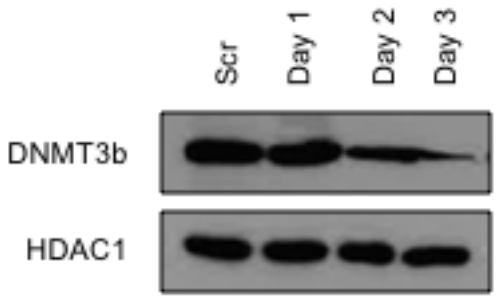

Figure 6.7: siRNA knockdown of DNMT3b in LP1. A marked reduction in DNMT3b protein expression was achieved with siRNA, greater than that seen in azacitidine treated LP1. However, this knockdown did not result in sensitivity to trametinib. HDAC1 is the nuclear loading control.

Treatment with nanaomycin A at doses greater than 200nM resulted in significant cell death. Treatment with sub-lethal doses, 10-100nM, for three days followed by trametinib did not recreate the effects seen with azacitidine.

6.3.3 Azacitidine does not consistently alter histone methylation marks associated with MMSET

MMSET is universally expressed in t(4;14) MM. We investigated whether its known targets are affected by azacitidine treatment. Effects on known MMSET histone methylation marks were inconsistent across the three t(4;14) HMCLs (Figure 6.8 A). As such azacitidine does not exert its effect through this process.

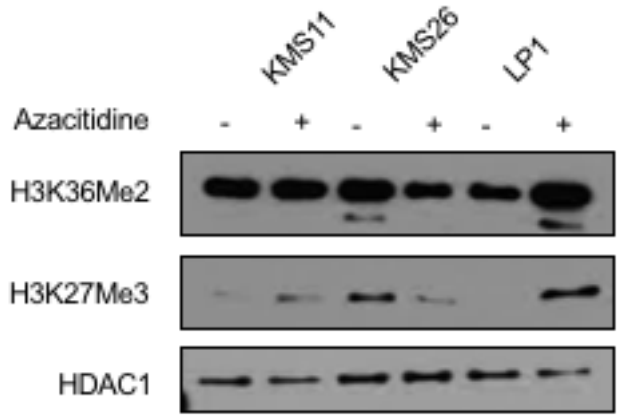

Figure 6.8: H3K36Me2 & H3K27Me3 marks pre & post-azacitidine. Azacitidine showed no consistent effects on the methylation states of two known histone targets of MMSET. HDAC1 is the nuclear loading control.

6.3.4 Azacitidine results in extensive gene expression changes and gene pathway changes irrespective of cytogenetic type

We evaluated gene expression changes associated with azacitidine treatment in both t(4;14) and WT HMCLs, with a view to establishing potential pathways associated with trametinib sensitivity. All HMCLs showed numerous gene expression changes, with more observed in WT than in t(4;14) HMCLs (Figure 6.9). No pattern of absolute gene expression changes was seen in relation to underlying cytogenetic status or the observed response to azacitidine.

Recurrent pathways analysis (using Gene Ontology (GO) and DAVID bioinformatics[322]) found markedly different gene expression changes in response to azacitidine between HMCLs. Few enriched pathways were shared within or distinguished the two cytogenetic groups (Table 6.1). As has previously been

reported in solid tumour cell lines in response to azacitidine, KMS11 and JJN3 both showed significant pathway enrichment for “MHC class II activity” “antigen presentation” and “immune response”. This response was also seen in KMS12BM and LP1 (although with lower p-values and “fold enrichment” scores) and did not correlate with response to trametinib.

Azacitidine has been reported to lead to re-expression of tumour suppressor genes. As our previous results (chapter 3 and kinome analysis) has suggested a role for cell cycle regulation and tumour suppressors for sensitivity to trametinib we interrogated gene expression changes in previously reported tumour suppressor genes[323,324] (Figure 6.10). A very heterogeneous pattern of tumour suppressor gene re-expression in response to azacitidine was seen. KMS11 and LP1 showed the greatest increase in reported tumour suppressor genes (n=5). Whilst KMS26 had no tumour suppressor gene changes.

Finally, we analysed expression changes in genes previously reported in MEK-sensitivity signatures. Whilst subtle changes in several of these were seen in the sensitive HMCLs, none were significant.

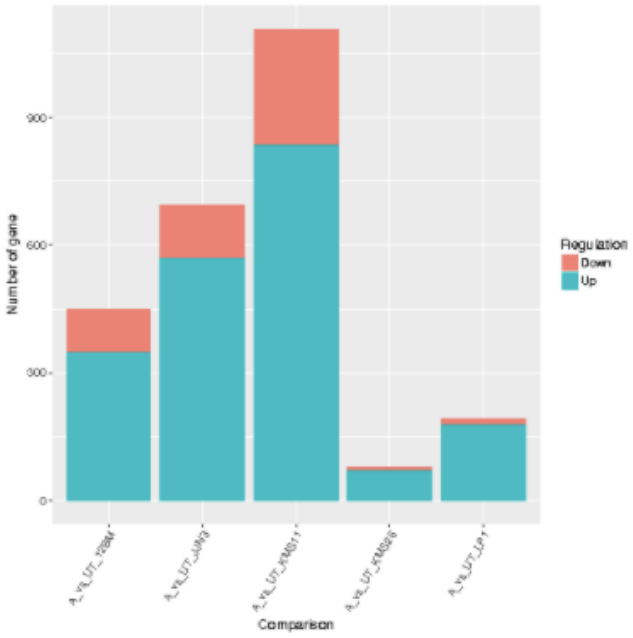

Figure 6.9: Absolute number of up- & down-regulated genes in response to azacitidine.

Figure 6.10: Heat map of tumour suppressor gene expression & changes in response to azacitidine. Generally more tumour suppressor genes had their expression increased in the t(4;14) HMCLs, KMS11 and LP1, although no changes were observed in KMS26. The WT HMCL JJN3 showed an increase in three tumour suppressor genes, which was fewer than that observed in t(4;14), whilst KMS12BM had only a single gene increase its expression. Green=expressed at baseline, red=not expressed and not changed with azacitidine, yellow=increased expression following azacitidine treatment.

HMCL	Enriched pathways	p-value
KMS11	i. Antigen processing and presentation	$9.45x10^{-10}$
	ii. MHC II complex/activity	$1.1x10^{-9}$
	iii. Cytosol	$2.92x10^{-8}$
KMS26	i. Protein homodimerization	0.001
	ii. Response to hypoxia	0.001
	iii. Basolateral plasma membrane	0.002
LP1	i. Extracellular space	$1.18x10^{-7}$
	ii. Type I interferon signalling	$1.78x10^{-5}$
	iii. Adaptive immune response	$4.12x10^{-5}$
JJN3	i. MHC II complex/activity	$1.50x10^{-11}$
	ii. Antigen processing and presentation	$2.19x10^{-11}$
	iii. Immune response	$5.45x10^{-11}$
KMS12BM	i. Cholesterol biosynthesis	$6.23x10^{-6}$
	ii. Extracellular space	$1.60x10^{-4}$
	iii. Lipoprotein metabolic processes	$7.09x10^{-4}$

Table 6.1: Most highly enriched pathways in response to azacitidine. KMS11 and JJN3 show the most consistently changed gene expression pathways, but opposite responses to trametinib. KMS26 shows very few enriched pathways consistent with the few gene changes observed.

(Pathway enrichment data presented in Supplementary Figure 9.5).

6.3.5 Combination azacitidine & MEK inhibition demonstrates anti-myeloma activity in murine xenograft models of MM

We evaluated the combination of azacitidine and trametinib in two murine xenograft models. The first recapitulates t(4;14) disease using the HMCL LP1, the second WT disease using the HMCL KMS12BM. In both instances, NOD scid gamma (NSG) mice were transplanted (IV via tail vein injection) with $4x10^6$ LP1 or $1x10^6$ KMS12BM cells stably expressing GFP and luciferase.

The LP1 model is moderately slow to engraft and establish tumour burden, occurring at approximately three weeks. The KMS12BM is a very robust disease model, establishing measurable disease within one week. Tumour burden was measured on a weekly basis, using in vivo bioluminescence imaging using

luciferin (IP) measuring median flux as photons/sec of averaged dorsal and ventral. Scientific end-points were high-limb paralysis (HLP) and/or >20% weight loss from baseline. On the basis of prior pilot studies, additional scientific end-points were included: LP1 - plasmacytomata causing distress, KMS12BM - overall poor condition as evidenced by general slowing, poor recovery post anaesthesia and/or a measured disease burden of $>1.5x10^{10}$ photons/sec on bio-luminescence imaging.

The treatment schemas were the same for both cohorts. Mice were treated with vehicle alone, azacitidine 5mg/kg (IP) daily, planned for 2 cycles of 1 week with 3 weeks off, trametinib 3mg/kg (OG) daily, planned for 2 cycles of 3 weeks with 1 week between cycles, or the combination planned for 2 cycles without a break between cycles. There were five mice per treatment group.

In the LP1 xenograft, disease establishes in the spine, progressing to the long bones and finally forms large tissue/spinal plasmacytomata (Figure 6.10). Trametinib monotherapy created no significant change in disease burden or kinetics nor a survival advantage. Azacitidine monotherapy resulted in a significant slowing of disease kinetics and no plasmacytomata. The addition of trametinib to azacitidine further slowed disease kinetics (Figure 6.11), significantly less than vehicle ($p=0.038$). Both groups treated with azacitidine succumbed to treatment toxicity following the second planned week of treatment with azacitidine. As such no survival advantage was observed in the azacitidine treated groups (Figure 6.12).

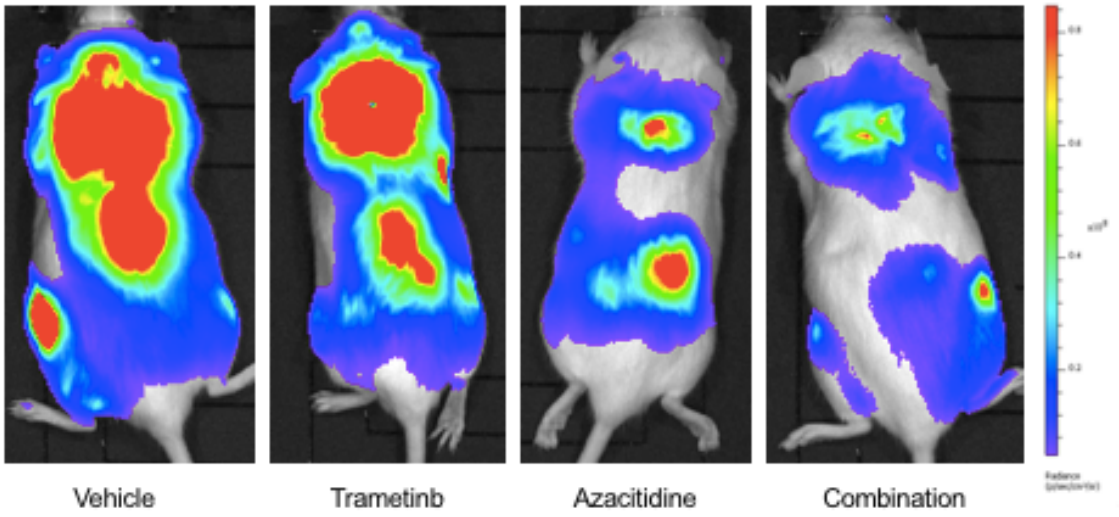

Figure 6.11: Disease pattern of LP1 xenograft. Images show disease measurement at five weeks. Disease establishes in the spine and long bones, before forming large plasmacytomata over the cervical and thoracic spine. Treatment group is listed beneath each mouse image.

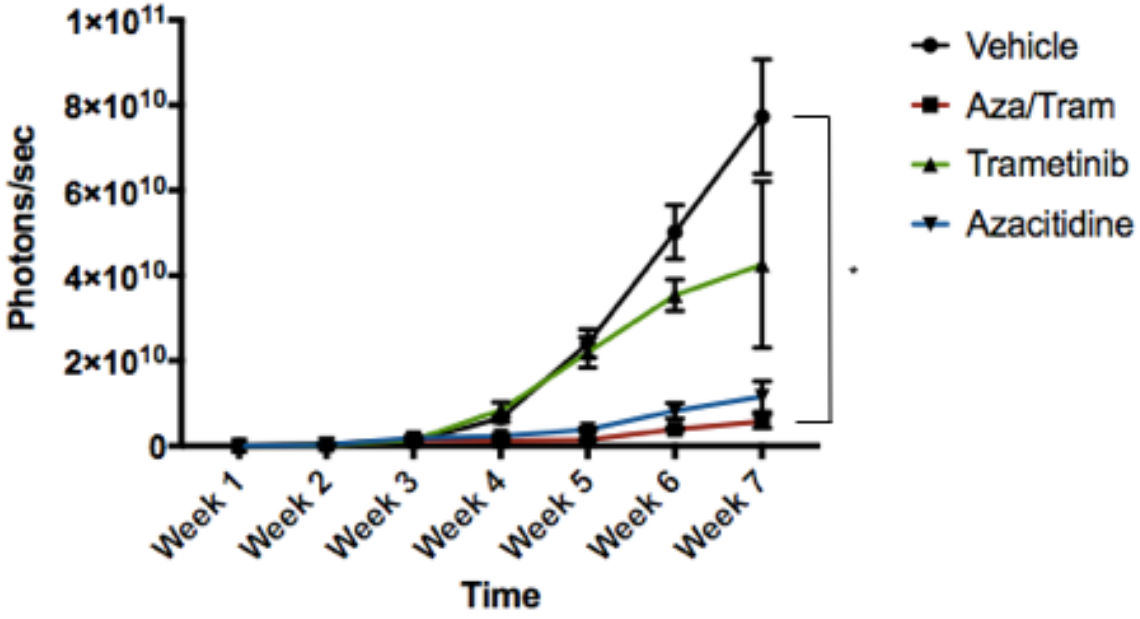

Figure 6.12: Disease bioluminescence measured over time in LP1. A profound reduction in disease burden and delayed growth kinetics was observed in both cohorts treated with azacitidine. The addition of trametinib to azacitidine significantly slowed disease growth compared with vehicle. (n=5, mean ±SEM). (*p=0.038 combination c/w vehicle. No other comparisons were significant).

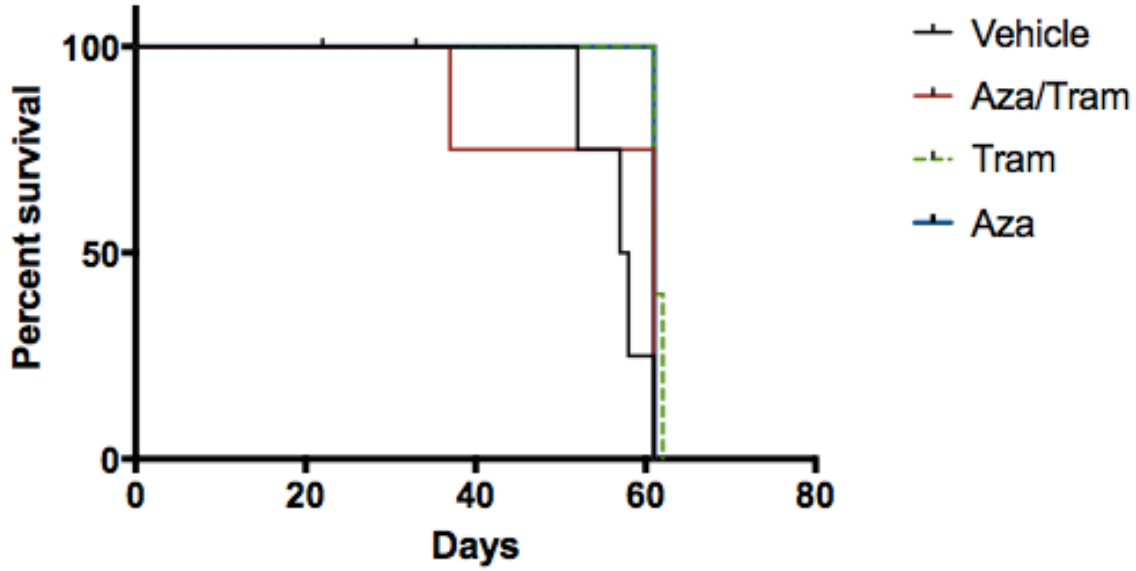

Figure 6.13: Survival curves of LP1 murine xenograft. No meaningful difference was observed between the cohorts. However, whilst the vehicle and trametinib alone met scientific endpoints, the azacitidine alone and in combination with trametinib succumbed to drug toxicity, rather than disease. (n=5/cohort).

In the KMS12B xenograft, disease establishes within one week in the liver, resulting in massive hepatomegaly (mean liver weight at end of study of 10.0g) (Figure 6.13, 6.14, A &B). Azacitidine treatment resulted in a significant slowing of disease kinetics (Figure 6.15), a reduced burden of disease within the liver (mean liver weight 4.26g) (Figure 6.14) and prolonged overall survival (Figure 6.16). Trametinib alone had no impact on disease kinetics or survival. The addition of trametinib to azacitidine provided no further survival benefit.

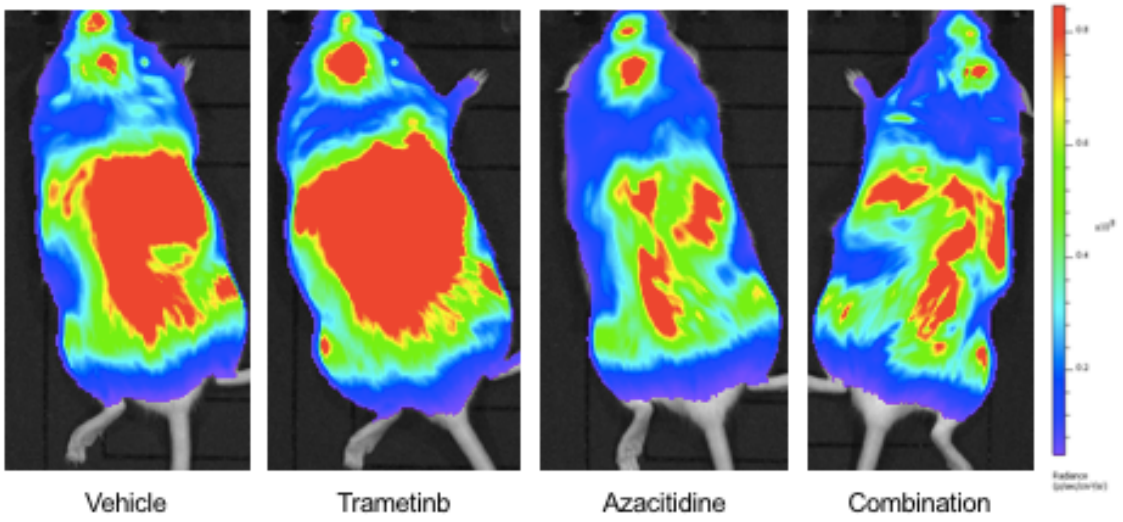

Figure 6.14: Disease pattern of KMS12BM xenograft. Images show disease at three weeks. Disease rapidly establishes in the liver leading to hepatomegaly. Treatment group is listed beneath each mouse image.

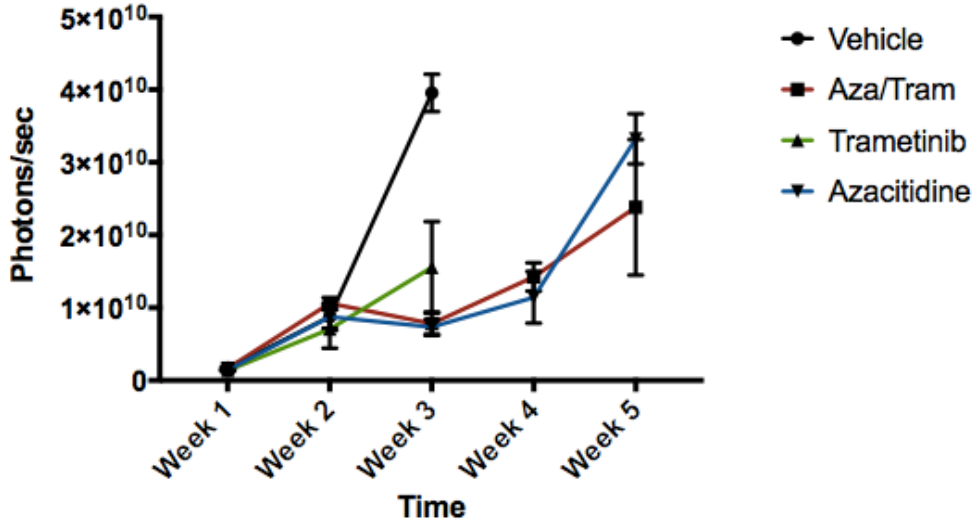

Figure 6.15: Disease bioluminescence measured over time in KMS12BM. Azacitidine profoundly slowed disease progression, whilst the addition of trametinib had no further impact. Trametinib alone appeared to slow disease progression, however did not translate into a survival advantage over vehicle. (n=5, mean ±SEM).

A

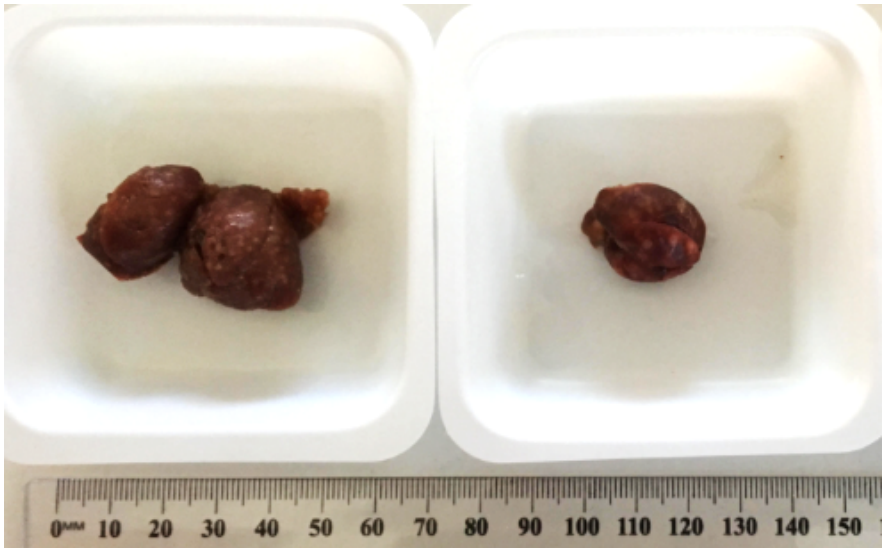

B

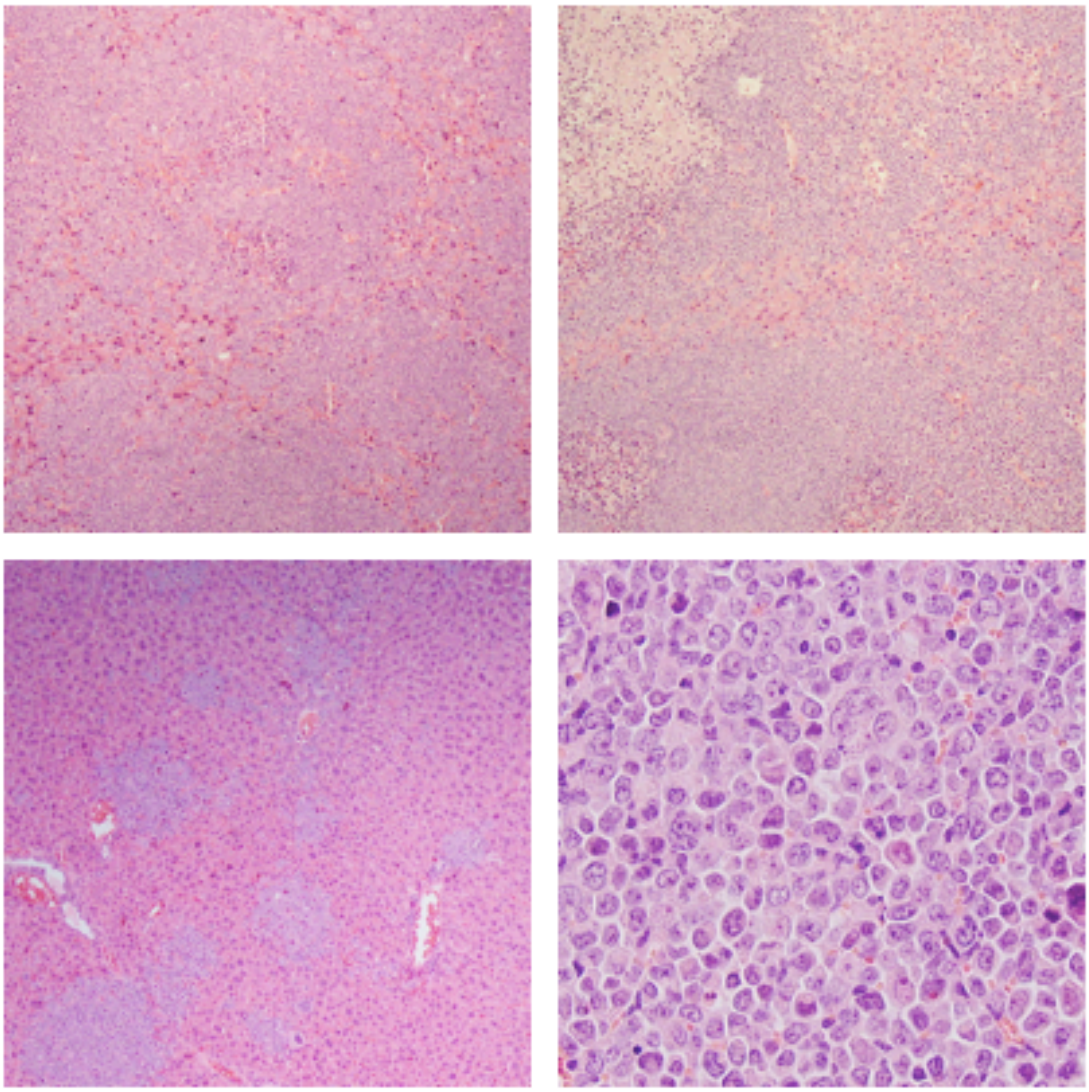

Figure 6.16: KMS12BM xenograft liver specimens and histology. (A) Liver on the left is from a vehicle mouse, showing massive hepatomegaly (weight 11.11g, 5cm) with a nodular surface. Liver on the right is from an azacitidine treated mouse, showing normal size (weight 4.25g, 2cm), nodules are still evident on the surface. **(B)** H+E staining of mice livers. Top panels are vehicle mice showing extensive replacement by tumour cells with little normal liver remaining. Areas of necrosis are present in the top right right-hand panel. Lower left-hand panel is from an azacitidine treated mouse showing fewer and smaller nodules of tumour cells with retention of normal liver architecture. Necrosis was not evident. Lower right panel is high power of a tumour nodule, demonstrating sheets of tumour cells.

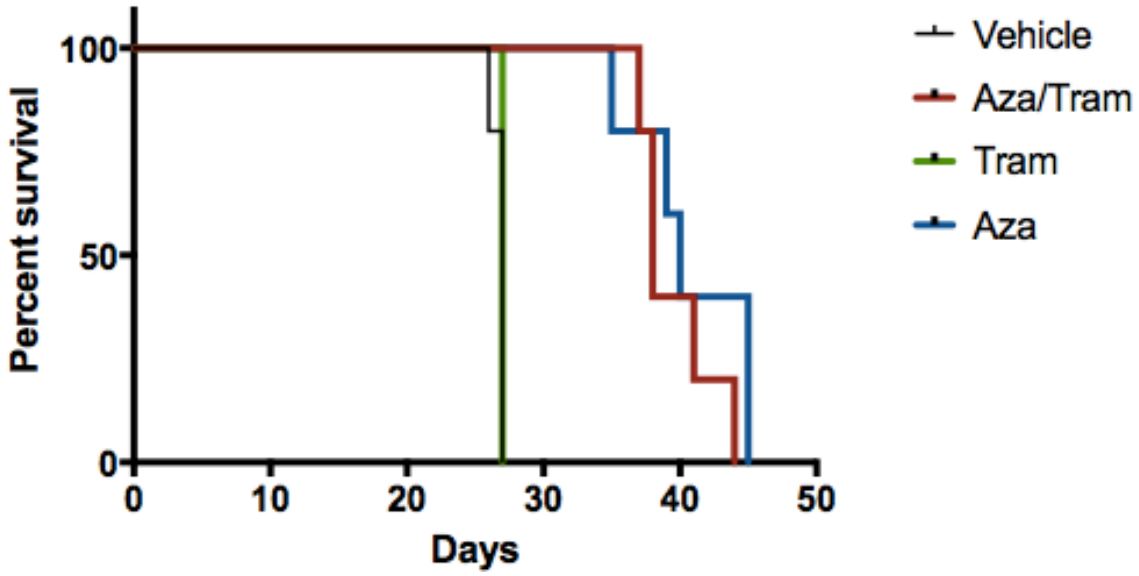

Figure 6.17: Survival curves of KMS12BM murine xenograft with combination treatment. Azacitidine treatment significantly prolonged survival over vehicle and trametinib alone (both azacitidine groups compared with vehicle or trametinib alone p=0.0002). The addition of trametinib to azacitidine provided no further survival benefit. (n=5/cohort).

6.4 DISCUSSION

The t(4;14) translocation occurs in approximately 15% of MM[298,325], resulting in juxtaposition of the MMSET/FGFR3 (multiple myeloma SET domain/fibroblast growth factor 3) locus on chromosome 4 and the IgH locus on chromosome 14. It is one of three high risk cytogenetic lesions (the others, t(14;16) and del17p) which confers a poor prognosis, an inferior response to therapy and worse OS[2]. A trial investigating the multi-targeted RTK (including FGFR3) inhibitor dovitinib, showed no single agent activity and was poorly tolerated[326]. Novel treatment approaches are required for this high-risk disease subtype.

Azacitidine pre-treatment of t(4;14) HMCLs results in sensitisation to MEK inhibition with trametinib. In 60% of cases the sensitisation was great enough that MEK inhibition resulted in complete arrest of growth and cell death. Cell cycle changes recapitulated those seen in *RAS*^{M} HMCLs with a marked shift to pre-G_0.

DNMT3a and DNMT3b are both known targets of azacitidine[327]. We found DNMT3b, but not DNMT3a, to be significantly overexpressed in t(4;14) compared with WT HMCLs. Its expression correlated with response to pre-treatment with azacitidine followed by trametinib. In an expanded panel of HMCLs (n=30) we confirmed overexpression of DNMT3b in t(4;14) compared with both *RAS*^{M} and WT HMCLs. As such DNMT3b overexpression in t(4;14) is a potential biomarker for MM sensitivity to azacitidine. These finding are consistent with previous descriptions in solid tumours where azacitidine sensitivity has also been ascribed to the overexpression of DNMT3b[328-330].

Neither siRNA knockdown of DNMT3b, nor DNMT3b inhibition with the specific inhibitor nanaomycin A, followed by trametinib treatment were able to recreate the effects of pre-treatment with azacitidine. In both instances, the duration of knockdown or inhibition may have been inadequate to induce the gene changes and sensitisation observed with azacitidine. Further, azacitidine may have pleiotropic effects not accounted for by simple knockdown/inhibition of one of its known targets. LP1 showed a change in DNMT3b expression following azacitidine treatment, however this was not universally seen in the t(4;14)

HMCLs. As such, the sensitising effects observed with azacitidine pre-treatment are unlikely to be due solely inhibition of DNMT3b.

The MMSET gene, overexpressed in 100% of t(4;14) cases, also known as the nuclear receptor-binding SET domain 2 (NSD2), is a histone methyltransferase involved in the methylation of several different histone marks including trimethylation of H3 at lysine residues K4 (H3K4me3), K27 (H3K27me3) and K36 (H3K36me3) and H4 dimethylation at lysine residues K20 (H4K20me2) and K36 (H4K36me2)[331,332]. Given its universal expression in t(4;14) MM, it is considered largely responsible for the negative prognosis of the subtype[295,325]. The effect of azacitidine on these histone targets was inconsistent between the t(4;14) HMCLs. Azacitidine's effects are not mediated by altering the methylation status of these histone marks.

The effect of azacitidine on gene expression continues to be investigated. It has been shown in myelodysplastic syndromes that azacitidine treatment results in the re-expression of silenced tumour suppressor genes[323,324,333,334]. Given the effects on cell cycle we have observed in *RAS*^{M} HMCLs we investigated the expression of these genes using RNA-seq in both t(4;14) and WT HMCLs pre- and post-treatment with azacitidine. Re-expression of a number of tumour suppressor genes was observed predominantly in the t(4;14) group. However, this was not universal as KMS26 showed no re-expression of any of the tumour suppressors analysed. Possibly confounding the expression of these genes as a cause of sensitivity to trametinib, is that several of the re-expressed genes were either already expressed or had their expression increased in JJN3, a WT HMCL, also.

It has been described that azacitidine induces gene expression changes related to innate and adaptive immunity[335]. These include expression of cancer antigens[336], interferon signalling,[337] antigen processing and presentation. The changes in these gene expression profiles is thought to result in an immune response against tumour cells[338]. Re-expression of these immunologic pathways was identified in three of the five HMCLs. It is unlikely the re-expression of these genes is responsible for trametinib sensitivity, as neither our in vitro nor in vivo

models have immune effectors cells present. However, this does raise the possibility of immune activation in clinical circumstances.

In a t(4;14) murine xenograft the combination of azacitidine and trametinib resulted in significant reduction of tumour burden and disease progression compared with vehicle treated mice. Further, spinal and soft tissue plasmacytomata did not develop in any of the azacitidine treated mice, which were seen in the vehicle and trametinib monotherapy mice. Unfortunately, drug toxicity was significant, with all azacitidine treated mice unable to tolerate a second cycle of treatment, succumbing to toxicity rather than disease. As such a survival benefit was likely but not demonstrable.

In a WT murine xenograft, azacitidine reduced tumour burden in extra-medullary sites of disease (liver) and prolonged overall survival. The addition of trametinib to the WT xenograft did not improve outcomes further.

The effectiveness of azacitidine in both these cases makes the argument that something intrinsic to the tumour cells is occurring rather than immune mediated effects. Alteration to the tumour micro-environment (i.e. the liver in the KMS12BM xenograft) may also occur, raising the possibility that azacitidine affects the tumour niche and may potentially prevent or slow disease establishing in extra-medullary sites.

To evaluate the potential role of immune mediated effects in response to azacitidine, the 5T33 murine myeloma model[339] in the immune competent C57BL/KaLwRij mouse, could be used.

The in-vitro combination of azacitidine pre-treatment resulting in trametinib sensitivity in t(4;14) MM potentially represents a novel targeted therapeutic approach against this high-risk disease and warrants further investigation. Further murine studies are required to validate this effect.

7. DISCUSSION & FUTURE DIRECTIONS

7.1 THE RAS-MAPK AS A TARGET IN MM

Multiple myeloma is a cytogenetically and molecularly heterogeneous disease[78]. Despite this heterogeneity, several groups have now demonstrated recurrent, aberrant signalling via the RAS-MAPK pathway. This occurs most frequently through *RAS*^{M}, but also through *RAF*^{M} albeit comparatively rarer (Table 1.1). Additionally, the high-risk cytogenetic lesion t(4;14) present in 15% of MM, results in overexpression of the RTK FGFR3 in 70% of cases, which also signals via the RAS-MAPK. Mutations in the RAS-MAPK and the cytogenetic lesion t(4;14) are considered mutually exclusive due to pathway redundancy, resulting in activity through the RAS-MAPK in up to 70% of MM. It is thought acquisition of these molecular mutations serve as secondary oncogenic drivers of disease progression from MGUS to clinically symptomatic disease, as these mutations are essentially not seen in MGUS[20]. Also, mutation prevalence is greater at relapse[18]. Taken together, these data support the RAS-MAPK as a pathway of dependence in MM and particularly of oncogene addiction to *RAS*^{M}. This provides the rationale for exploiting this dependence as a therapeutic target.

We have shown that targeting the RAS-MAPK, with the MEKi trametinib, abrogates pathway signalling, as demonstrated by the loss of phosphorylated ERK and significantly inhibits growth in *RAS*^{M} HMCLs (Figure 3.3). A similar effect, although blunted, was observed in a *RAF*^{M} HMCL. The most marked results (including cell death in a single instance) were observed in lines that harbour a WT *p53* gene (MM1s and NCI). The inhibition of ERK phosphorylation resulted in loss of its nuclear accumulation (Figure 3.8), affecting its role in cell cycling, and likely other nuclear activities (transcription factor activation). Similarly, we observed the loss of nuclear accumulation of cyclin B (Figure 3.8), a known cytoplasmic target of phosphorylated ERK for nuclear trafficking, confirming reduced activity of the MAPK.

Mutations in *p53* are typically late events in MM, consistent with later stages and multiply relapsed disease. A phase II study investigating the MEKi selumetinib as

a single agent in R/R MM (median prior lines 5, range 2-11) had disappointingly low response rates (ORR <5%)[184]. The overall poor responses may be accounted for by several reasons; (i) study inclusion was not limited to patients with evidence of MAPK signalling (*RAS*^{M} status was only present in 5 of 10 evaluated, one of whom achieved a VGPR to therapy), our data shows *RAS*^{M} as a predictive biomarker of response to MEK inhibition (ii) rates of *p53* mutation were not reported which were likely to be more prevalent in those with multiply relapsed disease, and (iii) our data suggests that MEK inhibition is primarily cytostatic not cytotoxic, suggesting it is unlikely that significant response rates to single agent therapy will be seen.

We investigated trametinib monotherapy in a murine xenograft of *RAS*^{M} disease (*p53* WT). Whilst a reduced tumour burden and slowing of disease progression was seen, this did not correlate with improved survival compared with vehicle mice. This disparity between in vitro and murine studies may in part be due to commencing therapy too late (once imaging data is measurable) whereby the disease is too aggressive for cytostatic therapy. Further, escalating dosing may have resulted in a better response. Finally the addition of dexamethasone warrants evaluation in the *RAS*^{M} model.

A cytostatic effect is clearly inadequate in achieving meaningful disease control. We have shown the addition of dexamethasone, a backbone of almost every MM therapy protocol, to trametinib can result in synergistic cytotoxicity (Figure 3.10). ERK signalling has a well-established role in pro-survival and anti-apoptotic functions. Inhibitory phosphorylation of the BH3 only pro-apoptotic protein BIM[245], by ERK leads to its degradation by the proteasome. Further, ERK phosphorylates ribosomal 6 family kinases (RSK), resulting in inhibitory phosphorylation of the pro-apoptotic protein BAD, further promoting cell survival[340,341]. Thus, inhibition of ERK activity may in fact be “priming” the cell for death, but a second insult is still required for apoptosis to occur. Measuring baseline pro-apoptotic proteins expression and phosphorylation and the effect of trametinib on these, would be a strategy for further identifying rational combination therapy.

Why this cytostatic effect is limited to *RAS*^{M} HMCLs and not seen in t(4;14) HMCLs is not immediately clear. The best response was seen in KMS11, with high rates of cell cytotoxicity with the combination of trametinib and dexamethasone (but not as a single agent). KMS11 shows high levels of FGFR3 overexpression and also harbours a FGFR3 mutation[233]. As such this may also be a predictive marker of response in t(4;14) disease. However, it is also known that t(4;14) is signalling via more pathways than just the RAS-MAPK[342]. Interrogation of alternative signalling pathways and their downstream effectors may better delineate these effects.

Optimising response to trametinib with combination therapy is key. Supporting this idea, a retrospective case series of 58 R/R MM patients treated with trametinib, reported a response rate of 40%[185]. Seventy-five percent of those responses were seen in those treated with combination therapy. However, as a cautionary note, a phase I trial of the combination of the MEKi trametinib with the AKT inhibitor afuresertib in a small number of patients, including one with MM, found the combination's toxicity too great, with only a single partial response to therapy observed[183].

A reason that targeted MEK inhibition might fail, beyond just mechanisms of resistance, is due to the clonal heterogeneity of MM itself. Extensive clonal architecture in both space and time has repeatedly been demonstrated in MM, which only increases with later stages of disease[18,78,108]. As such, targeting a single driver mutation that is present in only a portion of disease clones, would allow those not harbouring the mutation to proliferate unchecked. Perhaps counter to this is the dominant role assumed by these mutations. This is already seen with existing therapies with discordant responses sometimes seen at different sites of disease.

Given that *RAS*^{M} is essentially not observed in MGUS, a potentially interesting strategy to forestall the development of symptomatic disease would be to identify patients at significantly higher risk of developing both symptomatic MM and a *RAS*^{M} (i.e. those with underlying t(11;14) and features of high risk asymptomatic MM), and treating early with a MEKi. Inhibition of the RAS-MAPK might prevent

development of pathway mutations and subsequent progression to symptomatic disease. Appreciably this is a difficult but might represent an interesting therapeutic approach. Further, only a single trial has shown a trend to delaying progression to symptomatic disease when treating earlier (Brighton T. ASH abstract 2017 130:3155)

7.2 RATIONAL COMBINATION STRATEGIES

Chemo-resistance, including resistance to novel therapies, remains a significant issue in the treatment of MM. Mechanisms of therapeutic resistance are highly variable. Several mechanisms have been recognised that result in resistance to targeted kinase inhibition, including loss of feedback inhibition, alternative kinase isoform activation, gene amplification, binding site mutations, activating mutations in downstream targets, activation of parallel pathways and up-regulation of RTKs. Many of these mechanisms predictably result in reactivation of the same signalling pathway, given underlying pathway addiction. Predicting these mechanisms before they arise through in vitro studies is difficult given the techniques required to generate resistant cell lines are very artificial and remarkably different to that which occurs clinically. Further, exhaustive searches are required to identify mechanisms responsible in in vitro studies, which eventually may prove to be clinically irrelevant and but one of many.

A novel mechanism of resistance to targeted therapy is dynamic kinome reprogramming[250]. Dynamic kinome reprogramming occurs where in the face of targeted kinase inhibition, alternative kinases (including RTKs) results in activation of the same or other kinase pathways, circumventing the inhibitor. Using array-based platforms of dynamic changes in kinase activity, assessment of cell kinase responses to various perturbations, including drug treatments, can be made. This approach has been used to evaluate kinome responses in AML[255] and breast cancer[254] to MEK inhibition leading to successful combination therapy. Similarly, we used this approach to assess early responses at 24 hours in kinase activity in response to treatment with trametinib with a view to identifying additional therapeutic targets. Amongst several kinases/pathways identified we found recurrent changes in activity in CK2 and BCL-2 that when targeted in

combination with trametinib resulted in synergistic cytotoxicity in *RAS*^{M} and modest synergistic cytotoxicity in t(4;14).

Providing validation of our findings, both of the targets we identified are currently under investigation as therapeutic targets in haematologic and solid malignancies. CK2 has been found to be as overexpressed in a number of haematologic and solid malignancies, and is involved in enhancing oncogenic signalling, leading to the concept of "non-oncogene addiction"[258,259,262]. Targeting BCL-2, with the inhibitor ABT-199 (venetoclax), has proven resoundingly successful in CLL and broadening its role in haematologic malignancy, including MM, is an area of ongoing intense research[246,269,271].

Evaluating kinome responses at later time points (48 and 72 hours), may reveal additional delayed responses to MEK inhibition, and further therapeutic targets to enhance sensitivity to trametinib treatment.

A more extensive analysis of the extended family of pro and anti-apoptotic proteins activity in response to MEK inhibition may give greater insight into targeting. We observed differential expression of phosphorylated BCL-2 across the panel of HMCLs (Figure 4.8), including its expression in *KRAS*^{M} but not *NRAS*^{M}, and the t(4;14) KMS11 which has already shown several similarities in activity to the *RAS*^{M} HMCLs. The presence of phosphorylated BLC-2 would appear to serve as a predictive biomarker to sensitivity to the combination in *RAS*^{M} and t(4;14) disease. Similarly, identifying other anti-apoptotic proteins to potentially target may optimise the role of MEK inhibition in more subsets of disease. MCL1 has a well-recognised role in survival in MM[267], however the coverage of the array we utilised did not include this protein or several other members of the BLC-2 family.

7.3 EPIGENETIC STRATEGIES

Pre-treatment of t(4;14) HMCLs with azacitidine resulted in sensitisation to treatment with trametinib. Cell cycle analysis of t(4;14) HMCLs after combination treatment recapitulates that seen in *RAS*^{M} HMCLs treated with trametinib alone.

DNMT3b overexpression in t(4;14) HMCLs correlated with response to azacitidine, corroborating what has previously been reported in a selection of solid malignancies. However, siRNA knockdown or specific inhibition of DNMT3b followed by treatment with trametinib was unable to recreate the findings of azacitidine pre-treatment.

Interrogation of gene changes and enriched pathways in response to azacitidine found remarkable heterogeneity with no single gene set, or enriched pathway that accounted for the findings. This suggests a very pleiotropic effect of azacitidine, that may be cell specific on a background of hypermethylation.

Treatment of a t(4;14) murine xenograft with azacitidine and trametinib, resulted in a significant reduction in disease burden and progression, but mice succumbed to toxicity of a second cycle of azacitidine. As such no comment could be made on survival. Whilst in a WT xenograft, azacitidine alone not only reduced disease burden, but improved overall survival. The addition of trametinib provided no additional benefit.

In both cases, establishment of extra-medullary disease, spinal and soft tissue plasmacytomata in the t(4;14) xenograft and hepatic plasmacytomata in the WT xenograft, were both significantly delayed or reduced by treatment with azacitidine. This raises the possibility that azacitidine induces changes within the microenvironment as well as the tumour itself. Reclaiming tumour cells from the murine xenograft after treatment with azacitidine, may provide more realistic insight into the effects of azacitidine. Further, analysis of gene changes occurring within hepatocytes in the WT xenograft could account for microenvironment changes too.

The exact mechanisms by which azacitidine exerts these effects remains unclear, however we identified a small number of re-expressed tumour suppressor genes in the t(4;14) HMCLs, consistent with previously published experience with azacitidine. Further, in one t(4;14) and one WT HMCL, we found similar pathways of immune activation, interferon signalling, antigen processing and MHC class II activity that has previously been described in solid tumours in response to

azacitidine[308,336,337]. It is doubtful that these changes mediate the activity of azacitidine or sensitivity to trametinib as both our in vitro and in vivo studies are performed in the absence of immune effector cells.

To better characterise the effects of azacitidine, interrogating gene changes in in a broader panel of t(4;14) HMCLs would provide greater significance to gene changes observed. In addition, a longer, or permanent knockdown (e.g. CRISPR-Cas9 knockout), of the azacitidine targets, DNMT3b and/or DNMT3a, with investigation of gene expression changes, may better identify potential mechanisms related to sensitivity.

Azacitidine is already in clinical use for high risk myelodysplastic syndromes[324,333]. Using our data, a clinical trial might reasonably be established evaluating azacitidine +/- trametinib in patients, either t(4;14) disease, evidence of DNMT3b overexpression, or extramedullary disease.

Finally, given the response to seen to hypo-methylation, investigating other epigenetic modifiers (e.g. histone deacetylase inhibitors) in combination with trametinib may provide further therapeutic opportunities, and insights into sensitivity to MEK inhibition.

7.4 CONCLUSION

Multiple myeloma is a cytogenetically and molecularly heterogeneous disease that remains incurable with current therapy. Aberrant signalling through the RAS-MAPK is frequent in MM, typically through RAS^M which is present in up to 50% of cases. Additionally, the cytogenetic translocation t(4;14), also signals through the RAS-MAPK. This oncogenic addiction can be exploited using targeted MEK inhibition with trametinib. In RAS^M disease trametinib significantly inhibits proliferation, and in combination with rationally selected inhibitors results in synergistic cytotoxicity. The presence of RAS^M is a biomarker for response to targeted MEK inhibition.

Responses in both *RAS*^{M} and t(4;14) disease, can be further optimised by using rationally selected combination therapy. Pre-treatment with azacitidine can sensitise t(4;14) disease to MEK inhibition.

Targeted therapy with MEK inhibition could provide another previously unexploited treatment option in multiple myeloma.

8. REFERENCES

1. Palumbo A, Anderson K. Multiple myeloma. The New England journal of medicine 2011;364:1046-60.
2. Palumbo A, Avet-Loiseau H, Oliva S, et al. Revised International Staging System for Multiple Myeloma: A Report From International Myeloma Working Group. Journal of clinical oncology : official journal of the American Society of Clinical Oncology 2015;33:2863-9.
3. MacLennan IC, Toellner KM, Cunningham AF, et al. Extrafollicular antibody responses. Immunological reviews 2003;194:8-18.
4. Shlomchik MJ, Weisel F. Germinal center selection and the development of memory B and plasma cells. Immunological reviews 2012;247:52-63.
5. Radbruch A, Muehlinghaus G, Luger EO, et al. Competence and competition: the challenge of becoming a long-lived plasma cell. Nat Rev Immunol 2006;6:741-50.
6. Nutt SL, Hodgkin PD, Tarlinton DM, Corcoran LM. The generation of antibody-secreting plasma cells. Nat Rev Immunol 2015;15:160-71.
7. Oracki SA, Walker JA, Hibbs ML, Corcoran LM, Tarlinton DM. Plasma cell development and survival. Immunological reviews 2010;237:140-59.
8. Morgan GJ, Walker BA, Davies FE. The genetic architecture of multiple myeloma. Nature reviews Cancer 2012;12:335-48.
9. Kyle RA, Larson DR, Therneau TM, et al. Long-Term Follow-up of Monoclonal Gammopathy of Undetermined Significance. The New England journal of medicine 2018;378:241-9.
10. Therneau TM, Kyle RA, Melton LJ, 3rd, et al. Incidence of monoclonal gammopathy of undetermined significance and estimation of duration before first clinical recognition. Mayo Clin Proc 2012;87:1071-9.
11. Weiss BM, Kuehl WM. Advances in understanding monoclonal gammopathy of undetermined significance as a precursor of multiple myeloma. Expert review of hematology 2010;3:165-74.
12. Rajkumar SV, Dimopoulos MA, Palumbo A, et al. International Myeloma Working Group updated criteria for the diagnosis of multiple myeloma. Lancet Oncol 2014;15:e538-48.

13. Rajkumar SV, Larson D, Kyle RA. Diagnosis of smoldering multiple myeloma. The New England journal of medicine 2011;365:474-5.
14. Larsen JT, Kumar SK, Dispenzieri A, Kyle RA, Katzmann JA, Rajkumar SV. Serum free light chain ratio as a biomarker for high-risk smoldering multiple myeloma. Leukemia 2013;27:941-6.
15. Hillengass J, Fechtner K, Weber MA, et al. Prognostic significance of focal lesions in whole-body magnetic resonance imaging in patients with asymptomatic multiple myeloma. Journal of clinical oncology : official journal of the American Society of Clinical Oncology 2010;28:1606-10.
16. Carrasco DR, Tonon G, Huang Y, et al. High-resolution genomic profiles define distinct clinico-pathogenetic subgroups of multiple myeloma patients. Cancer cell 2006;9:313-25.
17. Fonseca R, Bergsagel PL, Drach J, et al. International Myeloma Working Group molecular classification of multiple myeloma: spotlight review. Leukemia 2009;23:2210-21.
18. Mithraprabhu S, Khong T, Ramachandran M, et al. Circulating tumour DNA analysis demonstrates spatial mutational heterogeneity that coincides with disease relapse in myeloma. Leukemia 2017;31:1695-705.
19. Bergsagel PL, Kuehl WM. Molecular pathogenesis and a consequent classification of multiple myeloma. Journal of clinical oncology : official journal of the American Society of Clinical Oncology 2005;23:6333-8.
20. Chesi M, Bergsagel PL. Molecular pathogenesis of multiple myeloma: basic and clinical updates. International journal of hematology 2013;97:313-23.
21. Chesi M, Bergsagel PL. Advances in the pathogenesis and diagnosis of multiple myeloma. Int J Lab Hematol 2015;37 Suppl 1:108-14.
22. Chng WJ, Huang GF, Chung TH, et al. Clinical and biological implications of MYC activation: a common difference between MGUS and newly diagnosed multiple myeloma. Leukemia 2011;25:1026-35.
23. McKay MM, Morrison DK. Integrating signals from RTKs to ERK/MAPK. Oncogene 2007;26:3113-21.
24. Zebisch A, Czernilofsky AP, Keri G, Smigelskaite J, Sill H, Troppmair J. Signaling through RAS-RAF-MEK-ERK: from basics to bedside. Current medicinal chemistry 2007;14:601-23.

25. Yoon S, Seger R. The extracellular signal-regulated kinase: multiple substrates regulate diverse cellular functions. Growth factors 2006;24:21-44.
26. Cullen PJ, Lockyer PJ. Integration of calcium and Ras signalling. Nature reviews Molecular cell biology 2002;3:339-48.
27. Malumbres M, Barbacid M. RAS oncogenes: the first 30 years. Nature reviews Cancer 2003;3:459-65.
28. Johnson L, Greenbaum D, Cichowski K, et al. K-ras is an essential gene in the mouse with partial functional overlap with N-ras. Genes & development 1997;11:2468-81.
29. Downward J. Targeting RAS signalling pathways in cancer therapy. Nature reviews Cancer 2003;3:11-22.
30. Boykevisch S, Zhao C, Sondermann H, et al. Regulation of ras signaling dynamics by Sos-mediated positive feedback. Current biology : CB 2006;16:2173-9.
31. Roskoski R, Jr. RAF protein-serine/threonine kinases: structure and regulation. Biochemical and biophysical research communications 2010;399:313-7.
32. Freeman AK, Morrison DK. 14-3-3 Proteins: diverse functions in cell proliferation and cancer progression. Seminars in cell & developmental biology 2011;22:681-7.
33. Rushworth LK, Hindley AD, O'Neill E, Kolch W. Regulation and role of Raf-1/B-Raf heterodimerization. Molecular and cellular biology 2006;26:2262-72.
34. Roskoski R, Jr. MEK1/2 dual-specificity protein kinases: structure and regulation. Biochemical and biophysical research communications 2012;417:5-10.
35. Roskoski R, Jr. ERK1/2 MAP kinases: structure, function, and regulation. Pharmacological research : the official journal of the Italian Pharmacological Society 2012;66:105-43.
36. Busca R, Pouyssegur J, Lenormand P. ERK1 and ERK2 Map Kinases: Specific Roles or Functional Redundancy? Front Cell Dev Biol 2016;4:53.
37. Fremin C, Saba-El-Leil MK, Levesque K, Ang SL, Meloche S. Functional Redundancy of ERK1 and ERK2 MAP Kinases during Development. Cell Rep 2015;12:913-21.

38. Morrison DK, Davis RJ. Regulation of MAP kinase signaling modules by scaffold proteins in mammals. Annual review of cell and developmental biology 2003;19:91-118.
39. Roy M, Li Z, Sacks DB. IQGAP1 binds ERK2 and modulates its activity. The Journal of biological chemistry 2004;279:17329-37.
40. Roy M, Li Z, Sacks DB. IQGAP1 is a scaffold for mitogen-activated protein kinase signaling. Molecular and cellular biology 2005;25:7940-52.
41. Torii S, Kusakabe M, Yamamoto T, Maekawa M, Nishida E. Sef is a spatial regulator for Ras/MAP kinase signaling. Developmental cell 2004;7:33-44.
42. Dhanasekaran DN, Kashef K, Lee CM, Xu H, Reddy EP. Scaffold proteins of MAP-kinase modules. Oncogene 2007;26:3185-202.
43. Li W, Han M, Guan KL. The leucine-rich repeat protein SUR-8 enhances MAP kinase activation and forms a complex with Ras and Raf. Genes & development 2000;14:895-900.
44. Ziogas A, Moelling K, Radziwill G. CNK1 is a scaffold protein that regulates Src-mediated Raf-1 activation. The Journal of biological chemistry 2005;280:24205-11.
45. Granovsky AE, Rosner MR. Raf kinase inhibitory protein: a signal transduction modulator and metastasis suppressor. Cell research 2008;18:452-7.
46. Masoumi-Moghaddam S, Amini A, Morris DL. The developing story of Sprouty and cancer. Cancer metastasis reviews 2014.
47. Hanafusa H, Torii S, Yasunaga T, Nishida E. Sprouty1 and Sprouty2 provide a control mechanism for the Ras/MAPK signalling pathway. Nature cell biology 2002;4:850-8.
48. Douville E, Downward J. EGF induced SOS phosphorylation in PC12 cells involves P90 RSK-2. Oncogene 1997;15:373-83.
49. Dougherty MK, Muller J, Ritt DA, et al. Regulation of Raf-1 by direct feedback phosphorylation. Molecular cell 2005;17:215-24.
50. Eblen ST, Slack-Davis JK, Tarcsafalvi A, Parsons JT, Weber MJ, Catling AD. Mitogen-activated protein kinase feedback phosphorylation regulates MEK1 complex formation and activation during cellular adhesion. Molecular and cellular biology 2004;24:2308-17.

51. Nikolaev SI, Vetiska S, Bonilla X, et al. Somatic Activating KRAS Mutations in Arteriovenous Malformations of the Brain. The New England journal of medicine 2018;378:250-61.
52. Anglesio MS, Papadopoulos N, Ayhan A, et al. Cancer-Associated Mutations in Endometriosis without Cancer. The New England journal of medicine 2017;376:1835-48.
53. Cox AD, Der CJ. Ras history: The saga continues. Small GTPases 2010;1:2-27.
54. Santos E, Tronick SR, Aaronson SA, Pulciani S, Barbacid M. T24 human bladder carcinoma oncogene is an activated form of the normal human homologue of BALB- and Harvey-MSV transforming genes. Nature 1982;298:343-7.
55. Der CJ, Krontiris TG, Cooper GM. Transforming genes of human bladder and lung carcinoma cell lines are homologous to the ras genes of Harvey and Kirsten sarcoma viruses. Proceedings of the National Academy of Sciences of the United States of America 1982;79:3637-40.
56. Parada LF, Tabin CJ, Shih C, Weinberg RA. Human EJ bladder carcinoma oncogene is homologue of Harvey sarcoma virus ras gene. Nature 1982;297:474-8.
57. Almoguera C, Shibata D, Forrester K, Martin J, Arnheim N, Perucho M. Most human carcinomas of the exocrine pancreas contain mutant c-K-ras genes. Cell 1988;53:549-54.
58. Kipp BR, Fritcher EG, Clayton AC, et al. Comparison of KRAS mutation analysis and FISH for detecting pancreatobiliary tract cancer in cytology specimens collected during endoscopic retrograde cholangiopancreatography. J Mol Diagn 2010;12:780-6.
59. Vaughn CP, Zobell SD, Furtado LV, Baker CL, Samowitz WS. Frequency of KRAS, BRAF, and NRAS mutations in colorectal cancer. Genes Chromosomes Cancer 2011;50:307-12.
60. Nikiforova MN, Lynch RA, Biddinger PW, et al. RAS point mutations and PAX8-PPAR gamma rearrangement in thyroid tumors: evidence for distinct molecular pathways in thyroid follicular carcinoma. The Journal of clinical endocrinology and metabolism 2003;88:2318-26.

61. Zhu Z, Gandhi M, Nikiforova MN, Fischer AH, Nikiforov YE. Molecular profile and clinical-pathologic features of the follicular variant of papillary thyroid carcinoma. An unusually high prevalence of ras mutations. Am J Clin Pathol 2003;120:71-7.
62. Nelson MA, Wymer J, Clements N, Jr. Detection of K-ras gene mutations in non-neoplastic lung tissue and lung cancers. Cancer Lett 1996;103:115-21.
63. Suzuki Y, Orita M, Shiraishi M, Hayashi K, Sekiya T. Detection of ras gene mutations in human lung cancers by single-strand conformation polymorphism analysis of polymerase chain reaction products. Oncogene 1990;5:1037-43.
64. Davies H, Bignell GR, Cox C, et al. Mutations of the BRAF gene in human cancer. Nature 2002;417:949-54.
65. Fukushima T, Suzuki S, Mashiko M, et al. BRAF mutations in papillary carcinomas of the thyroid. Oncogene 2003;22:6455-7.
66. Cohen Y, Xing M, Mambo E, et al. BRAF mutation in papillary thyroid carcinoma. J Natl Cancer Inst 2003;95:625-7.
67. Sanz-Garcia E, Argiles G, Elez E, Tabernero J. BRAF mutant colorectal cancer: prognosis, treatment, and new perspectives. Ann Oncol 2017;28:2648-57.
68. Paquette RL, Landaw EM, Pierre RV, et al. N-ras mutations are associated with poor prognosis and increased risk of leukemia in myelodysplastic syndrome. Blood 1993;82:590-9.
69. Kihara R, Nagata Y, Kiyoi H, et al. Comprehensive analysis of genetic alterations and their prognostic impacts in adult acute myeloid leukemia patients. Leukemia 2014;28:1586-95.
70. Irving J, Matheson E, Minto L, et al. Ras pathway mutations are prevalent in relapsed childhood acute lymphoblastic leukemia and confer sensitivity to MEK inhibition. Blood 2014;124:3420-30.
71. Tiacci E, Schiavoni G, Martelli MP, et al. Constant activation of the RAF-MEK-ERK pathway as a diagnostic and therapeutic target in hairy cell leukemia. Haematologica 2013;98:635-9.
72. Tiacci E, Trifonov V, Schiavoni G, et al. BRAF mutations in hairy-cell leukemia. The New England journal of medicine 2011;364:2305-15.

73. Waterfall JJ, Arons E, Walker RL, et al. High prevalence of MAP2K1 mutations in variant and IGHV4-34-expressing hairy-cell leukemias. Nature genetics 2014;46:8-10.
74. Arons E, Kreitman RJ. Molecular variant of hairy cell leukemia with poor prognosis. Leukemia & lymphoma 2011;52 Suppl 2:99-102.
75. Flaherty KT, Puzanov I, Kim KB, et al. Inhibition of mutated, activated BRAF in metastatic melanoma. The New England journal of medicine 2010;363:809-19.
76. Flaherty KT, Infante JR, Daud A, et al. Combined BRAF and MEK inhibition in melanoma with BRAF V600 mutations. The New England journal of medicine 2012;367:1694-703.
77. Long GV, Stroyakovskiy D, Gogas H, et al. Combined BRAF and MEK inhibition versus BRAF inhibition alone in melanoma. The New England journal of medicine 2014;371:1877-88.
78. Lohr JG, Stojanov P, Carter SL, et al. Widespread genetic heterogeneity in multiple myeloma: implications for targeted therapy. Cancer cell 2014;25:91-101.
79. Crowder C, Kopantzev E, Williams K, Lengel C, Miki T, Rudikoff S. An unusual H-Ras mutant isolated from a human multiple myeloma line leads to transformation and factor-independent cell growth. Oncogene 2003;22:649-59.
80. Millar BC, Bell JB, Barfoot R, Everard M. The proliferation of multiple myeloma colonies (MY-CFUc) in vitro is independent of prognosis and is not associated with mutated N- or K-ras alleles in human bone marrow aspirates. British journal of cancer 1995;71:259-64.
81. Yasuga Y, Hirosawa S, Yamamoto K, Tomiyama J, Nagata K, Aokia N. N-ras and p53 gene mutations are very rare events in multiple myeloma. International journal of hematology 1995;62:91-7.
82. Martin P, Santon A, Garcia-Cosio M, Bellas C. RAS mutations are uncommon in multiple myeloma and other monoclonal gammopathies. International journal of oncology 2005;27:1023-8.
83. Kalakonda N, Rothwell DG, Scarffe JH, Norton JD. Detection of N-Ras codon 61 mutations in subpopulations of tumor cells in multiple myeloma at presentation. Blood 2001;98:1555-60.

84. Ortega MM, Faria RM, Shitara ES, et al. N-RAS and K-RAS gene mutations in Brazilian patients with multiple myeloma. Leukemia & lymphoma 2006;47:285-9.
85. Ng MH, Lau KM, Wong WS, et al. Alterations of RAS signalling in Chinese multiple myeloma patients: absent BRAF and rare RAS mutations, but frequent inactivation of RASSF1A by transcriptional silencing or expression of a non-functional variant transcript. British journal of haematology 2003;123:637-45.
86. Melchor L, Brioli A, Wardell CP, et al. Single-cell genetic analysis reveals the composition of initiating clones and phylogenetic patterns of branching and parallel evolution in myeloma. Leukemia 2014.
87. Walker BA, Wardell CP, Melchor L, et al. Intraclonal heterogeneity and distinct molecular mechanisms characterize the development of t(4;14) and t(11;14) myeloma. Blood 2012;120:1077-86.
88. Neri A, Murphy JP, Cro L, et al. Ras oncogene mutation in multiple myeloma. The Journal of experimental medicine 1989;170:1715-25.
89. Chng WJ, Gonzalez-Paz N, Price-Troska T, et al. Clinical and biological significance of RAS mutations in multiple myeloma. Leukemia 2008;22:2280-4.
90. Rasmussen T, Kuehl M, Lodahl M, Johnsen HE, Dahl IM. Possible roles for activating RAS mutations in the MGUS to MM transition and in the intramedullary to extramedullary transition in some plasma cell tumors. Blood 2005;105:317-23.
91. Rasmussen T, Haaber J, Dahl IM, et al. Identification of translocation products but not K-RAS mutations in memory B cells from patients with multiple myeloma. Haematologica 2010;95:1730-7.
92. Mullins CD, Su MY, Hucthagowder V, et al. Germinal center B-cells resist transformation by Kras independently of tumor suppressor Arf. PloS one 2013;8:e67941.
93. Linden MA, Kirchhof N, Carlson CS, Van Ness BG. Targeted overexpression of an activated N-ras gene results in B-cell and plasma cell lymphoproliferation and cooperates with c-myc to induce fatal B-cell neoplasia. Experimental hematology 2012;40:216-27.
94. Liu P, Leong T, Quam L, et al. Activating mutations of N- and K-ras in multiple myeloma show different clinical associations: analysis of the Eastern Cooperative Oncology Group Phase III Trial. Blood 1996;88:2699-706.

95. Mulligan G, Lichter DI, Di Bacco A, et al. Mutation of NRAS but not KRAS significantly reduces myeloma sensitivity to single-agent bortezomib therapy. Blood 2014;123:632-9.
96. Greco C, Vitelli G, Vercillo G, et al. Reduction of serum IGF-I levels in patients affected with Monoclonal Gammopathies of undetermined significance or Multiple Myeloma. Comparison with bFGF, VEGF and K-ras gene mutation. Journal of experimental & clinical cancer research : CR 2009;28:35.
97. Rowley M, Liu P, Van Ness B. Heterogeneity in therapeutic response of genetically altered myeloma cell lines to interleukin 6, dexamethasone, doxorubicin, and melphalan. Blood 2000;96:3175-80.
98. Rowley M, Van Ness B. Activation of N-ras and K-ras induced by interleukin-6 in a myeloma cell line: implications for disease progression and therapeutic response. Oncogene 2002;21:8769-75.
99. Hu L, Shi Y, Hsu JH, Gera J, Van Ness B, Lichtenstein A. Downstream effectors of oncogenic ras in multiple myeloma cells. Blood 2003;101:3126-35.
100. Zhang B, Fenton RG. Proliferation of IL-6-independent multiple myeloma does not require the activity of extracellular signal-regulated kinases (ERK1/2). Journal of cellular physiology 2002;193:42-54.
101. Billadeau D, Jelinek DF, Shah N, LeBien TW, Van Ness B. Introduction of an activated N-ras oncogene alters the growth characteristics of the interleukin 6-dependent myeloma cell line ANBL6. Cancer research 1995;55:3640-6.
102. Billadeau D, Liu P, Jelinek D, Shah N, LeBien TW, Van Ness B. Activating mutations in the N- and K-ras oncogenes differentially affect the growth properties of the IL-6-dependent myeloma cell line ANBL6. Cancer research 1997;57:2268-75.
103. Mikulasova A, Wardell CP, Murison A, et al. The spectrum of somatic mutations in monoclonal gammopathy of undetermined significance indicates a less complex genomic landscape than that in multiple myeloma. Haematologica 2017;102:1617-25.
104. Xu J, Pfarr N, Endris V, et al. Molecular signaling in multiple myeloma: association of RAS/RAF mutations and MEK/ERK pathway activation. Oncogenesis 2017;6:e337.

105. Kortum KM, Mai EK, Hanafiah NH, et al. Targeted sequencing of refractory myeloma reveals a high incidence of mutations in CRBN and Ras pathway genes. Blood 2016;128:1226-33.
106. Walker BA, Boyle EM, Wardell CP, et al. Mutational Spectrum, Copy Number Changes, and Outcome: Results of a Sequencing Study of Patients With Newly Diagnosed Myeloma. Journal of clinical oncology : official journal of the American Society of Clinical Oncology 2015;33:3911-20.
107. Lionetti M, Barbieri M, Todoerti K, et al. Molecular spectrum of BRAF, NRAS and KRAS gene mutations in plasma cell dyscrasias: implication for MEK-ERK pathway activation. Oncotarget 2015;6:24205-17.
108. Bolli N, Avet-Loiseau H, Wedge DC, et al. Heterogeneity of genomic evolution and mutational profiles in multiple myeloma. Nature communications 2014;5:2997.
109. Mosca L, Musto P, Todoerti K, et al. Genome-wide analysis of primary plasma cell leukemia identifies recurrent imbalances associated with changes in transcriptional profiles. American journal of hematology 2013;88:16-23.
110. Hucthagowder V, Meyer R, Mullins C, et al. Resequencing analysis of the candidate tyrosine kinase and RAS pathway gene families in multiple myeloma. Cancer genetics 2012;205:474-8.
111. Chapman MA, Lawrence MS, Keats JJ, et al. Initial genome sequencing and analysis of multiple myeloma. Nature 2011;471:467-72.
112. Tiedemann RE, Gonzalez-Paz N, Kyle RA, et al. Genetic aberrations and survival in plasma cell leukemia. Leukemia 2008;22:1044-52.
113. Intini D, Agnelli L, Ciceri G, et al. Relevance of Ras gene mutations in the context of the molecular heterogeneity of multiple myeloma. Hematological oncology 2007;25:6-10.
114. Bezieau S, Devilder MC, Avet-Loiseau H, et al. High incidence of N and K-Ras activating mutations in multiple myeloma and primary plasma cell leukemia at diagnosis. Human mutation 2001;18:212-24.
115. Corradini P, Ladetto M, Voena C, et al. Mutational activation of N- and K-ras oncogenes in plasma cell dyscrasias. Blood 1993;81:2708-13.
116. Portier M, Moles JP, Mazars GR, et al. p53 and RAS gene mutations in multiple myeloma. Oncogene 1992;7:2539-43.

117. Tanaka K, Takechi M, Asaoku H, Dohy H, Kamada N. A high frequency of N-RAS oncogene mutations in multiple myeloma. International journal of hematology 1992;56:119-27.
118. Matozaki S, Nakagawa T, Nakao Y, Fujita T. RAS gene mutations in multiple myeloma and related monoclonal gammopathies. The Kobe journal of medical sciences 1991;37:35-45.
119. Paquette RL, Berenson J, Lichtenstein A, McCormick F, Koeffler HP. Oncogenes in multiple myeloma: point mutation of N-ras. Oncogene 1990;5:1659-63.
120. van der Spek E. Targeting the mevalonate pathway in multiple myeloma. Leukemia research 2010;34:267-8.
121. Harousseau JL. Farnesyltransferase inihibitors in hematologic malignancies. Blood reviews 2007;21:173-82.
122. Cafforio P, Dammacco F, Gernone A, Silvestris F. Statins activate the mitochondrial pathway of apoptosis in human lymphoblasts and myeloma cells. Carcinogenesis 2005;26:883-91.
123. Luckman SP, Hughes DE, Coxon FP, Graham R, Russell G, Rogers MJ. Nitrogen-containing bisphosphonates inhibit the mevalonate pathway and prevent post-translational prenylation of GTP-binding proteins, including Ras. Journal of bone and mineral research : the official journal of the American Society for Bone and Mineral Research 1998;13:581-9.
124. Le Gouill S, Pellat-Deceunynck C, Harousseau JL, et al. Farnesyl transferase inhibitor R115777 induces apoptosis of human myeloma cells. Leukemia 2002;16:1664-7.
125. Ochiai N, Uchida R, Fuchida S, et al. Effect of farnesyl transferase inhibitor R115777 on the growth of fresh and cloned myeloma cells in vitro. Blood 2003;102:3349-53.
126. Frassanito MA, Cusmai A, Piccoli C, Dammacco F. Manumycin inhibits farnesyltransferase and induces apoptosis of drug-resistant interleukin 6-producing myeloma cells. British journal of haematology 2002;118:157-65.
127. Frassanito MA, Mastromauro L, Cusmai A, Dammacco F. Blockade of the Ras pathway by manumycin, a farnesyltransferase inhibitor, overcomes the resistance of myeloma plasma cells to Fas-induced apoptosis. Clinical and experimental medicine 2005;4:174-82.

128. Bolick SC, Landowski TH, Boulware D, et al. The farnesyl transferase inhibitor, FTI-277, inhibits growth and induces apoptosis in drug-resistant myeloma tumor cells. Leukemia 2003;17:451-7.
129. Shi Y, Gera J, Hsu JH, Van Ness B, Lichtenstein A. Cytoreductive effects of farnesyl transferase inhibitors on multiple myeloma tumor cells. Molecular cancer therapeutics 2003;2:563-72.
130. Ochiai N, Yamada N, Uchida R, et al. Nitrogen-containing bisphosphonate incadronate augments the inhibitory effect of farnesyl transferase inhibitor tipifarnib on the growth of fresh and cloned myeloma cells in vitro. Leukemia & lymphoma 2005;46:1619-25.
131. Dai Y, Chen S, Pei XY, et al. Interruption of the Ras/MEK/ERK signaling cascade enhances Chk1 inhibitor-induced DNA damage in vitro and in vivo in human multiple myeloma cells. Blood 2008;112:2439-49.
132. Morgan MA, Sebil T, Aydilek E, Peest D, Ganser A, Reuter CW. Combining prenylation inhibitors causes synergistic cytotoxicity, apoptosis and disruption of RAS-to-MAP kinase signalling in multiple myeloma cells. British journal of haematology 2005;130:912-25.
133. David E, Sun SY, Waller EK, Chen J, Khuri FR, Lonial S. The combination of the farnesyl transferase inhibitor lonafarnib and the proteasome inhibitor bortezomib induces synergistic apoptosis in human myeloma cells that is associated with down-regulation of p-AKT. Blood 2005;106:4322-9.
134. Alsina M, Fonseca R, Wilson EF, et al. Farnesyltransferase inhibitor tipifarnib is well tolerated, induces stabilization of disease, and inhibits farnesylation and oncogenic/tumor survival pathways in patients with advanced multiple myeloma. Blood 2004;103:3271-7.
135. Cortes J, Albitar M, Thomas D, et al. Efficacy of the farnesyl transferase inhibitor R115777 in chronic myeloid leukemia and other hematologic malignancies. Blood 2003;101:1692-7.
136. Dai Y, Khanna P, Chen S, Pei XY, Dent P, Grant S. Statins synergistically potentiate 7-hydroxystaurosporine (UCN-01) lethality in human leukemia and myeloma cells by disrupting Ras farnesylation and activation. Blood 2007;109:4415-23.

137. van de Donk NW, Kamphuis MM, Lokhorst HM, Bloem AC. The cholesterol lowering drug lovastatin induces cell death in myeloma plasma cells. Leukemia 2002;16:1362-71.
138. Schmidmaier R, Baumann P, Bumeder I, Meinhardt G, Straka C, Emmerich B. First clinical experience with simvastatin to overcome drug resistance in refractory multiple myeloma. European journal of haematology 2007;79:240-3.
139. Dmoszynska A, Podhorecka M, Klimek P, Grzasko N. Lovastatin and thalidomide have a combined effect on the rate of multiple myeloma cell apoptosis in short term cell cultures. European journal of clinical pharmacology 2006;62:325-9.
140. Slawinska-Brych A, Zdzisinska B, Mizerska-Dudka M, Kandefer-Szerszen M. Induction of apoptosis in multiple myeloma cells by a statin-thalidomide combination can be enhanced by p38 MAPK inhibition. Leukemia research 2013;37:586-94.
141. van der Spek E, Bloem AC, Lokhorst HM, van Kessel B, Bogers-Boer L, van de Donk NW. Inhibition of the mevalonate pathway potentiates the effects of lenalidomide in myeloma. Leukemia research 2009;33:100-8.
142. Drucker L, Afensiev F, Radnay J, Shapira H, Lishner M. Co-administration of simvastatin and cytotoxic drugs is advantageous in myeloma cell lines. Anti-cancer drugs 2004;15:79-84.
143. Hus M, Grzasko N, Szostek M, et al. Thalidomide, dexamethasone and lovastatin with autologous stem cell transplantation as a salvage immunomodulatory therapy in patients with relapsed and refractory multiple myeloma. Annals of hematology 2011;90:1161-6.
144. van der Spek E, Bloem AC, van de Donk NW, et al. Dose-finding study of high-dose simvastatin combined with standard chemotherapy in patients with relapsed or refractory myeloma or lymphoma. Haematologica 2006;91:542-5.
145. van der Spek E, Bloem AC, Sinnige HA, Lokhorst HM. High dose simvastatin does not reverse resistance to vincristine, adriamycin, and dexamethasone (VAD) in myeloma. Haematologica 2007;92:e130-1.
146. Sondergaard TE, Pedersen PT, Andersen TL, et al. A phase II clinical trial does not show that high dose simvastatin has beneficial effect on markers of bone turnover in multiple myeloma. Hematological oncology 2009;27:17-22.

147. Muller E, Bauer S, Stuhmer T, et al. Pan-Raf co-operates with PI3K-dependent signalling and critically contributes to myeloma cell survival independently of mutated RAS. Leukemia 2017;31:922-33.
148. Wan PT, Garnett MJ, Roe SM, et al. Mechanism of activation of the RAF-ERK signaling pathway by oncogenic mutations of B-RAF. Cell 2004;116:855-67.
149. Rustad EH, Dai HY, Hov H, et al. BRAF V600E mutation in early-stage multiple myeloma: good response to broad acting drugs and no relation to prognosis. Blood cancer journal 2015;5:e299.
150. Andrulis M, Lehners N, Capper D, et al. Targeting the BRAF V600E mutation in multiple myeloma. Cancer discovery 2013;3:862-9.
151. Baritaki S, Huerta-Yepez S, Cabrava-Haimandez MD, et al. Unique Pattern of Overexpression of Raf-1 Kinase Inhibitory Protein in Its Inactivated Phosphorylated Form in Human Multiple Myeloma. Forum on immunopathological diseases and therapeutics 2011;2.
152. Morgan GJ, He J, Tytarenko R, et al. Kinase domain activation through gene rearrangement in multiple myeloma. Leukemia 2018.
153. Wilhelm SM, Carter C, Tang L, et al. BAY 43-9006 exhibits broad spectrum oral antitumor activity and targets the RAF/MEK/ERK pathway and receptor tyrosine kinases involved in tumor progression and angiogenesis. Cancer research 2004;64:7099-109.
154. Ramakrishnan V, Timm M, Haug JL, et al. Sorafenib, a dual Raf kinase/vascular endothelial growth factor receptor inhibitor has significant anti-myeloma activity and synergizes with common anti-myeloma drugs. Oncogene 2010;29:1190-202.
155. Kharaziha P, De Raeve H, Fristedt C, et al. Sorafenib has potent antitumor activity against multiple myeloma in vitro, ex vivo, and in vivo in the 5T33MM mouse model. Cancer research 2012;72:5348-62.
156. Udi J, Schuler J, Wider D, et al. Potent in vitro and in vivo activity of sorafenib in multiple myeloma: induction of cell death, CD138-downregulation and inhibition of migration through actin depolymerization. British journal of haematology 2013;161:104-16.
157. Yordanova A, Hose D, Neben K, et al. Sorafenib in patients with refractory or recurrent multiple myeloma. Hematological oncology 2013;31:197-200.

158. Kumar SK, Jett J, Marks R, et al. Phase 1 study of sorafenib in combination with bortezomib in patients with advanced malignancies. Investigational new drugs 2013;31:1201-6.
159. Breitkreutz I, Podar K, Figueroa-Vazquez V, et al. The orally available multikinase inhibitor regorafenib (BAY 73-4506) in multiple myeloma. Annals of hematology 2018;97:839-49.
160. Wilhelm SM, Dumas J, Adnane L, et al. Regorafenib (BAY 73-4506): a new oral multikinase inhibitor of angiogenic, stromal and oncogenic receptor tyrosine kinases with potent preclinical antitumor activity. International journal of cancer Journal international du cancer 2011;129:245-55.
161. Bohn OL, Hsu K, Hyman DM, Pignataro DS, Giralt S, Teruya-Feldstein J. BRAF V600E mutation and clonal evolution in a patient with relapsed refractory myeloma with plasmablastic differentiation. Clinical lymphoma, myeloma & leukemia 2014;14:e65-8.
162. Mey UJM, Renner C, von Moos R. Vemurafenib in combination with cobimetinib in relapsed and refractory extramedullary multiple myeloma harboring the BRAF V600E mutation. Hematological oncology 2017;35:890-3.
163. Sharman JP, Chmielecki J, Morosini D, et al. Vemurafenib response in 2 patients with posttransplant refractory BRAF V600E-mutated multiple myeloma. Clinical lymphoma, myeloma & leukemia 2014;14:e161-3.
164. Raab MS, Lehners N, Xu J, et al. Spatially divergent clonal evolution in multiple myeloma: overcoming resistance to BRAF inhibition. Blood 2016;127:2155-7.
165. Khong T, Spencer A. Targeting HSP 90 induces apoptosis and inhibits critical survival and proliferation pathways in multiple myeloma. Molecular cancer therapeutics 2011;10:1909-17.
166. Gantke T, Sriskantharajah S, Sadowski M, Ley SC. IkappaB kinase regulation of the TPL-2/ERK MAPK pathway. Immunological reviews 2012;246:168-82.
167. Shi L, Wang S, Zangari M, et al. Over-expression of CKS1B activates both MEK/ERK and JAK/STAT3 signaling pathways and promotes myeloma cell drug-resistance. Oncotarget 2010;1:22-33.

168. Ramakrishnan V, Kimlinger T, Haug J, et al. Anti-myeloma activity of Akt inhibition is linked to the activation status of PI3K/Akt and MEK/ERK pathway. PloS one 2012;7:e50005.
169. Hurt EM, Wiestner A, Rosenwald A, et al. Overexpression of c-maf is a frequent oncogenic event in multiple myeloma that promotes proliferation and pathological interactions with bone marrow stroma. Cancer cell 2004;5:191-9.
170. Annunziata CM, Hernandez L, Davis RE, et al. A mechanistic rationale for MEK inhibitor therapy in myeloma based on blockade of MAF oncogene expression. Blood 2011;117:2396-404.
171. Herath NI, Rocques N, Garancher A, Eychene A, Pouponnot C. GSK3-mediated MAF phosphorylation in multiple myeloma as a potential therapeutic target. Blood cancer journal 2014;4:e175.
172. Liu Z, Li T, Reinhold MI, Naski MC. MEK1-RSK2 contributes to Hedgehog signaling by stabilizing GLI2 transcription factor and inhibiting ubiquitination. Oncogene 2014;33:65-73.
173. Tsubaki M, Kato C, Nishinobo M, et al. Nitrogen-containing bisphosphonate, YM529/ONO-5920, inhibits macrophage inflammatory protein 1 alpha expression and secretion in mouse myeloma cells. Cancer science 2008;99:152-8.
174. Tsubaki M, Kato C, Isono A, et al. Macrophage inflammatory protein-1alpha induces osteoclast formation by activation of the MEK/ERK/c-Fos pathway and inhibition of the p38MAPK/IRF-3/IFN-beta pathway. Journal of cellular biochemistry 2010;111:1661-72.
175. Breitkreutz I, Raab MS, Vallet S, et al. Targeting MEK1/2 blocks osteoclast differentiation, function and cytokine secretion in multiple myeloma. British journal of haematology 2007;139:55-63.
176. Hideshima T, Catley L, Yasui H, et al. Perifosine, an oral bioactive novel alkylphospholipid, inhibits Akt and induces in vitro and in vivo cytotoxicity in human multiple myeloma cells. Blood 2006;107:4053-62.
177. Nelson EA, Walker SR, Kepich A, et al. Nifuroxazide inhibits survival of multiple myeloma cells by directly inhibiting STAT3. Blood 2008;112:5095-102.
178. Pei XY, Dai Y, Tenorio S, et al. MEK1/2 inhibitors potentiate UCN-01 lethality in human multiple myeloma cells through a Bim-dependent mechanism. Blood 2007;110:2092-101.

179. Pei XY, Li W, Dai Y, Dent P, Grant S. Dissecting the roles of checkpoint kinase 1/CDC2 and mitogen-activated protein kinase kinase 1/2/extracellular signal-regulated kinase 1/2 in relation to 7-hydroxystaurosporine-induced apoptosis in human multiple myeloma cells. Molecular pharmacology 2006;70:1965-73.
180. Chatterjee M, Stuhmer T, Herrmann P, Bommert K, Dorken B, Bargou RC. Combined disruption of both the MEK/ERK and the IL-6R/STAT3 pathways is required to induce apoptosis of multiple myeloma cells in the presence of bone marrow stromal cells. Blood 2004;104:3712-21.
181. Lunghi P, Giuliani N, Mazzera L, et al. Targeting MEK/MAPK signal transduction module potentiates ATO-induced apoptosis in multiple myeloma cells through multiple signaling pathways. Blood 2008;112:2450-62.
182. Tai YT, Fulciniti M, Hideshima T, et al. Targeting MEK induces myeloma-cell cytotoxicity and inhibits osteoclastogenesis. Blood 2007;110:1656-63.
183. Tolcher AW, Patnaik A, Papadopoulos KP, et al. Phase I study of the MEK inhibitor trametinib in combination with the AKT inhibitor afuresertib in patients with solid tumors and multiple myeloma. Cancer Chemother Pharmacol 2015;75:183-9.
184. Holkova B, Zingone A, Kmieciak M, et al. A Phase II Trial of AZD6244 (Selumetinib, ARRY-142886), an Oral MEK1/2 Inhibitor, in Relapsed/Refractory Multiple Myeloma. Clinical cancer research : an official journal of the American Association for Cancer Research 2016;22:1067-75.
185. Heuck CJ, Jethava Y, Khan R, et al. Inhibiting MEK in MAPK pathway-activated myeloma. Leukemia 2016;30:976-80.
186. Fan L, Hong J, Huang H, et al. High Expression of Phosphorylated Extracellular Signal-Regulated Kinase (ERK1/2) is Associated with Poor Prognosis in Newly Diagnosed Patients with Multiple Myeloma. Med Sci Monit 2017;23:2636-43.
187. Chen H, Shi L, Yang X, Li S, Guo X, Pan L. Artesunate inhibiting angiogenesis induced by human myeloma RPMI8226 cells. International journal of hematology 2010;92:587-97.
188. Ma Y, Jin Z, Huang J, et al. IQGAP1 plays an important role in the cell proliferation of multiple myeloma via the MAP kinase (ERK) pathway. Oncology reports 2013;30:3032-8.

189. Ma Y, Jin Z, Huang J, et al. Quercetin suppresses the proliferation of multiple myeloma cells by down-regulating IQ motif-containing GTPase activating protein 1 expression and extracellular signal-regulated kinase activation. Leukemia & lymphoma 2014.
190. Gocke CB, McMillan R, Wang Q, et al. IQGAP1 Scaffold-MAP Kinase Interactions Enhance Multiple Myeloma Clonogenic Growth and Self-Renewal. Molecular cancer therapeutics 2016;15:2733-9.
191. Chapman PB, Hauschild A, Robert C, et al. Improved survival with vemurafenib in melanoma with BRAF V600E mutation. The New England journal of medicine 2011;364:2507-16.
192. Van Allen EM, Wagle N, Sucker A, et al. The genetic landscape of clinical resistance to RAF inhibition in metastatic melanoma. Cancer discovery 2014;4:94-109.
193. Lito P, Pratilas CA, Joseph EW, et al. Relief of profound feedback inhibition of mitogenic signaling by RAF inhibitors attenuates their activity in BRAFV600E melanomas. Cancer cell 2012;22:668-82.
194. Hatzivassiliou G, Song K, Yen I, et al. RAF inhibitors prime wild-type RAF to activate the MAPK pathway and enhance growth. Nature 2010;464:431-5.
195. Poulikakos PI, Zhang C, Bollag G, Shokat KM, Rosen N. RAF inhibitors transactivate RAF dimers and ERK signalling in cells with wild-type BRAF. Nature 2010;464:427-30.
196. Nazarian R, Shi H, Wang Q, et al. Melanomas acquire resistance to B-RAF(V600E) inhibition by RTK or N-RAS upregulation. Nature 2010;468:973-7.
197. Shi H, Moriceau G, Kong X, et al. Melanoma whole-exome sequencing identifies (V600E)B-RAF amplification-mediated acquired B-RAF inhibitor resistance. Nature communications 2012;3:724.
198. Poulikakos PI, Persaud Y, Janakiraman M, et al. RAF inhibitor resistance is mediated by dimerization of aberrantly spliced BRAF(V600E). Nature 2011;480:387-90.
199. Wagle N, Emery C, Berger MF, et al. Dissecting therapeutic resistance to RAF inhibition in melanoma by tumor genomic profiling. Journal of clinical oncology : official journal of the American Society of Clinical Oncology 2011;29:3085-96.

200. Johannessen CM, Boehm JS, Kim SY, et al. COT drives resistance to RAF inhibition through MAP kinase pathway reactivation. Nature 2010;468:968-72.
201. Corcoran RB, Dias-Santagata D, Bergethon K, Iafrate AJ, Settleman J, Engelman JA. BRAF gene amplification can promote acquired resistance to MEK inhibitors in cancer cells harboring the BRAF V600E mutation. Science signaling 2010;3:ra84.
202. Das Thakur M, Salangsang F, Landman AS, et al. Modelling vemurafenib resistance in melanoma reveals a strategy to forestall drug resistance. Nature 2013;494:251-5.
203. Hatzivassiliou G, Liu B, O'Brien C, et al. ERK inhibition overcomes acquired resistance to MEK inhibitors. Molecular cancer therapeutics 2012;11:1143-54.
204. Akinleye A, Furqan M, Mukhi N, Ravella P, Liu D. MEK and the inhibitors: from bench to bedside. Journal of hematology & oncology 2013;6:27.
205. Chang-Yew Leow C, Gerondakis S, Spencer A. MEK inhibitors as a chemotherapeutic intervention in multiple myeloma. Blood cancer journal 2013;3:e105.
206. Sheth PR, Liu Y, Hesson T, et al. Fully activated MEK1 exhibits compromised affinity for binding of allosteric inhibitors U0126 and PD0325901. Biochemistry 2011;50:7964-76.
207. Gilmartin AG, Bleam MR, Groy A, et al. GSK1120212 (JTP-74057) is an inhibitor of MEK activity and activation with favorable pharmacokinetic properties for sustained in vivo pathway inhibition. Clinical cancer research : an official journal of the American Association for Cancer Research 2011;17:989-1000.
208. Emery CM, Vijayendran KG, Zipser MC, et al. MEK1 mutations confer resistance to MEK and B-RAF inhibition. Proceedings of the National Academy of Sciences of the United States of America 2009;106:20411-6.
209. Wang H, Daouti S, Li WH, et al. Identification of the MEK1(F129L) activating mutation as a potential mechanism of acquired resistance to MEK inhibition in human cancers carrying the B-RafV600E mutation. Cancer research 2011;71:5535-45.
210. Garon EB, Finn RS, Hosmer W, et al. Identification of common predictive markers of in vitro response to the Mek inhibitor selumetinib (AZD6244; ARRY-

142886) in human breast cancer and non-small cell lung cancer cell lines. Molecular cancer therapeutics 2010;9:1985-94.
211. Meng J, Peng H, Dai B, et al. High level of AKT activity is associated with resistance to MEK inhibitor AZD6244 (ARRY-142886). Cancer biology & therapy 2009;8:2073-80.
212. Tentler JJ, Nallapareddy S, Tan AC, et al. Identification of predictive markers of response to the MEK1/2 inhibitor selumetinib (AZD6244) in K-ras-mutated colorectal cancer. Molecular cancer therapeutics 2010;9:3351-62.
213. Dry JR, Pavey S, Pratilas CA, et al. Transcriptional pathway signatures predict MEK addiction and response to selumetinib (AZD6244). Cancer research 2010;70:2264-73.
214. Mithraprabhu S, Khong T, Spencer A. Overcoming inherent resistance to histone deacetylase inhibitors in multiple myeloma cells by targeting pathways integral to the actin cytoskeleton. Cell Death Dis 2014;5:e1134.
215. O'Brien SG, Guilhot F, Larson RA, et al. Imatinib compared with interferon and low-dose cytarabine for newly diagnosed chronic-phase chronic myeloid leukemia. The New England journal of medicine 2003;348:994-1004.
216. Weinstein IB. Cancer. Addiction to oncogenes--the Achilles heal of cancer. Science 2002;297:63-4.
217. Luo J, Solimini NL, Elledge SJ. Principles of cancer therapy: oncogene and non-oncogene addiction. Cell 2009;136:823-37.
218. Vogelstein B, Papadopoulos N, Velculescu VE, Zhou S, Diaz LA, Jr., Kinzler KW. Cancer genome landscapes. Science 2013;339:1546-58.
219. Pagliarini R, Shao W, Sellers WR. Oncogene addiction: pathways of therapeutic response, resistance, and road maps toward a cure. EMBO Rep 2015;16:280-96.
220. Zhao L, Lee VHF, Ng MK, Yan H, Bijlsma MF. Molecular subtyping of cancer: current status and moving toward clinical applications. Brief Bioinform 2018.
221. Huntsman DG, Ladanyi M. The molecular pathology of cancer: from pan-genomics to post-genomics. J Pathol 2018;244:509-11.
222. Malaney P, Nicosia SV, Dave V. One mouse, one patient paradigm: New avatars of personalized cancer therapy. Cancer Lett 2014;344:1-12.

223. Ferguson FM, Gray NS. Kinase inhibitors: the road ahead. Nat Rev Drug Discov 2018;17:353-77.
224. Lokhorst HM, Plesner T, Laubach JP, et al. Targeting CD38 with Daratumumab Monotherapy in Multiple Myeloma. The New England journal of medicine 2015;373:1207-19.
225. Boise LH, Kaufman JL, Bahlis NJ, Lonial S, Lee KP. The Tao of myeloma. Blood 2014;124:1873-9.
226. Ito T, Ando H, Suzuki T, et al. Identification of a primary target of thalidomide teratogenicity. Science 2010;327:1345-50.
227. Singhal S, Mehta J, Desikan R, et al. Antitumor activity of thalidomide in refractory multiple myeloma. The New England journal of medicine 1999;341:1565-71.
228. Schuster SR, Kortuem KM, Zhu YX, et al. The clinical significance of cereblon expression in multiple myeloma. Leukemia research 2014;38:23-8.
229. Oerlemans R, Franke NE, Assaraf YG, et al. Molecular basis of bortezomib resistance: proteasome subunit beta5 (PSMB5) gene mutation and overexpression of PSMB5 protein. Blood 2008;112:2489-99.
230. Balsas P, Galan-Malo P, Marzo I, Naval J. Bortezomib resistance in a myeloma cell line is associated to PSMbeta5 overexpression and polyploidy. Leukemia research 2012;36:212-8.
231. Ohren JF, Chen H, Pavlovsky A, et al. Structures of human MAP kinase kinase 1 (MEK1) and MEK2 describe novel noncompetitive kinase inhibition. Nat Struct Mol Biol 2004;11:1192-7.
232. Fabbro D, Cowan-Jacob SW, Moebitz H. Ten things you should know about protein kinases: IUPHAR Review 14. Br J Pharmacol 2015;172:2675-700.
233. Paterson JL, Li Z, Wen XY, et al. Preclinical studies of fibroblast growth factor receptor 3 as a therapeutic target in multiple myeloma. British journal of haematology 2004;124:595-603.
234. de la Puente P, Muz B, Jin A, et al. MEK inhibitor, TAK-733 reduces proliferation, affects cell cycle and apoptosis, and synergizes with other targeted therapies in multiple myeloma. Blood cancer journal 2016;6:e399.
235. Plotnikov A, Zehorai E, Procaccia S, Seger R. The MAPK cascades: signaling components, nuclear roles and mechanisms of nuclear translocation. Biochim Biophys Acta 2011;1813:1619-33.

236. Plotnikov A, Chuderland D, Karamansha Y, Livnah O, Seger R. Nuclear extracellular signal-regulated kinase 1 and 2 translocation is mediated by casein kinase 2 and accelerated by autophosphorylation. Molecular and cellular biology 2011;31:3515-30.
237. Caunt CJ, McArdle CA. ERK phosphorylation and nuclear accumulation: insights from single-cell imaging. Biochem Soc Trans 2012;40:224-9.
238. Chuderland D, Konson A, Seger R. Identification and characterization of a general nuclear translocation signal in signaling proteins. Molecular cell 2008;31:850-61.
239. Adachi M, Fukuda M, Nishida E. Two co-existing mechanisms for nuclear import of MAP kinase: passive diffusion of a monomer and active transport of a dimer. EMBO J 1999;18:5347-58.
240. Mebratu Y, Tesfaigzi Y. How ERK1/2 activation controls cell proliferation and cell death: Is subcellular localization the answer? Cell Cycle 2009;8:1168-75.
241. Porter LA, Donoghue DJ. Cyclin B1 and CDK1: nuclear localization and upstream regulators. Prog Cell Cycle Res 2003;5:335-47.
242. Gavet O, Pines J. Progressive activation of CyclinB1-Cdk1 coordinates entry to mitosis. Developmental cell 2010;18:533-43.
243. Gavet O, Pines J. Activation of cyclin B1-Cdk1 synchronizes events in the nucleus and the cytoplasm at mitosis. J Cell Biol 2010;189:247-59.
244. Walsh S, Margolis SS, Kornbluth S. Phosphorylation of the cyclin b1 cytoplasmic retention sequence by mitogen-activated protein kinase and Plx. Mol Cancer Res 2003;1:280-9.
245. Hubner A, Barrett T, Flavell RA, Davis RJ. Multisite phosphorylation regulates Bim stability and apoptotic activity. Molecular cell 2008;30:415-25.
246. Kumar S, Kaufman JL, Gasparetto C, et al. Efficacy of venetoclax as targeted therapy for relapsed/refractory t(11;14) multiple myeloma. Blood 2017;130:2401-9.
247. Peppelenbosch MP. Kinome profiling. Scientifica 2012;2012:306798.
248. Graves LM, Duncan JS, Whittle MC, Johnson GL. The dynamic nature of the kinome. The Biochemical journal 2013;450:1-8.
249. Johnson GL, Stuhlmiller TJ, Angus SP, Zawistowski JS, Graves LM. Molecular Pathways: Adaptive Kinome Reprogramming in Response to Targeted

Inhibition of the BRAF-MEK-ERK Pathway in Cancer. Clinical cancer research : an official journal of the American Association for Cancer Research 2014;20:2516-22.
250. Piersma SR, Labots M, Verheul HM, Jimenez CR. Strategies for kinome profiling in cancer and potential clinical applications: chemical proteomics and array-based methods. Analytical and bioanalytical chemistry 2010;397:3163-71.
251. Arsenault R, Griebel P, Napper S. Peptide arrays for kinome analysis: new opportunities and remaining challenges. Proteomics 2011;11:4595-609.
252. Kolch W, Mischak H, Pitt AR. The molecular make-up of a tumour: proteomics in cancer research. Clin Sci (Lond) 2005;108:369-83.
253. Fuhler GM, Diks SH, Peppelenbosch MP, Kerr WG. Widespread deregulation of phosphorylation-based signaling pathways in multiple myeloma cells: opportunities for therapeutic intervention. Molecular medicine 2011;17:790-8.
254. Duncan JS, Whittle MC, Nakamura K, et al. Dynamic reprogramming of the kinome in response to targeted MEK inhibition in triple-negative breast cancer. Cell 2012;149:307-21.
255. Kampen KR, Ter Elst A, Mahmud H, et al. Insights in dynamic kinome reprogramming as a consequence of MEK inhibition in MLL-rearranged AML. Leukemia 2014;28:589-99.
256. Siddiqui-Jain A, Drygin D, Streiner N, et al. CX-4945, an orally bioavailable selective inhibitor of protein kinase CK2, inhibits prosurvival and angiogenic signaling and exhibits antitumor efficacy. Cancer research 2010;70:10288-98.
257. Souers AJ, Leverson JD, Boghaert ER, et al. ABT-199, a potent and selective BCL-2 inhibitor, achieves antitumor activity while sparing platelets. Nat Med 2013;19:202-8.
258. Mandato E, Manni S, Zaffino F, Semenzato G, Piazza F. Targeting CK2-driven non-oncogene addiction in B-cell tumors. Oncogene 2016;35:6045-52.
259. Ruzzene M, Pinna LA. Addiction to protein kinase CK2: a common denominator of diverse cancer cells? Biochim Biophys Acta 2010;1804:499-504.
260. Meggio F, Pinna LA. One-thousand-and-one substrates of protein kinase CK2? FASEB J 2003;17:349-68.
261. Litchfield DW. Protein kinase CK2: structure, regulation and role in cellular decisions of life and death. The Biochemical journal 2003;369:1-15.

262. Piazza F, Manni S, Ruzzene M, Pinna LA, Gurrieri C, Semenzato G. Protein kinase CK2 in hematologic malignancies: reliance on a pivotal cell survival regulator by oncogenic signaling pathways. Leukemia 2012;26:1174-9.
263. Piazza F, Manni S, Semenzato G. Novel players in multiple myeloma pathogenesis: role of protein kinases CK2 and GSK3. Leukemia research 2013;37:221-7.
264. Piazza FA, Ruzzene M, Gurrieri C, et al. Multiple myeloma cell survival relies on high activity of protein kinase CK2. Blood 2006;108:1698-707.
265. Chon HJ, Bae KJ, Lee Y, Kim J. The casein kinase 2 inhibitor, CX-4945, as an anti-cancer drug in treatment of human hematological malignancies. Front Pharmacol 2015;6:70.
266. Czabotar PE, Lessene G, Strasser A, Adams JM. Control of apoptosis by the BCL-2 protein family: implications for physiology and therapy. Nature reviews Molecular cell biology 2014;15:49-63.
267. Peperzak V, Vikstrom I, Walker J, et al. Mcl-1 is essential for the survival of plasma cells. Nat Immunol 2013;14:290-7.
268. Gong JN, Khong T, Segal D, et al. Hierarchy for targeting prosurvival BCL2 family proteins in multiple myeloma: pivotal role of MCL1. Blood 2016;128:1834-44.
269. Roberts AW, Stilgenbauer S, Seymour JF, Huang DCS. Venetoclax in Patients with Previously Treated Chronic Lymphocytic Leukemia. Clinical cancer research : an official journal of the American Association for Cancer Research 2017;23:4527-33.
270. Gonsalves WI, Buadi FK, Kumar SK. Combination therapy incorporating Bcl-2 inhibition with Venetoclax for the treatment of refractory primary plasma cell leukemia with t (11;14). European journal of haematology 2018;100:215-7.
271. Moreau P, Chanan-Khan A, Roberts AW, et al. Promising efficacy and acceptable safety of venetoclax plus bortezomib and dexamethasone in relapsed/refractory MM. Blood 2017;130:2392-400.
272. Lee HJ, Cao Y, Pham V, et al. Ras-MEK Signaling Mediates a Critical Chk1-Dependent DNA Damage Response in Cancer Cells. Molecular cancer therapeutics 2017;16:694-704.
273. Estrada-Bernal A, Chatterjee M, Haque SJ, et al. MEK inhibitor GSK1120212-mediated radiosensitization of pancreatic cancer cells involves

inhibition of DNA double-strand break repair pathways. Cell Cycle 2015;14:3713-24.
274. Lubner SJ, Uboha NV, Deming DA. Primary and acquired resistance to biologic therapies in gastrointestinal cancers. J Gastrointest Oncol 2017;8:499-512.
275. Jing J, Greshock J, Holbrook JD, et al. Comprehensive predictive biomarker analysis for MEK inhibitor GSK1120212. Molecular cancer therapeutics 2012;11:720-9.
276. Ahn S, Brant R, Sharpe A, et al. Correlation between MEK signature and Ras gene alteration in advanced gastric cancer. Oncotarget 2017;8:107492-9.
277. Omolo B, Yang M, Lo FY, et al. Adaptation of a RAS pathway activation signature from FF to FFPE tissues in colorectal cancer. BMC medical genomics 2016;9:65.
278. Brant R, Sharpe A, Liptrot T, et al. Clinically Viable Gene Expression Assays with Potential for Predicting Benefit from MEK Inhibitors. Clinical cancer research : an official journal of the American Association for Cancer Research 2017;23:1471-80.
279. Wee S, Jagani Z, Xiang KX, et al. PI3K pathway activation mediates resistance to MEK inhibitors in KRAS mutant cancers. Cancer research 2009;69:4286-93.
280. Jong NN, McKeage MJ. Emerging roles of metal solute carriers in cancer mechanisms and treatment. Biopharm Drug Dispos 2014;35:450-62.
281. Pellegrino A, Antonaci F, Russo F, et al. CXCR3-binding chemokines in multiple myeloma. Cancer Lett 2004;207:221-7.
282. Moller C, Stromberg T, Juremalm M, Nilsson K, Nilsson G. Expression and function of chemokine receptors in human multiple myeloma. Leukemia 2003;17:203-10.
283. Giuliani N, Bonomini S, Romagnani P, et al. CXCR3 and its binding chemokines in myeloma cells: expression of isoforms and potential relationships with myeloma cell proliferation and survival. Haematologica 2006;91:1489-97.
284. Brufsky A. Trastuzumab-based therapy for patients with HER2-positive breast cancer: from early scientific development to foundation of care. Am J Clin Oncol 2010;33:186-95.

285. Ni QF, Tian Y, Kong LL, Lu YT, Ding WZ, Kong LB. Latexin exhibits tumor suppressor potential in hepatocellular carcinoma. Oncology reports 2014;31:1364-72.
286. Li Y, Basang Z, Ding H, et al. Latexin expression is downregulated in human gastric carcinomas and exhibits tumor suppressor potential. BMC cancer 2011;11:121.
287. Xue Z, Zhou Y, Wang C, et al. Latexin exhibits tumor-suppressor potential in pancreatic ductal adenocarcinoma. Oncology reports 2016;35:50-8.
288. Muthusamy V, Premi S, Soper C, Platt J, Bosenberg M. The hematopoietic stem cell regulatory gene latexin has tumor-suppressive properties in malignant melanoma. The Journal of investigative dermatology 2013;133:1827-33.
289. Liu Y, Howard D, Rector K, et al. Latexin is down-regulated in hematopoietic malignancies and restoration of expression inhibits lymphoma growth. PloS one 2012;7:e44979.
290. Watkins DB, Hughes TP, White DL. OCT1 and imatinib transport in CML: is it clinically relevant? Leukemia 2015;29:1960-9.
291. Witte T, Plass C, Gerhauser C. Pan-cancer patterns of DNA methylation. Genome Med 2014;6:66.
292. Liang G, Weisenberger DJ. DNA methylation aberrancies as a guide for surveillance and treatment of human cancers. Epigenetics 2017;12:416-32.
293. Baylin SB, Jones PA. A decade of exploring the cancer epigenome - biological and translational implications. Nature reviews Cancer 2011;11:726-34.
294. Pulukuri SM, Rao JS. Activation of p53/p21Waf1/Cip1 pathway by 5-aza-2'-deoxycytidine inhibits cell proliferation, induces pro-apoptotic genes and mitogen-activated protein kinases in human prostate cancer cells. International journal of oncology 2005;26:863-71.
295. Keats JJ, Reiman T, Maxwell CA, et al. In multiple myeloma, t(4;14)(p16;q32) is an adverse prognostic factor irrespective of FGFR3 expression. Blood 2003;101:1520-9.
296. Mirabella F, Wu P, Wardell CP, et al. MMSET is the key molecular target in t(4;14) myeloma. Blood cancer journal 2013;3:e114.
297. Marango J, Shimoyama M, Nishio H, et al. The MMSET protein is a histone methyltransferase with characteristics of a transcriptional corepressor. Blood 2008;111:3145-54.

298. Kalff A, Spencer A. The t(4;14) translocation and FGFR3 overexpression in multiple myeloma: prognostic implications and current clinical strategies. Blood cancer journal 2012;2:e89.
299. Kaiser MF, Johnson DC, Wu P, et al. Global methylation analysis identifies prognostically important epigenetically inactivated tumor suppressor genes in multiple myeloma. Blood 2013;122:219-26.
300. Geraldes C, Goncalves AC, Cortesao E, et al. Aberrant p15, p16, p53, and DAPK Gene Methylation in Myelomagenesis: Clinical and Prognostic Implications. Clinical lymphoma, myeloma & leukemia 2016;16:713-20 e2.
301. Pawlyn C, Kaiser MF, Heuck C, et al. The Spectrum and Clinical Impact of Epigenetic Modifier Mutations in Myeloma. Clinical cancer research : an official journal of the American Association for Cancer Research 2016;22:5783-94.
302. Krzeminski P, Corchete LA, Garcia JL, et al. Integrative analysis of DNA copy number, DNA methylation and gene expression in multiple myeloma reveals alterations related to relapse. Oncotarget 2016;7:80664-79.
303. Hajek R, Siegel D, Orlowski RZ, Ludwig H, Palumbo A, Dimopoulos M. The role of histone deacetylase inhibitors in patients with relapsed/refractory multiple myeloma. Leukemia & lymphoma 2014;55:11-8.
304. Hideshima T, Anderson KC. Histone deacetylase inhibitors in the treatment for multiple myeloma. International journal of hematology 2013;97:324-32.
305. Khong T, Sharkey J, Spencer A. The effect of azacitidine on interleukin-6 signaling and nuclear factor-kappaB activation and its in vitro and in vivo activity against multiple myeloma. Haematologica 2008;93:860-9.
306. Moreaux J, Reme T, Leonard W, et al. Development of gene expression-based score to predict sensitivity of multiple myeloma cells to DNA methylation inhibitors. Molecular cancer therapeutics 2012;11:2685-92.
307. Moreaux J, Bruyer A, Veyrune JL, Goldschmidt H, Hose D, Klein B. DNA methylation score is predictive of myeloma cell sensitivity to 5-azacitidine. British journal of haematology 2014;164:613-6.
308. Toor AA, Payne KK, Chung HM, et al. Epigenetic induction of adaptive immune response in multiple myeloma: sequential azacitidine and lenalidomide generate cancer testis antigen-specific cellular immunity. British journal of haematology 2012;158:700-11.

309. Ramachandran K, Speer C, Nathanson L, Claros M, Singal R. Role of DNA Methylation in Cabazitaxel Resistance in Prostate Cancer. Anticancer Res 2016;36:161-8.
310. Tsimberidou AM, Said R, Culotta K, et al. Phase I study of azacitidine and oxaliplatin in patients with advanced cancers that have relapsed or are refractory to any platinum therapy. Clin Epigenetics 2015;7:29.
311. Khan GN, Kim EJ, Shin TS, Lee SH. Azacytidine-induced Chemosensitivity to Doxorubicin in Human Breast Cancer MCF7 Cells. Anticancer Res 2017;37:2355-64.
312. Vendetti FP, Topper M, Huang P, et al. Evaluation of azacitidine and entinostat as sensitization agents to cytotoxic chemotherapy in preclinical models of non-small cell lung cancer. Oncotarget 2015;6:56-70.
313. Ramachandran K, Gordian E, Singal R. 5-azacytidine reverses drug resistance in bladder cancer cells. Anticancer Res 2011;31:3757-66.
314. Matei D, Fang F, Shen C, et al. Epigenetic resensitization to platinum in ovarian cancer. Cancer research 2012;72:2197-205.
315. Li XY, Wu JZ, Cao HX, et al. Blockade of DNA methylation enhances the therapeutic effect of gefitinib in non-small cell lung cancer cells. Oncology reports 2013;29:1975-82.
316. Wang X, Wang H, Jiang N, Lu W, Zhang XF, Fang JY. Effect of inhibition of MEK pathway on 5-aza-deoxycytidine-suppressed pancreatic cancer cell proliferation. Genet Mol Res 2013;12:5560-73.
317. Hu Q, Yu L, Chen R, et al. 5-aza-2'-deoxycytidine improves the sensitivity of endometrial cancer cells to progesterone therapy. Int J Gynecol Cancer 2012;22:951-9.
318. Wang L, Zhang Y, Li R, et al. 5-aza-2'-Deoxycytidine enhances the radiosensitivity of breast cancer cells. Cancer Biother Radiopharm 2013;28:34-44.
319. Valdez BC, Nieto Y, Murray D, et al. Epigenetic modifiers enhance the synergistic cytotoxicity of combined nucleoside analog-DNA alkylating agents in lymphoma cell lines. Experimental hematology 2012;40:800-10.
320. Gopalakrishnapillai A, Kolb EA, McCahan SM, Barwe SP. Epigenetic drug combination induces remission in mouse xenograft models of pediatric acute myeloid leukemia. Leukemia research 2017;58:91-7.

321. Cao Y, Qiu GQ, Wu HQ, et al. Decitabine enhances bortezomib treatment in RPMI 8226 multiple myeloma cells. Mol Med Rep 2016;14:3469-75.
322. Huang da W, Sherman BT, Lempicki RA. Systematic and integrative analysis of large gene lists using DAVID bioinformatics resources. Nat Protoc 2009;4:44-57.
323. Hagemann S, Heil O, Lyko F, Brueckner B. Azacytidine and decitabine induce gene-specific and non-random DNA demethylation in human cancer cell lines. PloS one 2011;6:e17388.
324. Tran HT, Kim HN, Lee IK, et al. DNA methylation changes following 5-azacitidine treatment in patients with myelodysplastic syndrome. J Korean Med Sci 2011;26:207-13.
325. Stewart AK, Bergsagel PL, Greipp PR, et al. A practical guide to defining high-risk myeloma for clinical trials, patient counseling and choice of therapy. Leukemia 2007;21:529-34.
326. Scheid C, Reece D, Beksac M, et al. Phase 2 study of dovitinib in patients with relapsed or refractory multiple myeloma with or without t(4;14) translocation. European journal of haematology 2015;95:316-24.
327. Oka M, Meacham AM, Hamazaki T, Rodic N, Chang LJ, Terada N. De novo DNA methyltransferases Dnmt3a and Dnmt3b primarily mediate the cytotoxic effect of 5-aza-2'-deoxycytidine. Oncogene 2005;24:3091-9.
328. Beyrouthy MJ, Garner KM, Hever MP, et al. High DNA methyltransferase 3B expression mediates 5-aza-deoxycytidine hypersensitivity in testicular germ cell tumors. Cancer research 2009;69:9360-6.
329. Cui M, Wen Z, Chen J, Yang Z, Zhang H. 5-Aza-2'-deoxycytidine is a potent inhibitor of DNA methyltransferase 3B and induces apoptosis in human endometrial cancer cell lines with the up-regulation of hMLH1. Med Oncol 2010;27:278-85.
330. Palii SS, Van Emburgh BO, Sankpal UT, Brown KD, Robertson KD. DNA methylation inhibitor 5-Aza-2'-deoxycytidine induces reversible genome-wide DNA damage that is distinctly influenced by DNA methyltransferases 1 and 3B. Molecular and cellular biology 2008;28:752-71.
331. Popovic R, Martinez-Garcia E, Giannopoulou EG, et al. Histone methyltransferase MMSET/NSD2 alters EZH2 binding and reprograms the

myeloma epigenome through global and focal changes in H3K36 and H3K27 methylation. PLoS Genet 2014;10:e1004566.

332. Martinez-Garcia E, Popovic R, Min DJ, et al. The MMSET histone methyl transferase switches global histone methylation and alters gene expression in t(4;14) multiple myeloma cells. Blood 2011;117:211-20.

333. Mund C, Hackanson B, Stresemann C, Lubbert M, Lyko F. Characterization of DNA demethylation effects induced by 5-Aza-2'-deoxycytidine in patients with myelodysplastic syndrome. Cancer research 2005;65:7086-90.

334. Tsai HC, Li H, Van Neste L, et al. Transient low doses of DNA-demethylating agents exert durable antitumor effects on hematological and epithelial tumor cells. Cancer cell 2012;21:430-46.

335. Li H, Chiappinelli KB, Guzzetta AA, et al. Immune regulation by low doses of the DNA methyltransferase inhibitor 5-azacitidine in common human epithelial cancers. Oncotarget 2014;5:587-98.

336. Wrangle J, Wang W, Koch A, et al. Alterations of immune response of Non-Small Cell Lung Cancer with Azacytidine. Oncotarget 2013;4:2067-79.

337. Roulois D, Loo Yau H, Singhania R, et al. DNA-Demethylating Agents Target Colorectal Cancer Cells by Inducing Viral Mimicry by Endogenous Transcripts. Cell 2015;162:961-73.

338. Chiappinelli KB, Strissel PL, Desrichard A, et al. Inhibiting DNA Methylation Causes an Interferon Response in Cancer via dsRNA Including Endogenous Retroviruses. Cell 2015;162:974-86.

339. Manning LS, Berger JD, O'Donoghue HL, Sheridan GN, Claringbold PG, Turner JH. A model of multiple myeloma: culture of 5T33 murine myeloma cells and evaluation of tumorigenicity in the C57BL/KaLwRij mouse. British journal of cancer 1992;66:1088-93.

340. Bonni A, Brunet A, West AE, Datta SR, Takasu MA, Greenberg ME. Cell survival promoted by the Ras-MAPK signaling pathway by transcription-dependent and -independent mechanisms. Science 1999;286:1358-62.

341. Zhao Y, Bjorbaek C, Moller DE. Regulation and interaction of pp90(rsk) isoforms with mitogen-activated protein kinases. The Journal of biological chemistry 1996;271:29773-9.

342. Turner N, Grose R. Fibroblast growth factor signalling: from development to cancer. Nature reviews Cancer 2010;10:116-29.
343. Mateos MV, Hernandez MT, Giraldo P, et al. Lenalidomide plus dexamethasone for high-risk smoldering multiple myeloma. The New England journal of medicine 2013;369:438-47.

9. SUPPLEMENTARY FIGURES

9.1 RIGOSERTIB

Rigosertib (ON-01910) is purportedly a RAS inhibitor. Western blot analysis did not reveal loss of phosphorylated ERK in treated HMCLs (figure 9.1 A, B). Rigosertib induced variable levels of cell death at 1μM doses only (figure 9.1 C). Growth inhibition was not observed at doses <1μM.

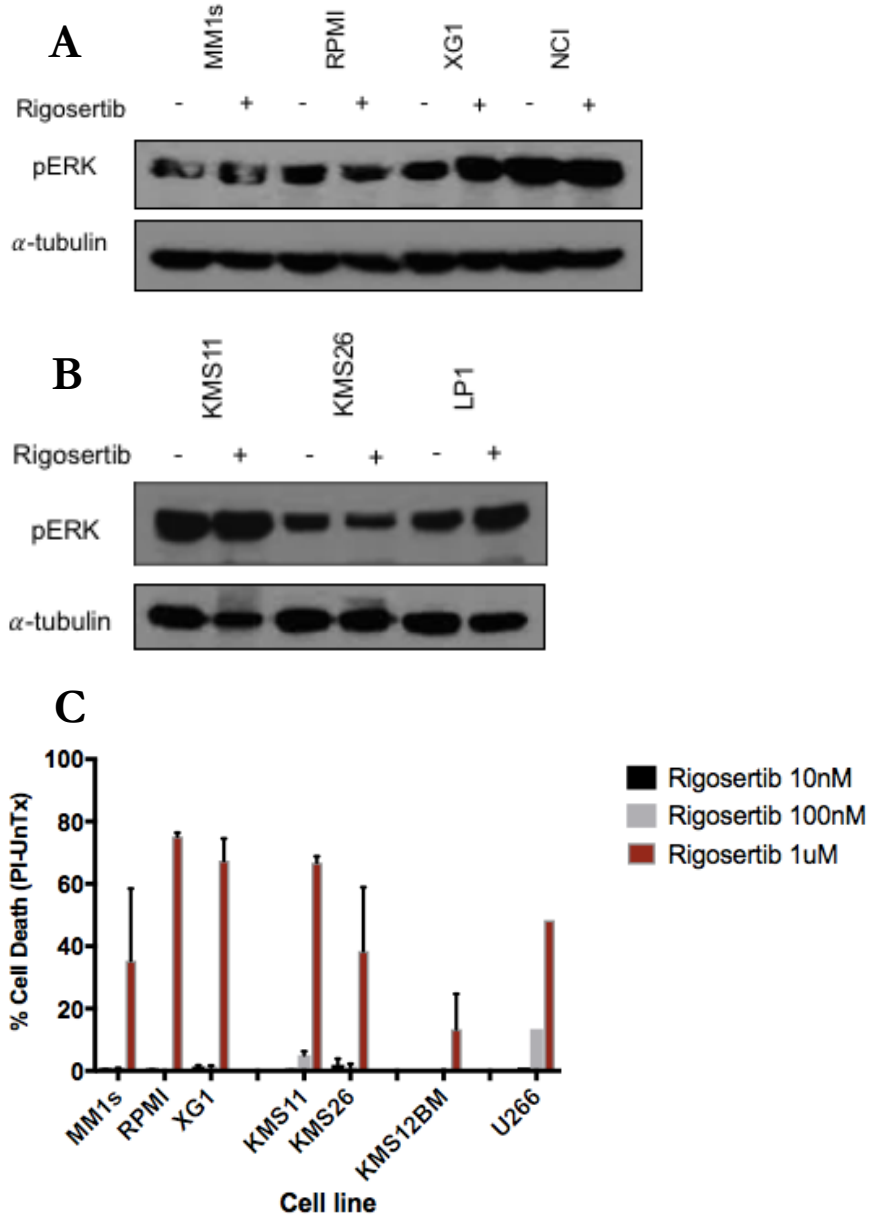

Figure 9.1: Rigosertib treatment does not result in loss of phosphorylated ERK. (A) RAS^M HMCLs. **(B)** t(4;14) HMCLs. P-ERK=phosphorylated ERK. α-tubulin is the loading control. **(C)** Cell death (by PI flow cytometry) was observed at 1μM doses. (n=3, mean ± SEM).

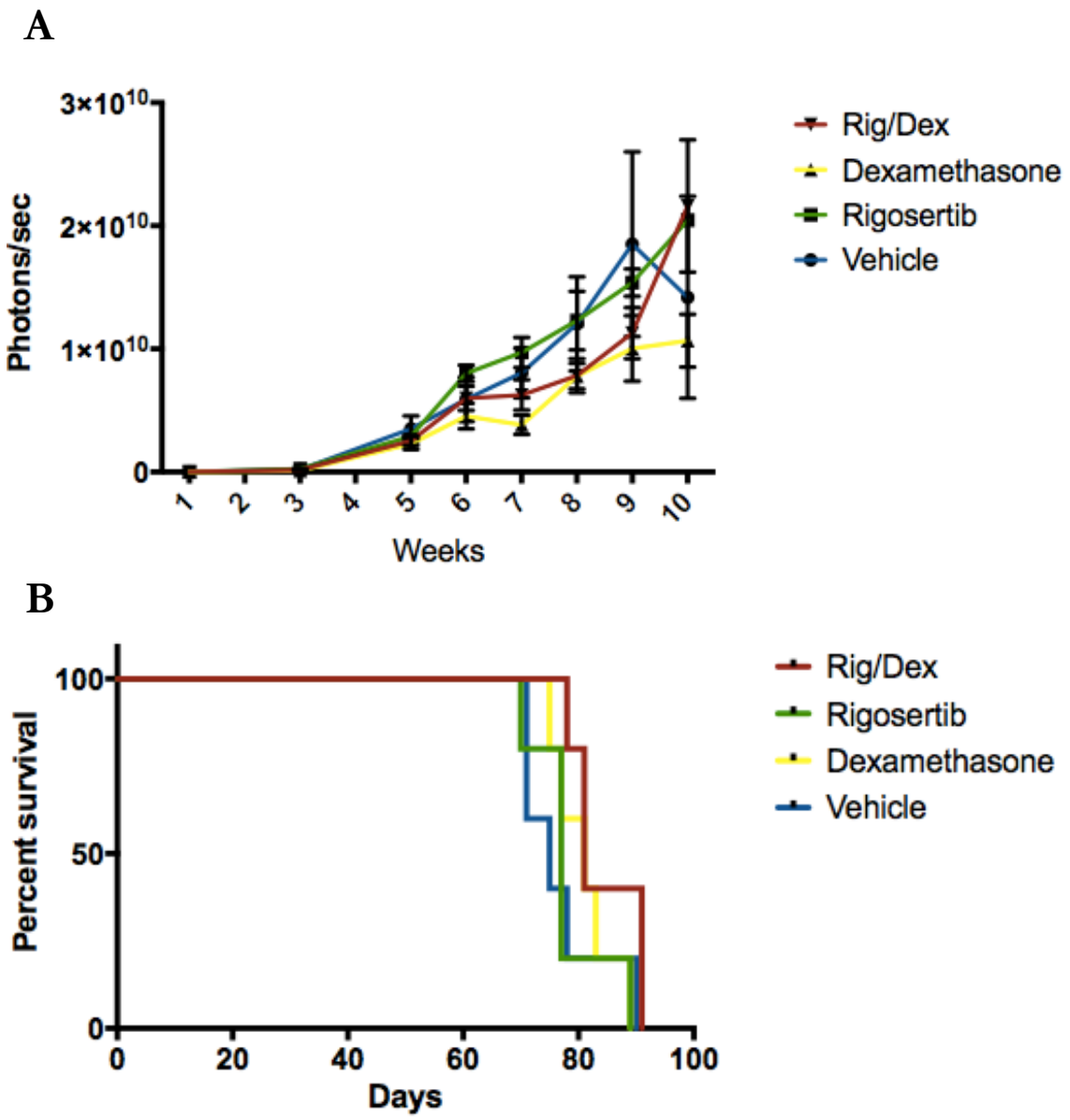

Figure 9.2(A, B): U266 murine xenograft treated with rigosertib, dexamethasone & combination. (A) Disease measurement by bioluminescence over time. No significant delay in disease progression was observed in any treatment arm. **(B)** Survival curve. No significant improvement in survival was observed in any treatment arm. Rig=rigosertib, Dex=dexamethasone. (n=5/treatment group).

In a U266 xenograft, mice were treated with vehicle alone, rigosertib 250mg/kg alone daily, dexamethasone 1mg/kg alone daily or both rigosertib 250mg/kg with dexamethasone 1mg/kg daily in combination. Treatment was continued for 2 cycles of 3 weeks with a single week break between cycles

9.3 MAPK GENE EXPRESSION PRE- & POST-TREATMENT RT^2 ARRAY

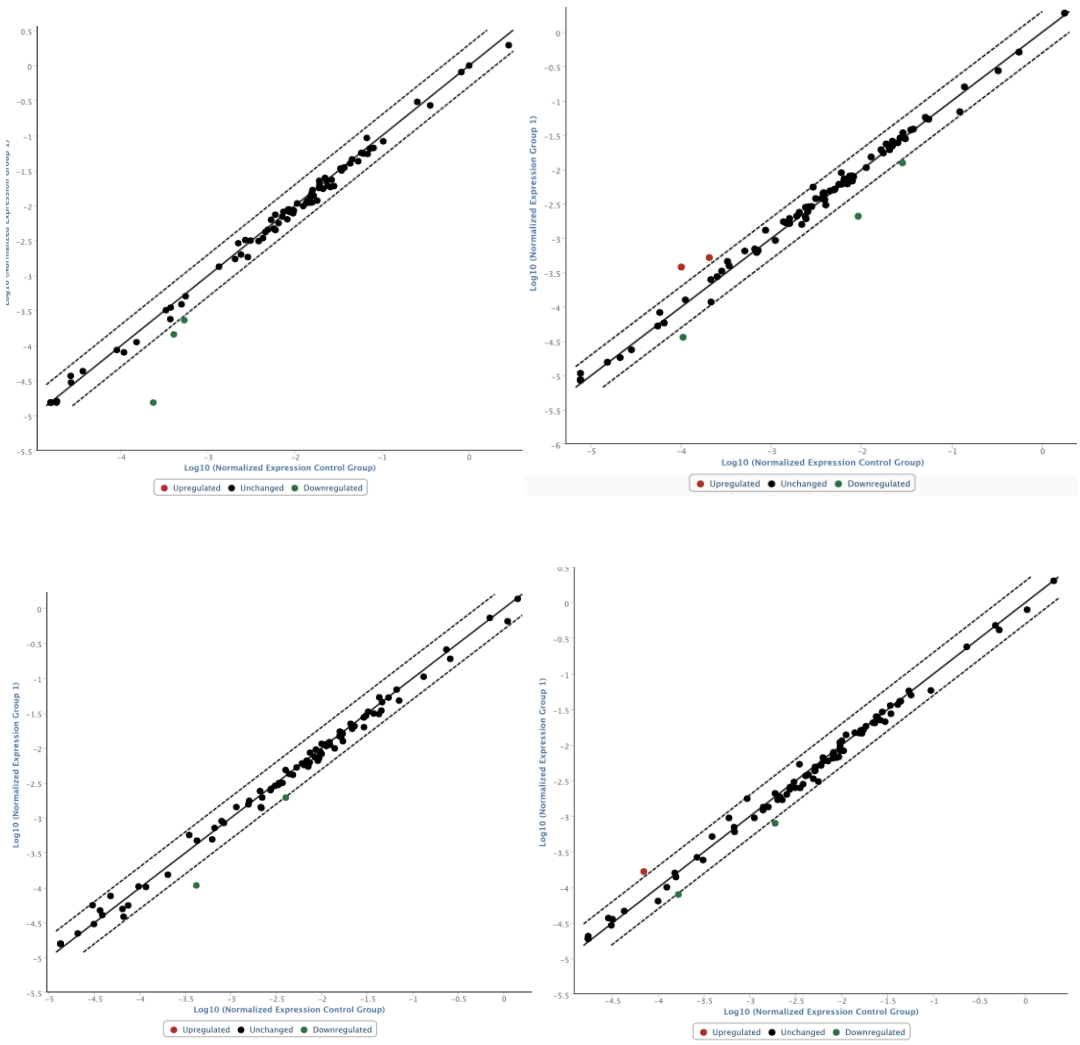

Figure 9.3: Gene expression changes pre- and post-treatment with trametinib RT^2 MAPK array. The QIAGEN RT^2 MAPK array, did not identify significant gene expression changes pre- and post-treatment with trametinib 1μM at 24 hours. (n=3). Top left – MM1s. Top right – NCI. Lower left – KMS26. Lower right – LP1.

9.4 SURFACE CXCR3 BY FLOW CYTOMETRY

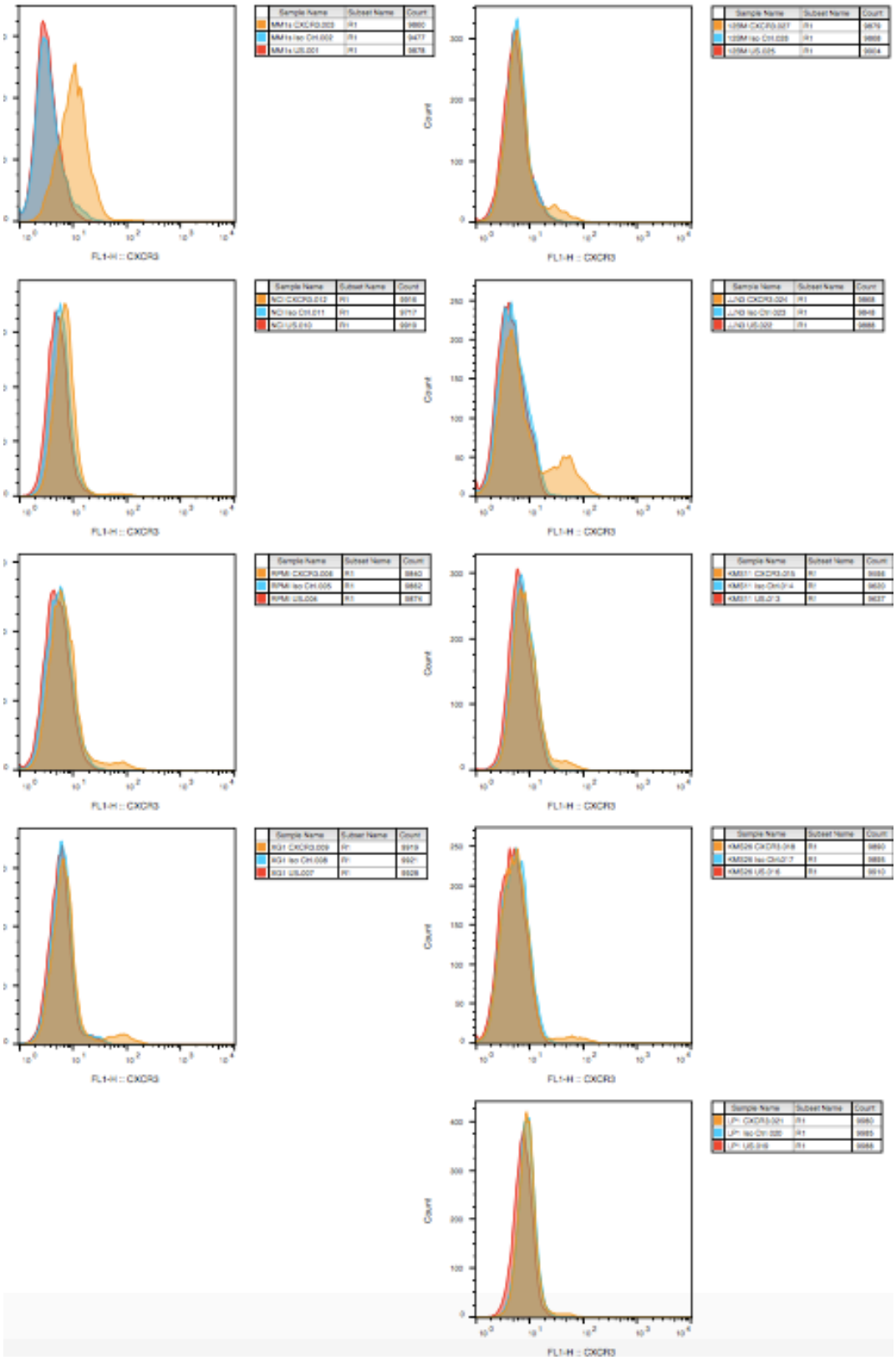

Figure 9.4: Surface CXCR3 by flow cytometry. MM1s is the only HMCL to show any surface expression of CXCR3.

9.5 RNA-SEQ PATHWAY ENRICHMENT DATA IN AZACITIDINE TREATED HMCLS

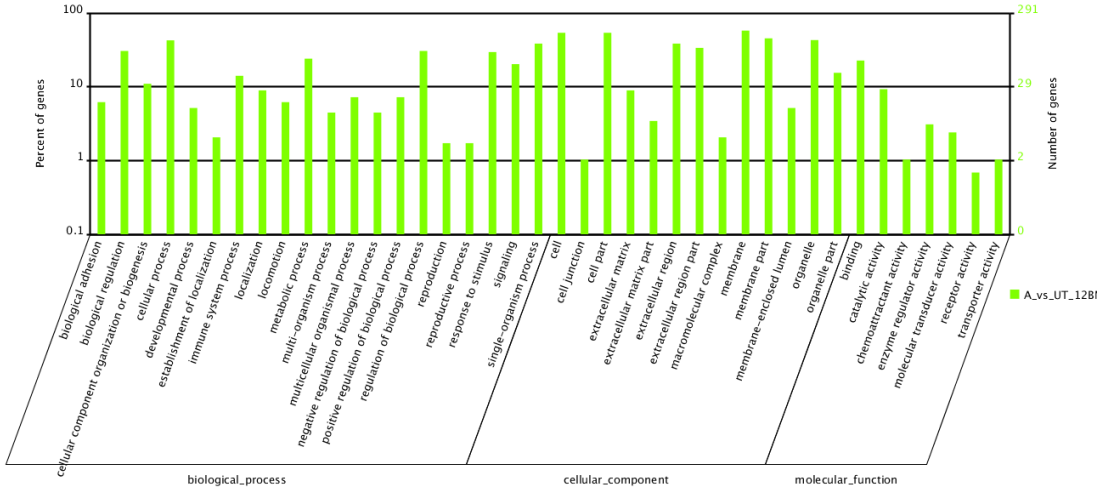

KMS12BM

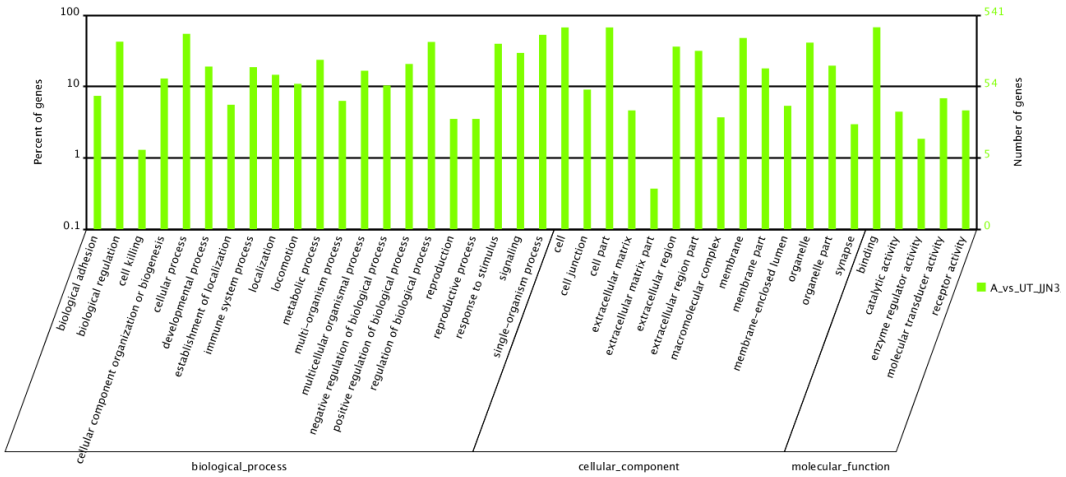

JJN3

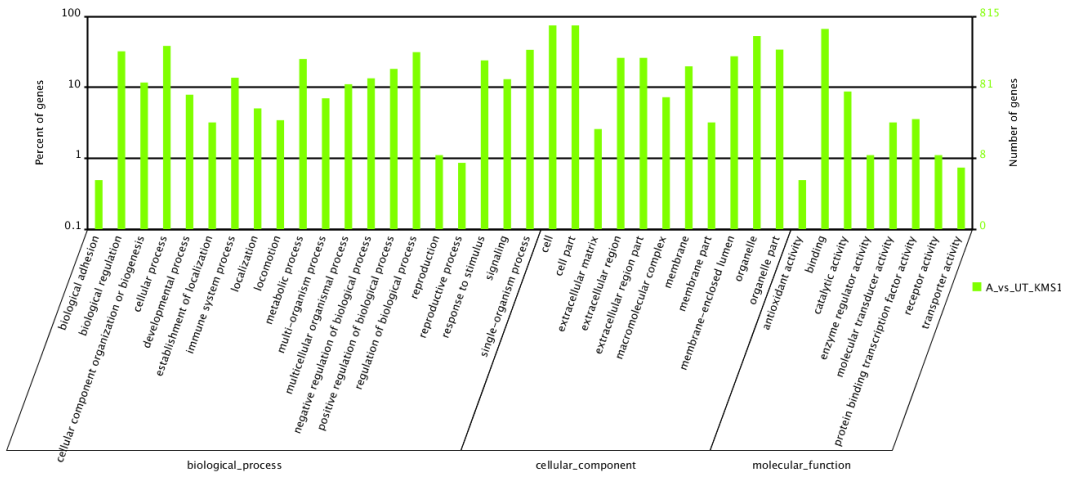

KMS11

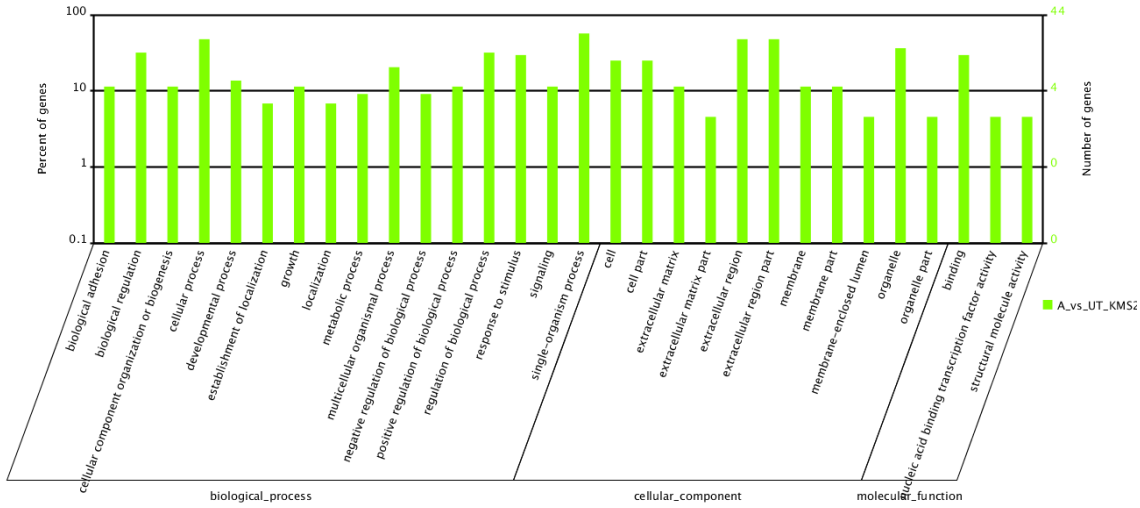

KMS26

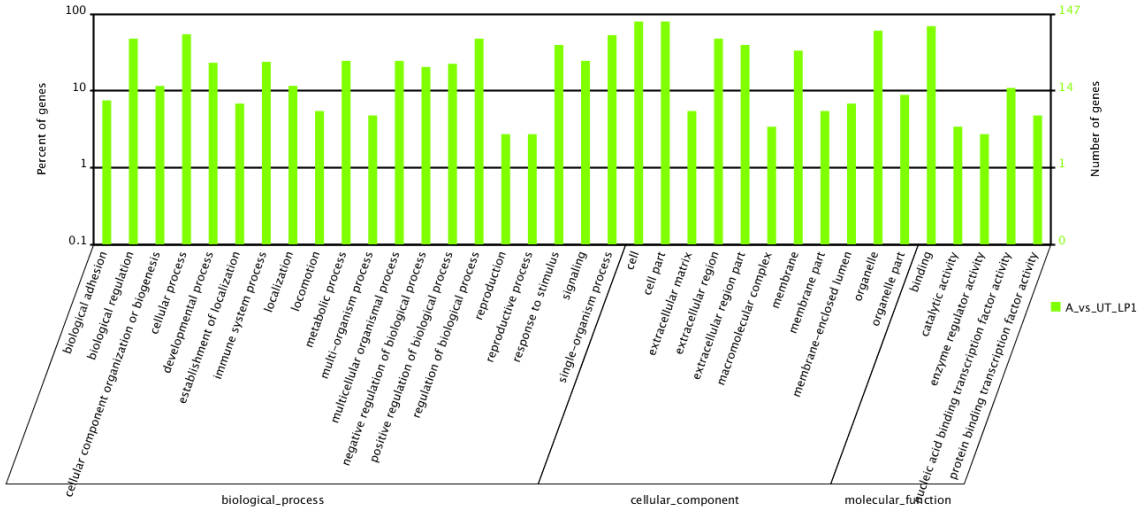

LP1

Figure 9.5: Gene enrichment pathways post azacitidine treatment.